DYNAMIC IMPEDENCE MATCHING AND PULSE SHAPING OF HIGH VOLTAGE HIGH PULSE POWER SUPPLY

A Thesis
Submitted in partial fulfillment of the requirements
for the award of the degree of

Doctor of Philosophy

in

Electrical Engineering

By

KRISHNA KUMAR RAI

(Roll No.716121)

Supervisors

Dr. A.V. Giridhar
Associate Professor
Department of Electrical Engineering
NIT Warangal
&
Dr. D.R. Jahagirdar
Outstanding Scientist
RCI, DRDO, Hyderabad

DEPARTMENT OF ELECTRICAL ENGINEERING
NATIONAL INSTITUTE OF TECHNOLOGY
WARANGAL

Dec 2023

APPROVAL SHEET

This Thesis entitled "**Dynamic Impedance Matching And Pulse Shaping Of High Voltage High Pulse Power Supply**" by **Krishna Kumar Rai (Roll No. 716121)** is approved for the degree of Doctor of Philosophy

Examiners

_____

_____

_____

Supervisor(s)

Dr. A.V. Giridhar
Associate Professor
Department of Electrical Engineering
NIT Warangal
&

Dr. D.R. Jahagirdar
Outstanding Scientist
RCI, DRDO, Hyderabad

Chairman

Dr. B.L. Narasimharaju
Professor & Head
Department of Electrical Engineering
NIT Warangal

Date: _____

DEPARTMENT OF ELECTRICAL ENGINEERING
NATIONAL INSTITUTE OF TECHNOLOGY WARANGAL
WARANGAL – 506 004

DEPARTMENT OF ELECTRICAL ENGINEERING
NATIONAL INSTITUTE OF TECHNOLOGY WARANGAL

CERTIFICATE

This is to certify that the thesis entitled **"Dynamic Impedance Matching And Pulse Shaping Of High Voltage High Pulse Power Supply"**, which is being submitted by **Krishna Kumar Rai (Roll No. 716121)**, is a bonafide work submitted to National Institute of Technology Warangal in partial fulfilment of the requirements for the award of the degree of **Doctor of Philosophy** in Electrical Engineering. To the best of my knowledge, the work incorporated in this thesis has not been submitted elsewhere for the award of any degree.

Date:
Place: Warangal

Dr. A.V.GIRIDHAR
(Thesis Supervisor)
Associate Professor
Department of Electrical Engineering
NIT Warangal

Dr. D.R. JAHAGIRDAR
(Thesis Co-Supervisor)
Outstanding Scientist
RCI, DRDO, Hyderabad

DECLARATION

This is to certify that the work presented in the thesis entitled "**Dynamic Impedance Matching And Pulse Shaping Of High Voltage High Pulse Power Supply"** is a bonafide work done by me under the supervision of **Dr. A.V. Giridhar, Department of Electrical Engineering, National Institute of Technology Warangal, India & Dr. D. R. Jahagirdar, RCI, DRDO, Hyderabad** and was not submitted elsewhere for the award of any degree.

I declare that this written submission represents my ideas in my own words and where others ideas or words have been included; I have adequately cited and referenced the original sources. I also declare that I have adhered to all principles of academic honesty and integrity and have not misrepresented or fabricated or falsified any idea/date/fact/source in my submission. I understand that any violation of the above will be a cause for disciplinary action by the institute and can also evoke penal action from the sources which have thus not been properly cited or from whom proper permission has not been taken when needed.

Date:
Place: NIT Warangal

Krishna Kumar Rai
(Roll No. 716121)

ACKNOWLEDGEMENT

I write this acknowledgement with great honor, pride and pleasure to pay respect to all those who have guided and supported me either directly or indirectly for the completion of this work.

I owe a debt of gratitude to my project guide **Dr. A.V.Giridhar** who was so generous with his time and expertise to guide all through my project work.

I wish to express a deep sense of respect and gratitude to my external project guide **Dr. D.R. Jahagirdar (Outstanding Scientist)** for his constant encouragement and support throughout the course. His able guidance and useful suggestions helped me in completing the project work.

I am grateful to **CHESS & RCI, DRDO, Hyderabad,** for all the aid provided for completing the project work successfully.

I am highly grateful to our Head of the Department & Chairman, DSC **Prof. B.L. Narasimharaju** for providing necessary facilities and encouragement during the course of the work.

My thankful regards go to my Doctoral Scrutiny Committee members **Prof. D. Vakula, ECE** and **Dr. A. Kirubakaran**, **EED**for their detailed review, constructive suggestions and excellent advice during the progress of this research work.

I also appreciate the encouragement from teaching, non-teaching members, and fraternity of Department of Electrical Engineering of NIT Warangal. They have always been encouraging and supportive.

I am very thankful to all the Research Scholars (PhD- NITW) for their support and guidance in the successful completion of this project work.

I wish to express my sincere thanks to the Directors, CHESS, DRDO and NIT Warangal for their official support and encouragement.

I would also like to express my sincere thanks to my family, parents and my friends for their support and blessings.

Krishna Kumar Rai
Roll No. 716121

ABSTRACT

High Voltage High Pulse Power Supply plays a vital role in the generation and amplification of high power RF and Microwave. High power RF and Microwave has various commercial and industrial applications in the field of fundamental research in physics, advanced applications in medical science, quality inspection in aerospace industry etc. Klystron is used as the microwave power generator which uses transmission line based Pulse Forming Network to generate required high voltage to the cathode of Klystron. These high voltage high pulse power are extensively used in rugged environment eventually leading to unavoidable technical issues frequently. This thesis discuss about the problems related to these High Voltage High Pulse Power Supply, their diagnosis techniques using various output parameter observations. The performance of pulse power systems were observed continuously on daily basis throughout the years and a considerably rich database of various parameters like signals, waveforms and trends have been analysed to predict the behavioural performance within the module. The analysis will be a key feedback factor for quick diagnosis, rectification and design modifications.

The performance of High Voltage High Pulse Power Supply (HVHPPS) changes with the change in the load parameters i.e. dynamic impedance, cable length, temperature variation, cavity dimension change, applied cathode voltage, magnetic strength etc. The High Voltage High Pulse Power Supply (HVHPPS) for RF and Microwave types of load requires always a very good impedance matching, to achieve maximum power transmission and minimum reflection. The mathematical modelling and analysis of High Voltage High Pulse Power Supply (HVHPPS) performance on various type of load like magnetron, klystron, particle accelerator etc. In this thesis the mathematical modelling of subsystem of High Voltage High Pulse Power Supply (HVHPPS) and load are generated. Accordingly the load behaviour changes incorporated and analysed the effect at the source side based on hardware results. The mathematical modelling analysis result is validated through the experimental hardware model.

In the present scenario of pulse power applications, transmission of high voltage pulses varies as per load condition. In the early days of its application, High Voltage High Pulse Power Supply (HVHPPS) designs were only for a short distance between the load and the source, where the effect of cable length was not taken into account for design.

The load under observation is Klystron based high energy particle accelerator system. The performance of pulse power systems were observed continuously on a daily basis throughout the year and detailed analysis was carried out. The model of pulse forming system provides details of pattern distortion of the pulse shape due to various dynamic parameter changes i.e. impedance, Load Voltage, Load Current, Cavity Dimensional Changes (Microwave components), temperature variations etc.

High Voltage High Pulse Power Supply (HVHPPS) systems are designed with the goal to match fixed load, so that precise pulse output can be achieved. The HVHPPS output pulse shape changes with load impedance variation due to various reasons. Due to changes in impedance, the performance of Pulse Power Supply degrades and reflects the power to the source end which causes component failure and system shut down. To overcome such problems, a scale down High Voltage High Pulse Power is designed and developed to match the dynamic impedance variations. In earlier days, all HVHPPS were designed using microcontroller where the problem of pulse to pulse monitoring and computational speed were compromised. The availability of variable and self-defined field programmable gate array (FPGA) controller, ensures flexibility to design pulse to pulse shaping and various vital parameter monitoring. This thesis presents the design and implementation of High Voltage High Pulse Power Supply over an FPGA platform to meet the fast response requirement. An experimental test hardware is designed and developed for HVHPPS to implement novel techniques of dynamic impedance matching and pulse shaping on klystron and results are validated experimentally.

Table of Contents

List of Figures

List of Tables

Chapter 1

Introduction

1.1 Introduction

High Voltage High Pulsed Power Supply (HVHPPS) is utilized for pulsed load applications i.e. magnetron, klystron accelerators etc. the performance will be better if pulse to pulse shaping and load matching achieved during initial design. So as to energize magnetron/ klystron at proper frequency and at appropriate level it is important to supply high voltage and high power pulses to it. In addition appropriate pulse voltage and power, the shape of the pulse is of essential significance for proper magnetron activity. The unit which outfits these pulses of voltage to the oscillator is known as the modulator; it is also known as the "pulser". So these pulsers will start exciting the magnetron/ klystron with high voltage pulses which then emits the electromagnetic waves. These electromagnetic waves will be transmitted by the transmitter in order to hit the object with the generated wave so as to know the position and velocity of the object under consideration. The pulse generators used for exciting the magnetron can be of various types though the main function is the same i.e. to excite the magnetron/ klystron with train of high voltage pulses.

High Voltage High Pulse Power Supply (HVHPPS) comprises of energy into nano to millisecond duration but intensive peak power as single pulse (with short rise and fall time, pulse width varies from Nano second to few micro second) at a particular repetitive rate. Pulse power supply in a compact form is always attractive for directed energy weapon system defense, space and commercial application like, particle accelerator, radar systems, plasma immersion ion implantation (PIII), food sterilization, package sealer, paint strippers, water treatment plants etc. here such high voltage pulse power has specific use as futuristic weapon system against aerial targets i.e. mini, micro UAV’s, main UAV and drones and space war counter attack.

The five basic functional blocks content in any pulse power generator system i.e. main power supply system, charging and discharging circuit, pulse generation system, pulse boosting system and various nature of loads as illustrated in Fig.1.1

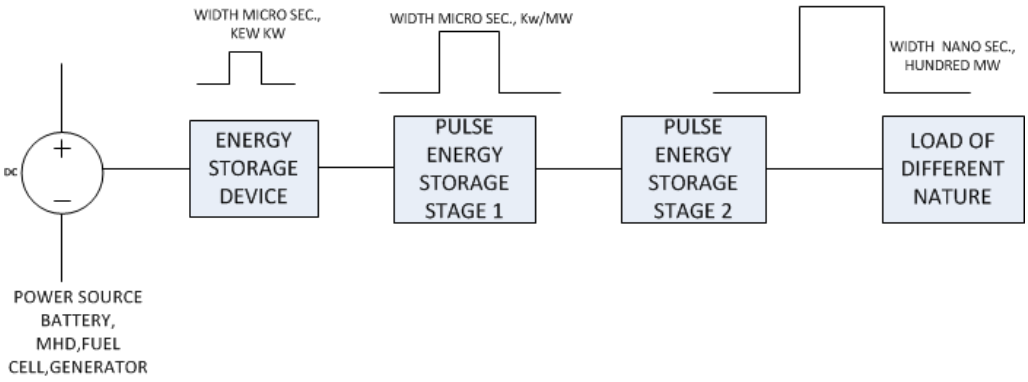

Fig 1.1. Functional Blocks of high voltage high pulse power supply

The sub-system begins at the steady power source (batteries, solar cells, turbo-alternators, utility electric power) followed by energy storage device and ends at the interface with the dynamic impedance change load (laser, RF, X-ray, particle beam).

There may be more blocks of pulse formation as per the requirements of pulse width amplitude. In industrial applications, where high voltage high pulse power needs to be transmitted across long distances, the length of transmission line has significant effect on the shape of high voltage pulses. There are two main domains of application, one at low voltage low pulse power level and another at high voltage high pulse power. Basically low voltage low pulse power is used in commercial and some industrial sectors while all military applications require High Voltage High Pulse Power Supply under rough terrain conditions. HVHPPS has varieties of load (impedance) for carrying out research in nuclear power/ domain. Thus efficient HVHPPS design and development is essential. The change in length of transmission line, temperature effect on overall oxygen free cavity dimensions, dynamic impedance characteristics of amplifiers /oscillators, etc. causes impedance change in the load and impacts the performance of HVHPPS because of back reflection on power loss.

Pulse power system in a compact form is always desirable for defense, space and commercial applications. High Voltage High Pulse Power System generates peak power for very short duration as a single pulse at a particular Pulse Repetition Frequency (PRF).

Pulse generators are generally utilized in Radar applications to energize magnetron/ Klystron so it produces high power RF. The production of high power pulses is broadly utilized in numerous fields like in military, in medical and so forth. The fundamental

standard associated with pulse generators is that energy is stored as electrical or in magnetic form and by closing switch it was discharged into load in type of pulses.

In terms of energy storage and discharging path pulse generators are of two sorts a) Hard tube pulser, b) Line type pulser. Today a large portion of pulse generators are line type pulser on the grounds that the efficiency acquired from hard tube pulser is low contrasted with line type pulser. The line type pulsers are utilized for both energy storage and for pulse shaping. So they are called Pulse Forming Networks (PFN). The PFN Marx generator is appropriate for moderate to low energy applications. In order to obtain pulse widths of rectangular in shape of very small duration of hundreds of nanoseconds and very small rising time of tens of nanoseconds, several PFNs which are identical in nature together with the Marx generator can be used. These can be utilized as an X-ray generator or microwave generator control supply.

Repetitive high-voltage pulses are of extraordinary significance for delivering pulse electron beams and high power microwaves. One of potential advances for the age of such pulses is a Marx generator utilizing PFN stages, regularly joined with a pulses sharpening technique to diminish the rise time to a couple of nanoseconds. As of late there has been an extensive development in use of PFNs for empowering rail guns. A strategy for optimal design of a PFN feeding an optimal launcher is presented. Given the design parameters (pulse length, pulse rise time, pulse repetition frequency), the technique gives the estimation of the inductances and capacitances for an optimal design of an L-C ladder feeding network.

In line type of pulser all energy is dissipated during pulse henceforth it is important to charge the PFN amid inter pulse interval. For this reason charging component is required. This component will charge the PFN to twofold of the power supply voltage. Generally the charging component can be either resistor or inductor. Mostly in all applications inductor is utilized as charging component in light of the fact that the efficiency is high if there should be an occurrence of inductor as charging element.

The discharging circuit consists of a PFN, switch, and the load. As for the load, a magnetron/ klystron is used for the radar application. A magnetron/ klystron is a powerful vacuum tube that fills in as self-energized microwave oscillator. If a magnetron/ klystron is excited with pulsed power or continuous high voltage pulses of

required magnitude, required width and required pulse recurrence frequency it emits electromagnetic waves which is used in the radar application. As for the switches, with improvement of solid state devices like vacuum switch SCR, MOSFETs, IGBTs they are utilized in pulse generator applications.

Depending upon the switching frequency and performance a switch of desired choice is used and the switch is turned on or off at a particular interval to get the required switching frequency or pulse recurrence frequency. By utilizing vacuum switch solid state devices as switch the voltage levels can be expanded to wanted esteem. The efficiency and switching losses are additionally limited by utilizing semiconductor devices.

1.2 Pulse Generators

Pulsed power applications requires the use of high quality rectangular pulses i.e. it should have very fast rise and very fast fall time with a flat pulse top. The rising time of the pulse, its fall time, duration and repetition rate are some of the important specifications for the pulse generator. Basically there are two Types of pulse generators:

1.2.1 Hard-tube Pulsers

In hard tube pulser, the energy-storage device is basically a condenser which is charged to some voltage V initially, thus making available the amount of electrical energy of $\frac{1}{2}$CV2. The term “hard-tube” here actually refers to the nature of which the switch is used in the pulser, which is mainly a high-vacuum tube having a control grid. For this switch closing and opening is therefore accomplished by applying required controlled voltages to its grid. Since during the discharging period only a small fraction of the total energy which is stored during the charging period in the condenser is discharged during the pulse, across the switch the voltage obtained from this pulser immediately after the pulse and also during the charging interval is almost the same as it is found at the beginning of the pulse. The circuit is given in Fig 1.2 below.

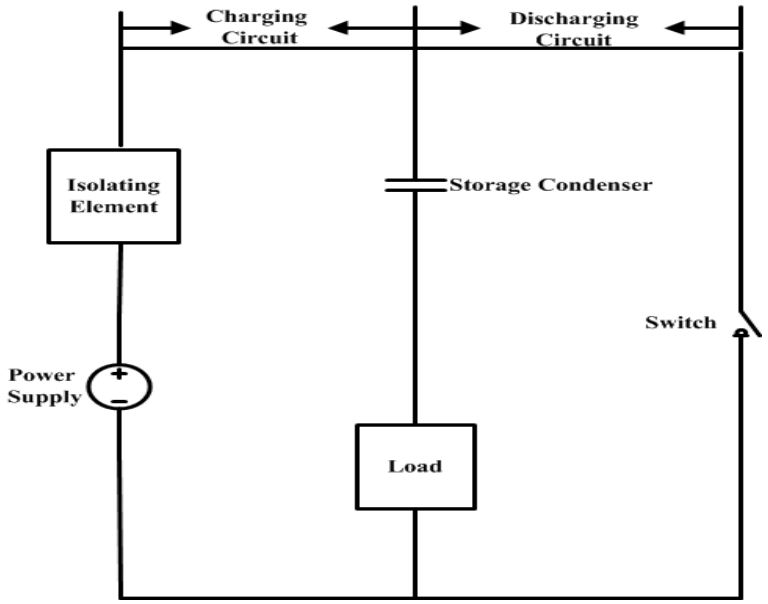

Fig 1.2. Hard tube pulser

1.2.2 Line-type Pulsers

In line type pulsers the energy-storage device is basically a lumped-constant transmission line and hence this category of Pulse generators are referred to as "line-type" pulsers. Since this part of the pulser in the line type not only serves as source of electrical energy but also as the pulse-shaping element during the pulse and hence it has become popularly known as a Pulse Forming Network (PFN). There are notably two types of pulse-forming networks, namely, those in which the energy is stored as an electrostatic field in the amount $\frac{1}{2}$CV2 where C is the total PFN capacitance and V is the voltage that the PFN is charged toand the other is those in which the energy is stored in a magnetic field in the amount $\frac{1}{2}LI^2$. The first class is popularly referred to as the "voltage-fed networks" where the stored energy obtained in the PFN is completely discharged to the load when the switch is closed at the load side and the second as "current fed networks'' where the switch is used to charge the PFN for a certain duration and allows current in the inductances to build up and when switch is turned off.

Energy is discharged to the load. The circuit is as shown in Fig 1.3.

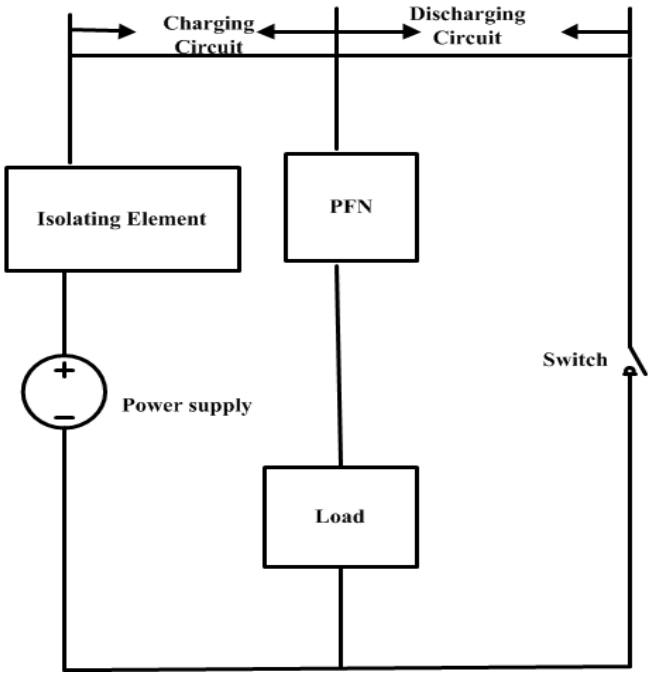

Fig 1.3. Line type pulser

The Pulse-Forming Network in a line type pulser consists of capacitances and inductances which can be put together depending upon the performance in any one of a number of possible configurations.

1.3 Applications

Here we are discussing the use of Pulse Generators for radar application but today they are utilized in numerous applications like in medical applications, in biological fields, in defence area, in water treatment applications, in environmental applications. They are utilized in ecological applications to expel contaminated gases like O, OH, N radicals. In defence industry they are utilized being developed of lasers, launchers and RADAR. In water treatment applications they are utilized for expelling organisms from water and air.

In medical applications, for sterilization and for cancer disease treatment. Some different utilizations of pulse generators are in food processing industry and in plasma science.

Water treatment: The sterilization procedure in water treatment is a pivotal step before piping the water to homes and organizations. For the most part, it happens after filtration, where a disinfectant (for instance chlorine, and chloramine) is added to the water. The purification procedure plans to execute any residual parasites, bacteria, and infections to shield the water

from germs before its piping. Then again, sterilization can be effectively accomplished by applying deadly electroporation to the water under treatment. Usually we can say that applying High-Voltage (HV) pulses over a biological cell membrane called as electroporation.

Food sterilization: Too wide and narrow high-voltage pulse waveforms are of importance for food cleansing industry. Wide pulses joined with narrow pulses for food sterilization in free space, was proposed as another pulse wave shape. It was tentatively demonstrated that consolidated wide and narrow pulses can accomplish preferred disinfection execution over that with limited pulses, and it requires lower control utilization than that with wide pulses. At the point when a wide pulse with sufficiently high power, reiteration rate, and pulse width is connected to the suspension and makes high voltage over the phone layer, it will incite irreversible pore changes and execute organisms with a system of cracking the cell film (electroporation).

Medical Applications: The most progressive of these applications is by all accounts electro chemotherapy, where clinical investigations are in progress. In electro chemotherapy, a chemotherapeutic medication is infused into the tumor and the tumor is then treated with pulse electric fields of 10– 100μs term and amplitudes on the request of 1 kV/cm. It is done by methods for an anode array that is embedded into the affected tissue. The medication is chosen so it has no impact outside the cells and does not enter into intact cells either. So even high centralizations of the medication have no impact aside from in the neighborhood the cells are harmed by electroporation. Pulse generators can also be used for surface modification of Geo Materials, bio fouling prevention and many other applications.

1.4 Literature Review

In 2005, J.h.Kim et al, The pulse generator uses six IGBT stacks and a step-up pulse transformer to generate high voltage pulse.

Twelve IGBTs are connected in series in each IGBT to increase voltage rating of the pulse generator. Each IGBT stack uses a very simple driving method that has only two active drivers and eleven passive drivers (are composed of passive components such as resistors, capacitors, and diodes) to have solid state switching circuit to support the generator of high voltage pulses.

In 2005, N. Carleto et al, designed the PFN based on the Guillemin network synthesis theory. Using this approach, a 31 /spl Omega/ of impedance level and 11.4 nF of capacitance PFN was simulated and then assembled to supply 9 kV and 0.7 /spl mu/s voltage pulses in a pulse transformer primary circuit, at a pulse recurrence frequency (PRF) of 2 kHz. The pulse transformer was designed to impedance matching and d-c isolation between the PFN to magnetron, with transformation ratio 1:7, supplying 30 kV voltage pulses with 93% of efficiency.

In 2007, Yifan Wu et al, developed Marx modulator employs high voltage (HV) insulated gate bipolar transistors (IGBT) as switches and series- connected diodes as isolated components. They used Self-supplied IGBT drivers and optic signals in the system to avoid insulation problem. Experimental results of 20 stages generating pulses with 60 kV, 20-100 micro sec and 50 ~ 500 Hz are validated.

In 2007 A.V.Akimov et al, provided the modulator circuit providing for supply of inductive-resistive load in double-pulse mode with currents up to 10 kA and pulse duration of 300 ns. As switching components thyratron TPI1-10k/50 with anode voltage up to 50 kV are used. The thyratron considered as an alternative to well-known switches, including hot cathode hydrogen thyratron and up-to-date power solid state switches, especially for switching of high-currents with sub-nanosecond jitter, turn-on time of 3-5 ns and average current up to 0.3 A.

In 2010, Dongdong Wang et al, developed all-solid-state pulsed-power generator based on Marx modulator on discrete IGBTs and a magnetic pulse-sharpening circuit, which is employed to compress the rising edge of the Marx output pulse and experimental results are presented with a maximum voltage of 20 kV, a rise time of 200 ns, a pulse duration of 500 ns (full-width at half-maximum), and a repetition rate of 5 kHz on a 285 resistive load. The output power of the generator is 2.5 kW, and the average power in one pulse is 1 MW.

In 2016 Sizhuang Liang et al, the application of superconducting inductive pulsed power supplies in electromagnetic launchers by presenting a dynamic model. In this model, the load of the pulsed power supply is a rail-type electromagnetic launcher. A prototype launcher and a superconducting inductive pulsed power supply were designed. Finite-element analysis was carried out to obtain parameters for the launcher.

In 2016, Haitao Li et al, the feasibility of two discharge methods, high-current testing is carried out with the two HTSPPTs. a higher amplitude of current pulse can be achieved using synchronous parallel discharge and a larger pulse width of current pulse can be achieved using asynchronous parallel discharge.

In 2018, Haitao Li et al explained the main principle of the circuit is that the recaptured energy in the capacitor and the residual energy in the secondary are used to pre charge the primary inductor for the next cycle, which shortens the charging time, generates continuous current pulses, and improves the energy transfer efficiency.

In 2018, Falong Lu et al, Based on two high-temperature superconducting pulsed power transformers, a double-module pulse power supply is presented and the collaborative discharge of the two modules is discussed. Seven discharge modes are compared and four evaluation criterions are used to evaluate the output current of the seven discharge modes.

In 2018 Zhenmei Li et al, a mathematical model of electromagnetic launching system driven by multiple superconducting inductive pulsed PS modules is established. The fixed resistance and inductance load are replaced by the dynamic load model of the rail gun; the effects of dynamic load and fixed load on the discharge characteristics are analyzed; the parallel discharge characteristics of multiple high-temperature superconducting pulsed-power transformer (HTSPPT) modules are studied.

In 2018, Falong Lu et al, The influence of the mutual inductance between two modules on three discharge modes of the system is researched. Simulations and experiments on synchronous discharge, time-delay discharge, and asynchronous discharge are carried out, respectively. The results demonstrate that taking the mutual inductance into consideration, the amplitude and the pulse width of the output currents are both improved a lot, especially the obtainable energy of load is improved by nearly half.

In 2020, Andrey Ponomarev et al, A new approach to the construction of powerful power supplies with stable output voltage for pulsed power devices are proposed. The solution allows to almost completely eliminate the ripple of the power source output voltage and at the same time reduce the requirements for the capacitive filter. This additional power source replaces the function of the output capacitive filter with the value of capacity tending to infinity.

In 2020, Q.Wang et al, for a pulsed power system using capacitors as an energy storage unit, the performance of the capacitor charging power supply determines the stability of the output voltage. The series resonant power supply has inherent constant current charging characteristics, and the correctness of the theoretical analysis was verified by simulation calculation.

In 2021, Yuchen Wang et al, designs a series resonant high-voltage constant current power supply, which includes transformer design, main topology research and component selection and compared with other well-known topologies of charging power supply, the proposed full-bridge-based series resonant circuit allows the power supply to charge the load capacitance in constant current mode.

In 2021 Chan-Gi Cho et al, they proposed compact solid-state modulator for the generation of high-power electromagnetic (HPEM) pulses uses a lithium polymer battery as the input power source and was capable of achieving a 100-Hz pulse discharge rate with a peak voltage of 400 kV for 2 min with 200-A battery current. The resonant components are intentionally placed on the secondary side of the three-phase transformer, which was characterized by low current and high voltage conditions.

In 2022, Leming Zhou et al, an enhanced virtual synchronous generator (VSG) control with self-adaptive dynamic synchronous torque was proposed to suppress the low-frequency power oscillation by narrowing the acceleration gap between the diesel generator and the internal converters during the dynamic adjustment period. Then, the synchronous power supply for the three power supply channels is realized under high-energy pulse load conditions.

In 2022, Shanshan Jin et al, introduced high-voltage pulse current power supply (HV-PCPS) with an energy storage pulse transformer based on fly back topology of output microsecond pulse widths with high-power, ultrahigh voltage, and high reliability, which are suitable for most dielectric barrier discharge (DBD) plasma applications. A novel resistor–diode–diode (RDD) shaping method to solve the problem of poor quality of the output pulse power from the HV-PCPS, guaranteeing stable discharge for various DBD electrodes, it can also limit the maximum output voltage amplitude.

From the literature review, it is observed that the voltage fed series resonance pulse forming network techniques are widely utilized by many Industries & R & D units for optimal and efficient operation of HVHPPS. The real time pulse deformation and fault identification is essential to restore the HVHPPS condition. Many researchers have proposed various pulse shaping techniques for solving the impedance matching and pulse shaping problem in the literature. Moreover, an effective novel dynamic algorithm is required to attain an optimum solution. The following are the research gaps have been pinpointed as motivation of the dissertation.

- Majority of literature proposes conventional methods and component level optimization method and very few proposed pulse transformer based impedance matching techniques.
- Need an effective and universal solution that can work for both field and laboratory used for pulse shaping techniques.
- Most of researchers in the literature have not yet discussed the dynamic impedance matching of the designed HVHPPS and very few researchers have mentioned the pulse shaping method.
- Still today not yet framed a standard method for the calculation of Dynamic impedance matching in the literature.
- Still research is going on various type of HVHPPS but not even thought of dynamic impedance matching for universal power supply for such application.

1.5 Objective and organization of the thesis

The main objectives of the thesis are:

- To perform Mathematical Modelling and Analysis of High Voltage High Pulse Power Supply Performance on Various Loads.
- To design a Pulse Generator of 15 kV, 4-6 μs pulse width, 10-400 Hz Pulse Repetition Frequency (PRF).
- To Investigate on the Effect of Cable Length on Pulse Shape of High Voltage High Pulse Power Supply
- To develop experimentally a scaled down model to verify the Simulation results.
- To design and develop High Voltage High Pulse Power Supply Using FPGA for Dynamic Impedance Matching.

- To study Novel Techniques of Active Pulse Shaping of High Voltage High Pulse Power Supply on Klystron.
- Analytical Approach of Fault Diagnosis of High Voltage High Pulse Power Supply for High Power Klystron.

This chapter provides the introduction part, various types of pulse generators, applications, an in depth literature survey, research gap, need of improvement and the main objectives of the thesis.

Chapter 2

Modelling of Pulse Forming Network

2.1 Basic circuit for generating pulses

The pulse-forming network serves the dual purpose of precisely storing the amount of energy required for a single pulse and of releasing the energy into the load as a pulse of specified shape. Fundamentally a PFN is a lumped constant transmission line of L and C. Now look at the basic circuit for generating pulses of arbitrary shape as given in Fig 2.1 where capacitor C_N is pre-charged up to V_N.

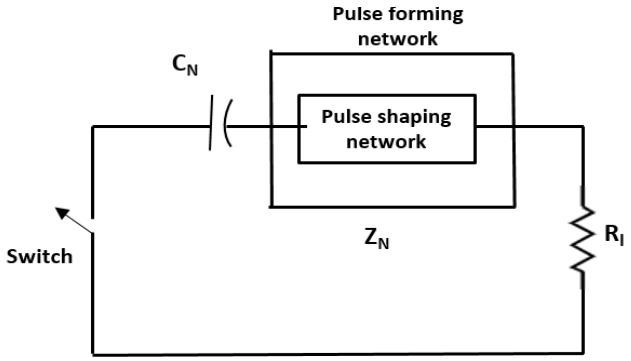

Fig 2.1. Basic circuit for generating pulses of arbitrary shape

From Laplace Transform, the current is given by

$$i(s) = \int_0^\infty i(t)e^{-st}dt \qquad \text{.....(1)}$$

Now apply the basic KVL equation in Laplace domain for the circuit, we get

$$(R_l + Z_{N(s)} + 1/C_N s)\, i(s) = Q_N/C_N s = V_N/s \qquad \text{.....(2)}$$

Where R_l=load resistance, Z_N=network impedance, C_N= network capacitance, Q_N=Initial charge on capacitor, V_N=Initial voltage on capacitor

Now rearranging equation (2),

$$Z_{N(s)} = \frac{V_N}{si(s)} - R_l - \frac{1}{C_N s} \qquad \text{..... (3)}$$

Let the current is specified as a rectangular pulse with amplitude I_l, duration τ, and that the load is a resistive one of value R_l. Then current i(s) is found from Eq.(1) to be-

$$i(s) = I_l/s\,(1-e^{-s\tau}) \qquad \text{.....(4)}$$

Substituting in Eq. (3), Z_N is obtained as-

$$Z_{N(s)} = \frac{sV_N}{sI_l(1-e^{-s\tau})} - R_l - 1/C_N s \qquad \text{.....(5)}$$

On rearranging,

$Z_{N(s)} + 1/C_N s = R_l\left[\frac{\left(\frac{V_N}{I_l R_l}-1\right)+e^{-s\tau}}{1-e^{-s\tau}}\right]$ ……..(6)

If the numerator and denominator are multiplied by, $e^{s\tau/2}$,

$Z_{N(s)} + 1/C_N s = R_l\left[\frac{\left(\frac{V_N}{I_l R_l}-1\right)e^{\frac{s\tau}{2}}+e^{\frac{-s\tau}{2}}}{e^{\frac{s\tau}{2}}-e^{\frac{-s\tau}{2}}}\right]$ …….....(7)

$= R_l\left[coth\frac{s\tau}{2} + \frac{\left(\frac{V_N}{I_l R_l}-2\right)e^{\frac{s\tau}{2}}}{e^{\frac{s\tau}{2}}-e^{\frac{-s\tau}{2}}}\right]$ ……..(8)

Choosing $V_N=2I_lR_l$, there is obtained

$Z_{N(s)} + 1/C_N s = R_l coth(s\tau/2)$ ……..(9)

The right-side member of Eq. (9) is seen as the impedance function of an open-circuited lossless transmission line of characteristic impedance $Z_0= R$, and transmission time $\delta= \tau/2$. Thus, in this case, either the pulse-shaping circuit plus the capacitance C_N must be an electrical proportional to the transmission line.

2.2 Pulses Generated by a Lossless Transmission Line

Since the microwave amplifiers for which most pulsers have been designed require the application of an essentially rectangular pulse, the lossless open-ended transmission line considered in the foregoing example may be taken as a starting point in the discussion as shown in the schematic diagram in Fig 2.2.

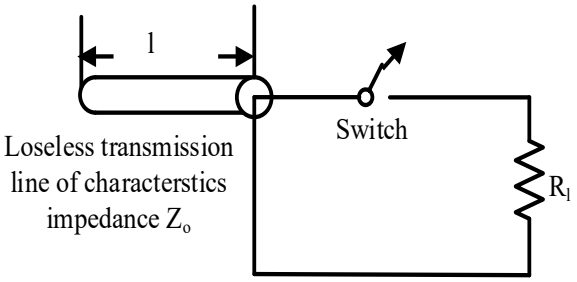

Fig 2.2. Schematic diagram for producing an ideal rectangular pulse

The a-c impedance, Z, of the transmission line, is given by elementary transmission line theory as: $Z=Z_0 cothjw\delta$, Its LT: $Z(s) = Z_0 coths\delta$.

The current transform is then:

$i(s) = \frac{V_0}{s}$ ……..(10)

$= \frac{V_0}{s(Z_0+R_l)}\frac{1-e^{-2s\delta}}{1+\frac{Z_0-R_l}{Z_0+R_l}e^{-2s\delta}}$ ……(11)

$$= \frac{V_0(1-e^{-2s\delta})}{s(Z_0+R_l)}\left[1 - \frac{Z_0-R_l}{Z_0+R_l}e^{-2s\delta} + \left(\frac{Z_0-R_l}{Z_0+R_l}\right)^2 e^{-4s\delta} - \cdots\right] \qquad \text{……..…..(12)}$$

Where V_0 is the initial voltage on the transmission line. The inverse transform gives the current as

$$i(t) = \frac{Vo}{Zo+R_l})\text{-}\frac{Zo-Rl}{Zo+Rl}[U(t-2\delta)\text{-}U(t-4\delta)]+\text{…….)} \qquad \text{..……(13)}$$

If $R_l = Z_0$, i.e. if the line impedance is matched to the load impedance, the current consists of a single rectangular pulse of amplitude $I_l = V_0/2Z_0$ and duration $\tau = 2\delta$. Current and voltage pulses for $R_l=Z_0$, $R_l=2Z_0$, and $R_l=1/2Z_0$ are shown in Fig 2.3.

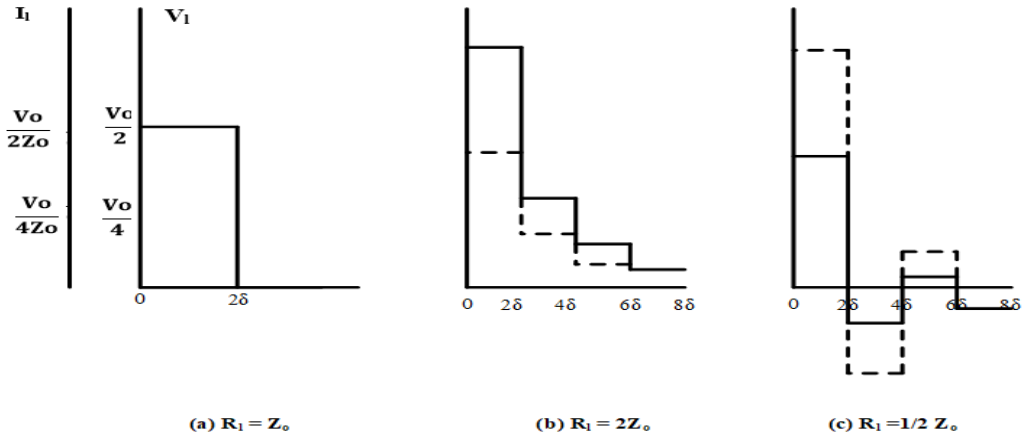

Fig 2.3.Discharging of Current (broken lines) and voltage (solid lines) pulses in a lossless transmission line to a resistance load

The effect of mismatching the load is to introduce a series of steps into the transient discharge. These steps are the majority of a similar sign when $R_l>Z_0$, and opposite in sign when $R_l<Z_0$. A transmission line having a single direction transmission time of δ produces a pulse of span 2δ; assuming a pulse of 1 microsecond term and a signal speed on the line of 500 ft/microsecond , a line of length = 500 x ½= 250 ft. is required. Clearly a high-voltage line or cable of this length would be unreasonable as a result of its extensive size and weight, and subsequently, that a substitute as a line-reproducing system is essential for any practical equipment.

2.3 Line simulating network

In line simulating network the transmission line is having lumped parameters. As the quantity of parameters is expanded, the degree of simulation will improve. The line simulating network appears as follows as in Fig 2.4.

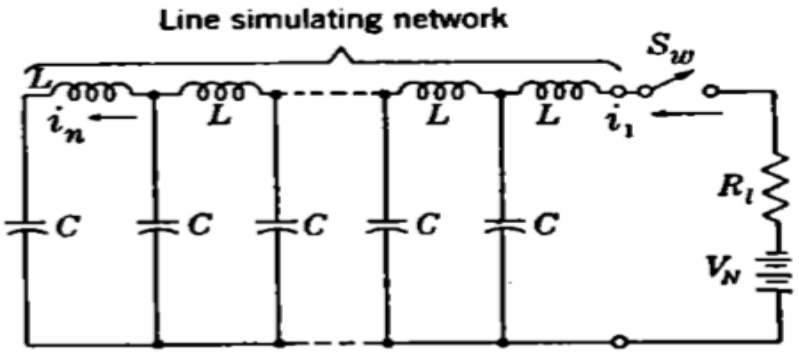

Fig 2.4. Line simulating network. Source:DSJ ,72(2),243-249,May 2022

Now look at current equation in Laplace domain:

$$\lim_{n\to\infty} i_l(s) = \frac{V_N}{2\sqrt{\frac{L_N}{C_N}}s}\left(1-e^{-2\sqrt{L_N C_N}s}\right) \qquad \text{……..(14)}$$

This is the Laplace transform for a rectangular current pulse of amplitude $V_N/(2\sqrt{L_N/C_N}$ and of duration $2\sqrt{L_N C_N}$ where L_N and C_N are the total inductance and capacitance of the network. In these kind of networks, pulses show overshoots and oscillations towards the start and end of the pulse. Since we don't utilize infinite sections, pulses display overshoots and oscillations. Fig 2.5. shows such an oscillation characteristics.

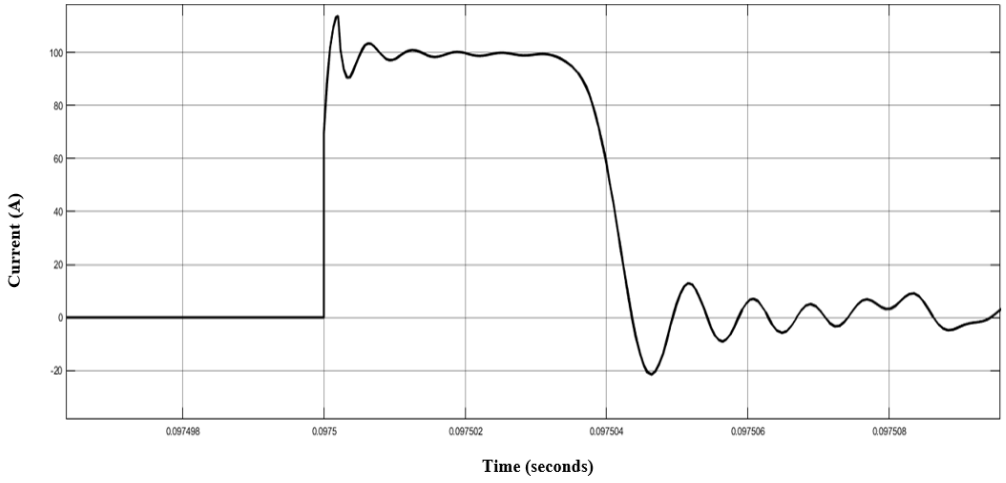

Fig 2.5.Oscillation of seven section network

Different techniques that reproduce a transmission line is acquired by expanding the transmission line as impedance and admittance functions in an infinite series of rational function. But they also display overshoots.

2.4 Guillemin's theory

Guillemin's precisely broke down these difficulties are a direct result of the attempt to deliver a discontinuous pulse by lumped network with infinite rate of rise and fall. Guillemin then concluded that it is hard to make such an ideal rectangular pulse by techniques for a lumped system if pulse is having infinite rise and fall. The theoretical pulse that is chosen should purposely have limited rise and fall times. The first Guillemin's network were designed dependent on a trapezoidal pulse shape having an rise time of generally 8% as in Fig 2.6.The method used by Guillemin's theory to structure of the PFN relies upon the Fourier series arrangement of the desired output pulse. Now take the case of trapezoidal pulse:

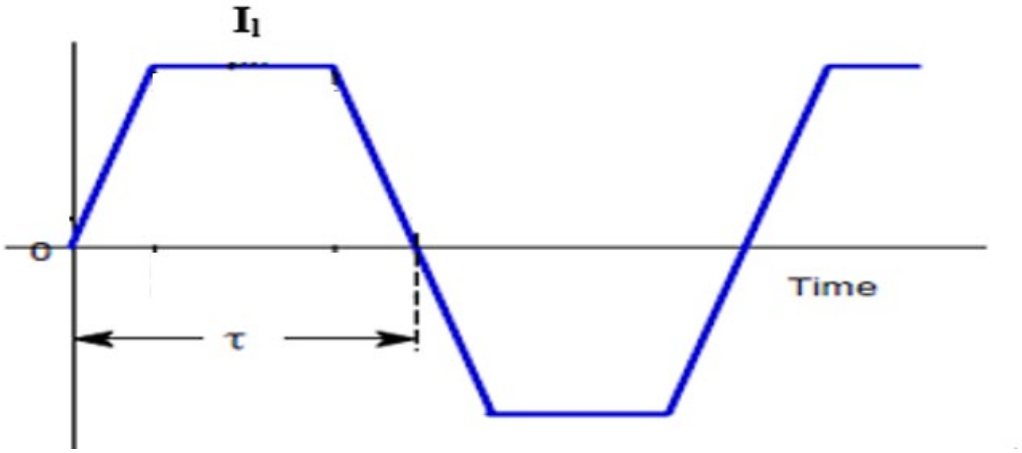

Fig 2.6. Trapezoidal alternating current wave

As i (t) is an odd function and we know from Fourier series that it contains only sine terms and there is no cosine and constant term. Then

$i(t) = I_l \sum_{n=1,2,3\ldots}^{\infty} b_n sin \frac{n\pi t}{\tau}$ ……..(15)

Here, I_l is the peak amplitude and τ is the pulse duration. Each term of the Fourier series represents a sine wave of amplitude b_n and frequency n/2τ. Now consider the LC loop for generating sine terms given in Fig 2.7.

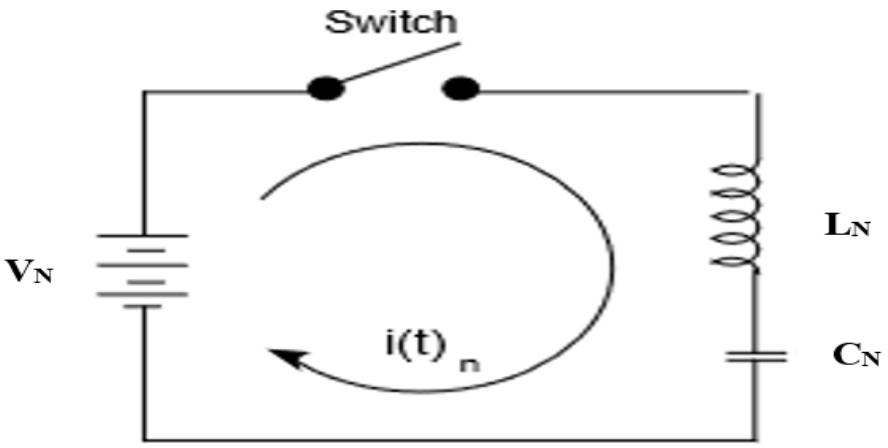

Fig 2.7.Circuit for generating a sinusoidal steady state current. Source:DSJ ,72(2),243-249,May 2022

Current produced by the circuit is:

$i(t)_n = \frac{V_N}{\sqrt{\frac{L_N}{C_N}}}\sin(\frac{t}{\sqrt{L_N C_N}})$ .....……(16)

$i(t)_n = \frac{V_N}{Z_N}\sin w_0 t$ ...……...(17)

Comparing the amplitude and frequency terms for the Fourier coefficients and the LC loop of eq.(15) and (16):

$I_l b_n \sin\frac{n\pi t}{\tau} = \frac{V_N}{\sqrt{\frac{L_N}{C_N}}}\sin(\frac{t}{\sqrt{L_N C_N}})$

$I_l bn = \frac{V_N}{\sqrt{\frac{L_N}{C_N}}}$ and $\frac{n\pi}{\tau} = \frac{1}{\sqrt{L_N C_N}}$

Solving for L_N and C_N:

$L_N = \frac{Z_N \tau}{n\pi b_n}$ where $Z_N = \frac{V_N}{I_l}$,$C_N = \frac{\tau b_n}{n\pi Z_N}$ …….(18)

The resultant network required to produce the given wave shape consists of a number of such resonant LC-sections in parallel, as shown below:

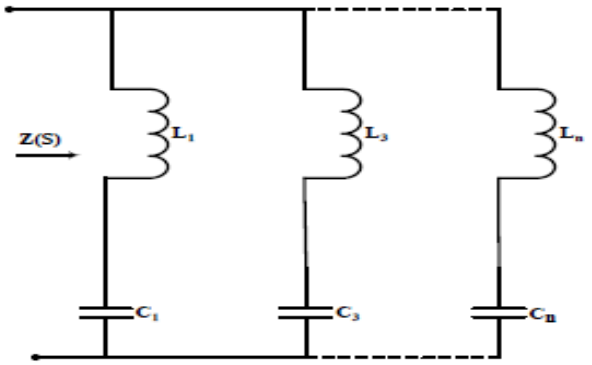

Fig 2 8. Type C PFN, Source: DSJ ,72(2),243-249,May 2022

Where $L_1, L_{2.....}, C_1, C_2$……are found out from equation(18)

Regardless, the issue of this circuit is that physical inductors have stray shunt capacitance which distorts the wave shape and values of capacitors, so the capacitor values have a wide range which increases cost and manufacturing labour. So distinctive networks are derived from this system having same impedance function.

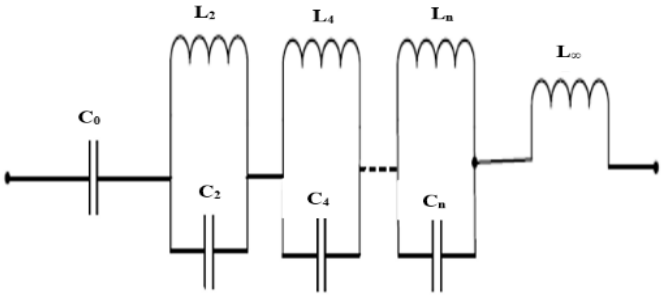

Fig 2.9. Type A PFN , Source:DSJ ,72(2),243-249,May 2022

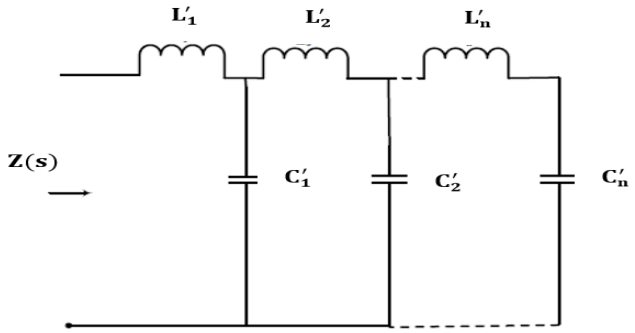

Fig 2.10. Type B PFN, Source:DSJ ,72(2),243-249,May 2022

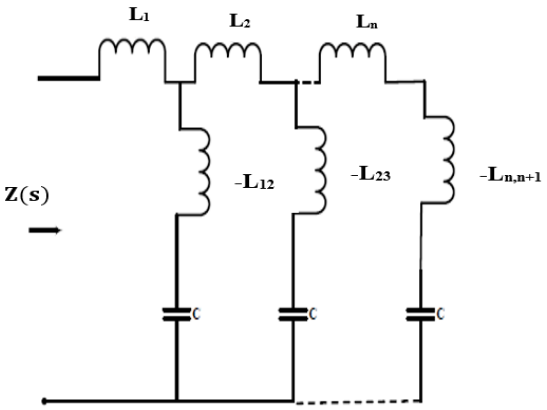

Fig 2.11. Type D PFN , Source:DSJ ,72(2),243-249,May 2022

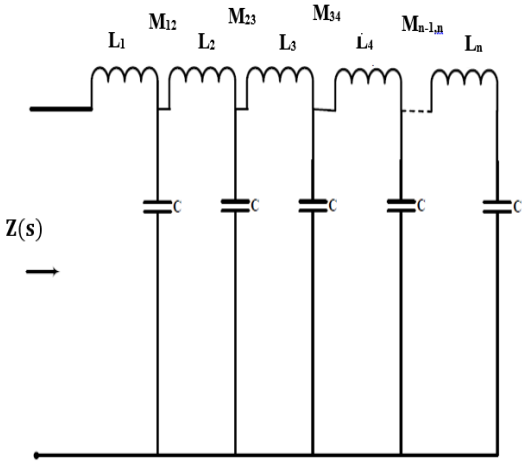

Fig 2.12: Type E PFN, Source:DSJ ,72(2),243-249,May 2022

Among them Type D is of significance as it has equal capacitances. The negative inductance in Type D is used to compensate for the increased capacitances from Type B. The negative inductance can be recognized in every way using mutual inductance concept. In Type E we will use a long solenoid and at suitable points tappings are taken out with the objective that the loop inductance is same as that in Type B. Type E having the best reaction with total inductance $\tau Z_N/2$ and total capacitance $\tau/2Z_N$ divided equally between all areas and each condenser is related with a tap on solenoid. The taps are arranged to get equal inductances for all segments aside from the ends which should have 20 to 30 percent more inductance and the shared inductance is 15-20% of self-inductance of each portion.

In this chapter Mathematical modeling of Pulse Forming Network of type E is generated for simplified transmission line and pulse formation generation discussed. The impedance mismatch basic reasons were generated and find out the effect of impedance mismatch. Here discussed about of pulse forming network and available configurations of lossless Transmission line.

Chapter 3

Charging & Discharging Circuit for Line Type Pulse Generator

3.1 Need of Charging Circuit

In line-type pulsers, all the energy stored in the pulse-forming network is typically dispersed during the pulse and it is important to energize the system during the interpulse interim. One of the significant considerations in the design of the circuit is that a same amount of energy must be stored in the system for each pulse. Another thought is that the charging component must isolate the power supply from the switch amid the pulse and for a brief span following the pulse. The charging component can be either a resistance or an inductance. A resistance in series with the energy-storage condenser of a voltage-fed network and the power supply is a straightforward technique yet the efficiency will be very poor. The utilization of an inductance as the charging component, however, makes it possible to structure the charging circuit for a high effectiveness and to get better isolation between the source power supply and the switch.

3.2 Assumptions made in the Charging Circuit

The following assumptions are made to study the behaviour of charging circuit:

1) The pulse-forming network is represented by the capacitance C, showing up between its terminals. The impact of the PFN inductances on the charging voltage wave can be dismissed.

2) The pulser switch is thought to be perfect—that is, its deionization is thought to be immediate after the discharge of the network and can be assumed as an open circuit.

3.3 Inductance Charging from a DC Power Supply

The proportional charging circuit can be represented by Fig 3.1. The differential condition for this circuit, as far as the momentary charge Q_N for the system, is

$$L_c\frac{d^2q_N}{dt^2} + R_c\frac{dq_N}{dt} + \frac{q_N}{C_N} = E_{bb} \quad \text{.....(19)}$$

where Rc is the resistance of the charging inductor and Ebb is the power supply voltage.

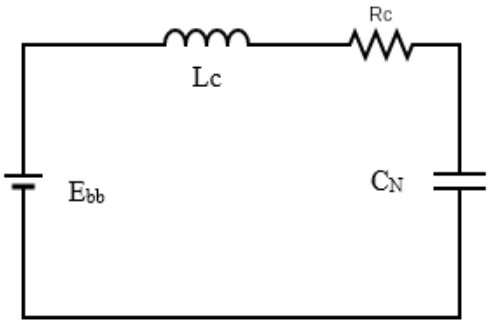

Fig 3.1: Equivalent charging circuit for a line type pulser

In the event that it is expected that there is an initial current $i_c(0)$ in the charging inductance L_c and an initial voltage $V_N(0)$ over the system capacitance C_N, considering the initial conditions on Eq. above are:

$q_N(0) = C_N V_N(0)$ and

$\frac{dq_N}{dt}(t=0) = i_c(0)$

Considering all these initial conditions, Eq.(19) leads to the following Laplace transform(L.T.) equation:

$$q_N(s) = \frac{E_{bb}}{L_c s}\frac{1}{s^2+\frac{R_c}{L_c}s+\frac{1}{L_c C_N}} + \; + \frac{i_c(0)}{s^2+\frac{R_c}{L_c}s+\frac{1}{L_c C_N}} \qquad \text{.....(20)}$$

Let $a=\frac{R_c}{2L_c}$; $\omega_0^2=\frac{1}{L_c C_N}$; $\omega^2= w_0^2 - a^2 = \frac{1}{L_c C_N} - \frac{R_c^2}{4L_c^2}$

Then eq.(20) becomes-

$$q_N(s) = C_N E_{bb}\left[\frac{1}{s} - \frac{(s+a)+a}{(s+a)^2+\omega^2}\right] + q_N(0)\frac{(s+a)+a}{(s+a)^2+\omega^2} + i_c(0)\frac{1}{(s+a)^2+\omega^2}. \qquad \text{.....(21)}$$

The time function is

$$q_N(t)=C_N E_{bb}\left[1 - e^{-at}\left(coswt + \frac{a}{w}sinwt\right)\right] + q_N(0)e^{-at}\left(coswt + \frac{a}{w}sinwt\right) +$$

$$i_c(0)e^{-at}\frac{sinwt}{w} \qquad \text{.....(22)}$$

Now the network voltage cam be expressed as

$$V_N(t) = \frac{q_{N(t)}}{C_N} = E_{bb} + e^{-at}\left\{[V_N(0) - E_{bb}]\left[coswt + \frac{a}{w}sinwt\right] + \frac{i_c(0)}{C_N w}sinwt\right\} \text{..(23)}$$

Now by differentiating eq (22) and simplifying, current can be expressed as

$$i_c(t) = e^{-at}\left\{\frac{E_{bb}-V_N(0)}{L_C}\frac{sinwt}{w} + i_c(0)\left[coswt - \frac{a}{w}sinwt\right]\right\} \qquad \text{.....(24)}$$

It is vital that the pulse shaping system be charged to a similar potential each time the switch closes if all the output pulses are to be of the equivalent amplitude.

Then $i_c(0) = i_c(T_r)$.From eq.(24)

$i_c(0) = i_c(T_r) = e^{-aT_r}\left[\frac{E_{bb}-V_N(0)}{L_C}\frac{sinwT_r}{w} + i_c(0)\left[coswT_r - \frac{a}{w}sinwT_r\right]\right]$ .....(25)

Solving eq.(25)

$i_c(0) = \frac{E_{bb}-V_N(0)}{L_C\omega}\frac{sinwT_r}{e^{aT_r}+\frac{a}{w}sinwT_r-coswT_r}$ .....(26)

Now the expression for network voltage $V_N(t)$ is obtained by putting Eq. (26) into Eq. (23):

$V_N(t)=E_{bb}+[E_{bb}-V_N(0)]e^{-at}$ .....(27)

The value of network voltage during discharge is given by

$V_N(T_r)=E_{bb}+[E_{bb}-V_N(0)]e^{-aT_r}$ ..... (28)

Now putting Eq. (26) in Eq. (24) current that charges the network is obtained as

$i_c(t) = \frac{E_{bb}-V_N(0)}{L_C\omega}e^{-at}$ .....(29)

If now the resistance R_c is neglected, then there are no network losses, a = 0, the equations (28) and (29) for voltage and current can be found as

$V_N(t)=E_{bb}+[E_{bb}-V_N(0)]\frac{sin\frac{2t-T_r}{2\sqrt{L_CC_N}}}{sin\frac{T_r}{2\sqrt{L_CC_N}}}$ .....(30)

And $i_c(t) = \frac{E_{bb}-V_N(0)}{\sqrt{\frac{L_C}{C_N}}}\frac{cos\frac{-2t+T_r}{2\sqrt{L_CC_N}}}{sin\frac{T_r}{2\sqrt{L_CC_N}}}$ .....(31)

The network voltage at the time of discharge given by Eq. (30) reduces to

$V_N(T_r) = 2E_{bb}-V_N(0)$ .....(32)

Resonant charging is utilized for this modulator. At the time switch is shut Lc and C_N will consolidate to form resonant circuit. The voltage on the system will be double the supply voltage till principle switch is turned ON. The case where $i_c(0) = O$ is designated “resonant charging" and corresponds to the initial zero of $sinwT_r$, as the argument increments, got when

$wT_r = \pi$ .....(33)

The estimation of inductance comparing to resonant charging is promptly found from Eq. (33),

$L_r = 1/\pi^2 f_r^2 C_N$ where $f_r = 1/T_r$ .....(34)

Since the resonant frequency of the circuit is given by $f_0 = \frac{1}{2\pi\sqrt{LcCn}}$

We can conclude that $f_r = 2f_0$

The waveform for voltage and current are shown in fig.3.2 below.

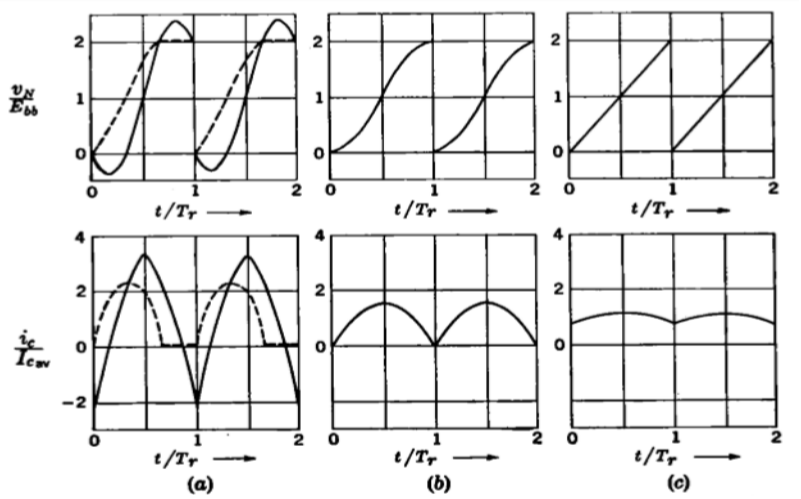

Fig 3.2:Charging voltage of current and voltage waveshapes (a)Lc<Lr (b) Lc=Lr (c)LC>Lr.The dotted line corresponds the use of a charging diode. Source: DSJ ,72(2),243-249,May 2022

For any estimation of inductance bigger than Lr, so-called “linear charging" results i.e. the voltage obtained for the system is as yet increasing at the time the pulser switch is closed. Care has to be taken to guarantee that the switch task is free from the unwanted time jitter, and that the current in the inductor is small enough to enable the switch to actually deionize. If the charging inductance is made smaller than that relating to resonant charging, the charging current i_c (0) is negative. Thus, extra misfortunes happen in the circuit, and the pulse shaping system must probably withstand a voltage higher than that at which the release of energy takes place. Advantages of resonant charging is that: 1) .The rate of change in the voltage is little in the area of most extreme value.2) Slow development of the voltage just after the pulse thus permitting a greater amount of time for the switch to deionize.

3.4 Basic discharging circuit

The discharging circuit incorporates Pulse Forming Network, switch and load, given in Fig 3.3. The PFN needs to create rectangular pulse output if it is connected through a switch to load, whose magnitude is equivalent to characteristic impedance of PFN. At whatever point the switch is closed the complete energy which was stored in PFN needs to release into load, for that the characteristic impedance of PFN ought to be equivalent to load impedance. This exchange of energy happens in between the interim $\tau = 2\delta$. But in practical cases 20% of mismatch is allowable for operation of Pulsers. This mismatch in impedances has little impact on releasing circuit. The energy discharged in load under matched conditions is equivalent to energy that is stored in PFN.

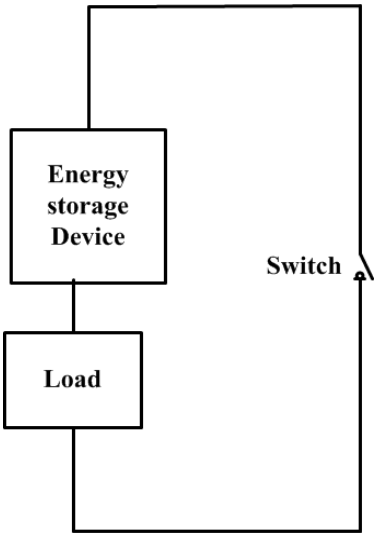

Fig 3.3: Basic Discharging Circuit of Pulser, Source: DSJ ,72(2),243-249,May 2022

The energy storage device that is used is a cascaded combination of L and C i.e. a pulse-forming network. Here as one can see, switch is a very important device as it is the one which initiates the discharge of the energy from the pulse-forming network to the load. So the proper selection of the switch is a very important task. Now there are few important things which are to be considered for selection of switches.

3.5 Conditions for choice of Switches

Switches are used to initiate discharge of PFN into load to get Pulsed output. So switch should be selected in such a way that it has following requirements:

- The switch should not conduct during the time when it is charging i.e. when the supply charges the pulse-forming network the switch should remain off till the PFN remain a particular voltage and a particular recurrence time.
- The switch should be able to close at a very fast speed and at predetermined times i.e. it should be able to close at a very high pulse recurrence frequency.
- The switch resistance has to be as small as possible during discharge of the pulse so that energy loss is as small as possible in the switch and most of the stored energy in the pulse-forming network is available at the output.
- As soon as the discharge of the pulse is ended the switch should regain its non-conducting state very fast.
- The switch should be able to carry high current during the pulse i.e.it should have high current carrying capability with minimum voltage drop across the switch.

3.6 Options available as switch for Pulse Generators

Different switching schemes which can be used in pulse generators is discussed below.

3.6.1 Vacuum tubes as switch

A customary way to deal with high voltage switching operation is to utilize a vacuum tube switch used as a series switch for pulse modulator. By this methodology, we can provide high voltage switching required to pulser however it has significant disadvantages as referenced underneath:

- The tube in vacuum tube as switch itself acts as current limiting. As a result of that pulse rise time is deteriorated.
- The second disadvantage is that there is huge amount of voltage drop all across the tube of the switch. Large voltage drops means a huge amount of power loss in the switch during the high current discharge of the pulse.

3.6.2 Thyratron as switch

Normally, the energy in the PFN is released into the load circuit by using a hydrogen thyratron or other quick closing switch. With this sort of switch is utilized when constant load impedance and pulse width is required. It has a few downsides:

- A thyratron can just fill in as a closing switch, and can't open during a pulse in case of an arc. This will lead to extra equipment for opening of switch which increase the cost which is also an important factor.
- The thyratron commonly used to drive a PFN has a limited lifetime, and must be replaced at normal interims. At high levels of operation, this can be a recognizable cost factor in the task of Pulser.

3.6.3 Solid State devices as Switch

Amid the most recent couple of years the interest for substitution of thyratrons and ignitrons has expanded steeply, and the innovation for solid state switches has improved definitely, particularly in the medium frequency range. The characteristic for this power device is long life time and having high stability. Pulse generator with solid state devices as switches

can deliver high repetition rate. Some of switching device utilized by pulsed power generators are SCRs, IGBTs and MOSFETs. The pulse can be produced by utilizing transistors and Silicon Controlled Rectifiers (SCRs) as switch yet their performance by and large is not as much as that obtained with a power MOSFET. The voltage levels can be increased by cascading a number of MOSFETS in series. Consequently, solid state devices, for example, power MOSFETs are turning the consideration of scientists towards the structure of new pulse generators of high speed with limited size and cost. With innovation progressions in the high voltage MOSFETs the conduction and exchanging misfortune are diminished which empowers high influence thickness and better effectiveness. Another preferred standpoint of utilizing MOSFET as switch is it's ON state resistance is less.

3.7 Klystron Load

Klystron is best RF source with frequency range higher than 3.0 GHz. Klystron has high gain of around 50 dB, Klystron is a voltage driven device and if applied voltage is stable, phase property is excellent. It is a matured device with its simplicity, availability and long life. It is a best device for average and peak power capability. Klystron consists of key components such as electron gun, RF cavity, drift tube, RF window, beam collector, focusing magnet, and cooling system. Electron is velocity modulated in the input cavity and forms bunch i.e. density modulation. Bunches are de-accelerated in the output cavity (beam energy to RF power) which is inverse process of accelerator (RF power to beam energy)

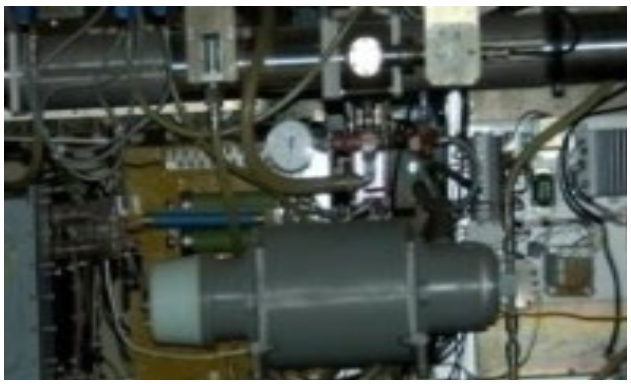

Fig 3.4. Photograph of Klystron based high voltage high pulse power supply (HVHPPS) Source: DRDO, MOD, India

3.7.1 Klystron basic operation:

Klystron characteristics is as follows,
Child's Law- In space charge limit current, emission current is,

$$I = P_r V^{3/2} \qquad (1)$$

Where P_r is Perveance, I is current and V is applied voltage

Then Power is,

$$P = I.V = P_r V^{5/2} \qquad (2)$$

Power's variation,

$$\frac{\delta P}{P} = \frac{2.5 P_r V^{3/2} \delta V}{P_r V^{5/2}} = \frac{5}{2}\frac{\delta V}{V} \quad (3)$$

Klystron's Impedance,

$$Z = \frac{V}{I} = \frac{V}{P_r V^{3/2}} = \frac{1}{P_r \sqrt{V}} \quad (4)$$

Therefore, Klystron's impedance varies with applied voltage.

This chapter gives the information about Charging circuit and discharging circuit for Line type Pulser, need of Charging Circuit, assumptions made in the charging circuit and Inductance charging from DC Power Supply, Conditions for choice of switches, Option available as switch for Pulse Generators, Klystron load and its operation.

Chapter 4

Simulation, Experimental Results and Analysis

Simulation studies have been done with following parameters: Single Phase AC Voltage Source with a peak voltage of 220V, 50Hz, Non-Linear Load as Diode Rectifier with R-Load with resistance, 12.5 Ω. The High Voltage High Power Pulse Generation Simulation Model is as shown in Fig.4.1.

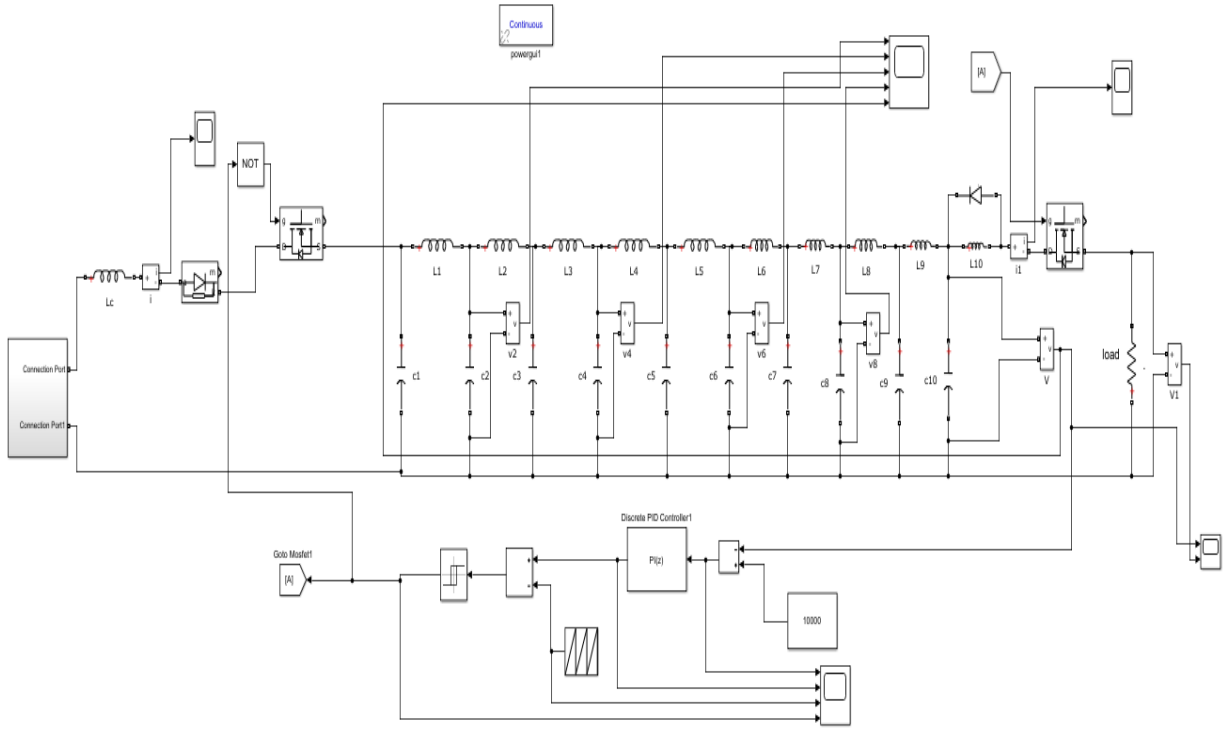

Fig 4.1. Simulation Model of High Voltage High Power Pulse Generation

4.1 Simulation Results And Analysis

Developed High Voltage High Pulse Power Supply tested with 12.5 Ω resistor connected through four RG8 (tri-axial) cables to match the transmission line impedance of 12.5Ω.The system is fed from Single Phase AC Voltage Source with a peak voltage of 220V, 50Hz frequency.

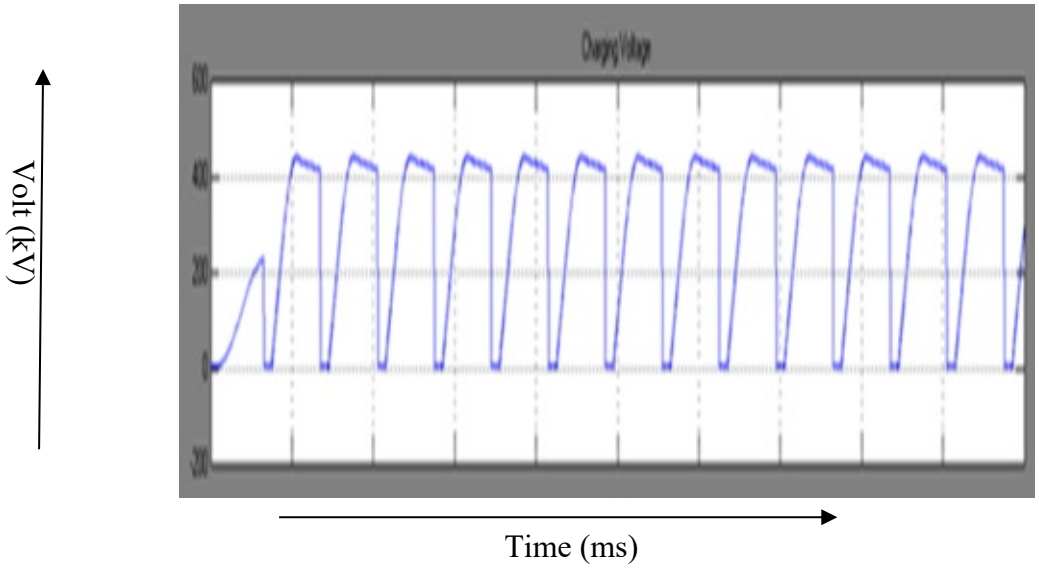

Fig 4.2. Charging Voltage waveform

Fig 4.2. shows charging voltage waveform shows the series resonance charging phenomenon between charging choke and the capacitor (lumped) of pulse forming network in order to verify the proper charging, a fast RC compensation network (1:4) is developed and ensured low side end of charging choke voltage is V and due to resonance, the capacitor of Pulse forming network it charge up to 2V.

Decreasing Quality (DeQ) trigger and Choke voltage waveforms are shown in Fig.4.3. Fast RC Compensation network sensed the extra charging voltage of choke. Then controller gives the trigger signal to DeQ switch to operate and dissipate the excess power across resistor network for pulse to pulse regulation to maintain constant charging voltage. Setting is done in such a way that maximum power dissipation should not exceed more than 25%.

During DeQ switching the charging voltage fall to zero, this can be seen in charging choke voltage waveform. If charging voltage is negative (between 5% -10%) due to mismatch between pulse forming network and dynamic load, then reverse diode protection scheme reduce the pulse repetition rate by 20%. Due to action of shunt diode protection circuit the reverse overvoltage at the main switch stack is tolerant. The developed high voltage high pulse power supply has high flexibility to reduce up to 50% of the output voltage with respect to the pulse width, the pulse reputation rate and voltage magnitude during reveres charging more the 25%.

Fig 4.4. shows the charging current and forward diode voltage. Charging current and time is sensed through 1Ω resistor assembly. The overcurrent protection circuit turns off EHT supply when output current rapidly increases due to arc. The charging time depends upon the inductor value as the inductance is high the time will increase but the peak current will reduce and vice

versa. The diode voltage which is used to protect the reverse flow of current from PFN to the supply side.

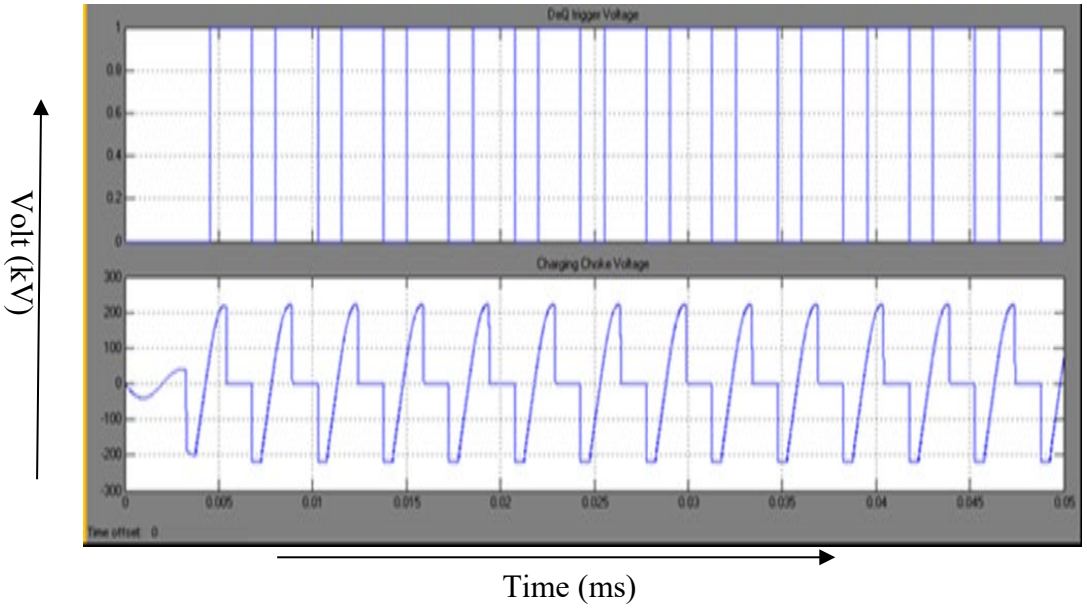

Fig 4.3. DeQ trigger pulse and Choke voltage

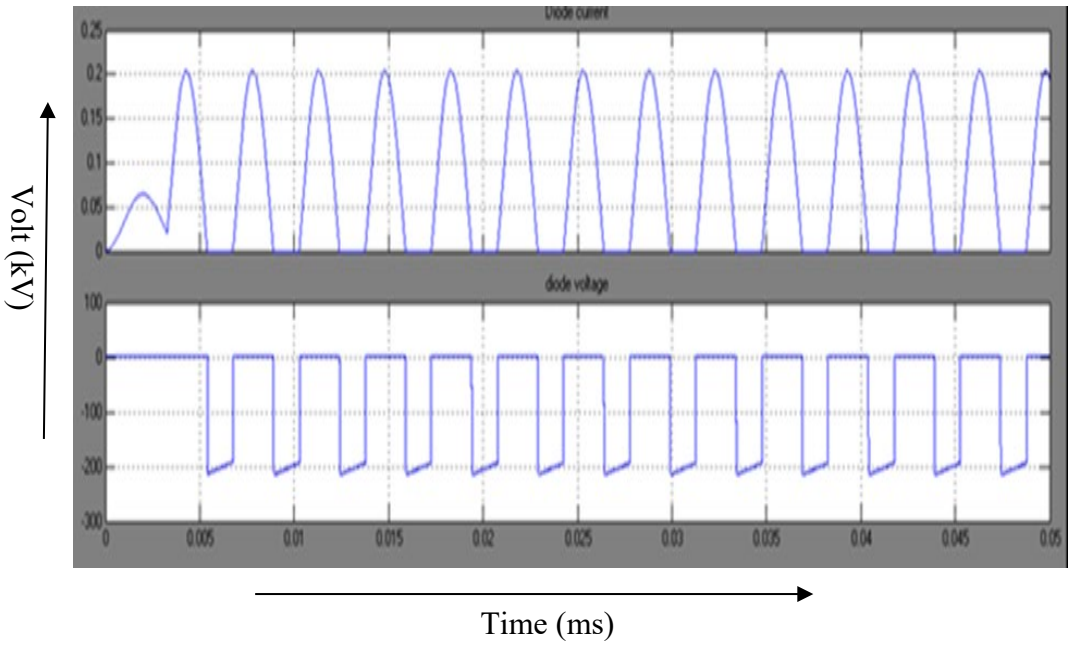

Fig 4.4. Charging current and forward diode voltages

Pulse Transformer is conventionally designed with bifilar winding. It is used to deliver a high voltage to the load and main switch stacks at low voltage. Six pieces of ferrite core are used in the pulse transformer. Fig 4.5. shows waveforms of output voltage at load.

To sense 35 kV a fast compensation network is designed. For a load resistance of 1.5 kΩ and a charging voltage of 3.2 kV, the resulting output pulse voltage is 1.6 kV. The rise time

of load voltage is approx. 100 ns (10%-90%), the initial peak of 5% is due to the first combination of L and C of pulse forming network. Second and third overshoot is due to mismatch of second and third combination of L and C of pulse forming network.

The initial few µsecond is required to settle down the initial mismatch of network and load. Rest of the pulse top is flat to make the total pulse width of 10 micro second. The replica of initial pulse forming network, performance is seen during fall time of pulse.

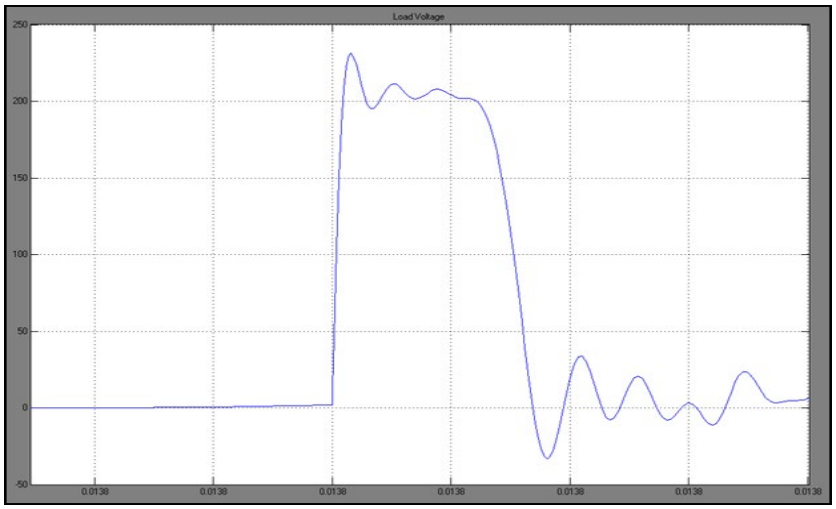

Fig 4.5 .Simulated Output voltage at load

It has been experimented that, the output voltage waveform at load will deteriorate with increase of transmission line length. To compensate this deterioration on output wave form, a compensation circuit is designed and put across the primary side of pulse transformer.

Fig.4.6. waveform shows that resistive load will have no impedance mismatch but R-L load will have heavy negative mismatch. To minimize the negative mismatch on active impedance change of pulse forming network is implemented.

The simulated results were verified on klystron based high voltage high pulse power supply, output performance of power supply is being seen through high voltage compensation network of 135 kV through klystron voltage .The klystron which is used here is of 6 MW peak power and duty of .001, pulse width of 6 µsec. The observed waveform of klystron current is shown in Fig 4.6.This waveform is almost perfectly matched and having no positive and negative mismatch.

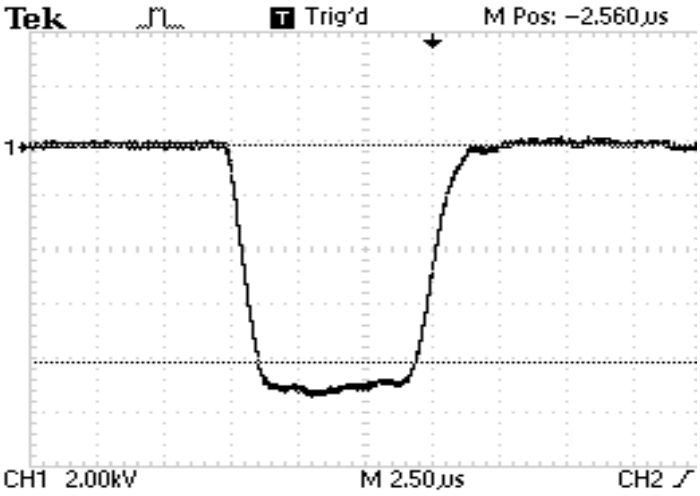

Fig 4.6. Klystron voltage waveform

4.2 DC power input for the system

Here, to obtain DC voltage a single phase full bridge diode rectifier is used. First the AC input voltage from the mains is stepped up using a step up transformer to the required level. Then the AC voltage from the secondary of transformer is applied as input to the rectifier.

DC voltage obtained from the rectifier has some ripples which is removed using a suitable value of RC circuit as discussed in chapter 5 section 5.5. The rectifier with filter is as shown in Fig 4.7.

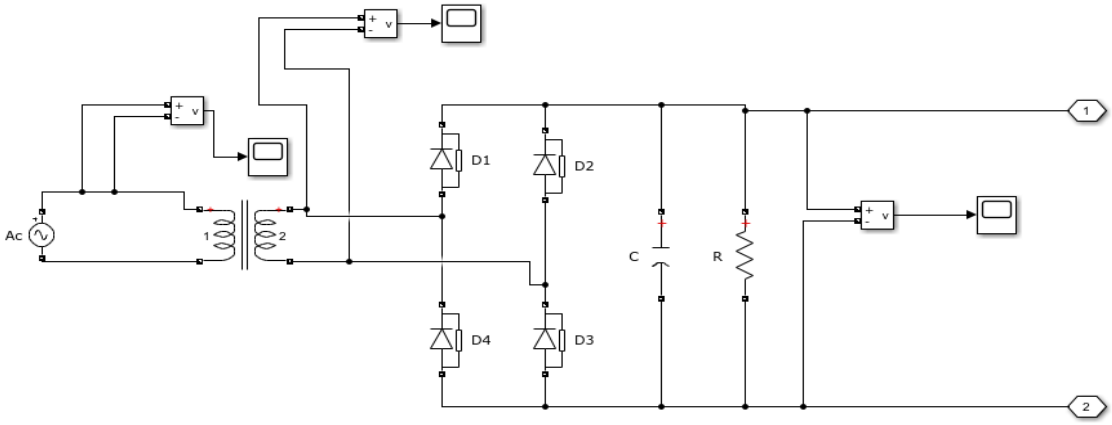

Fig 4.7. 1-Ø Diode full bridge rectifier with capacitive Filter

4.2.1 Input Voltage at the primary of transformer

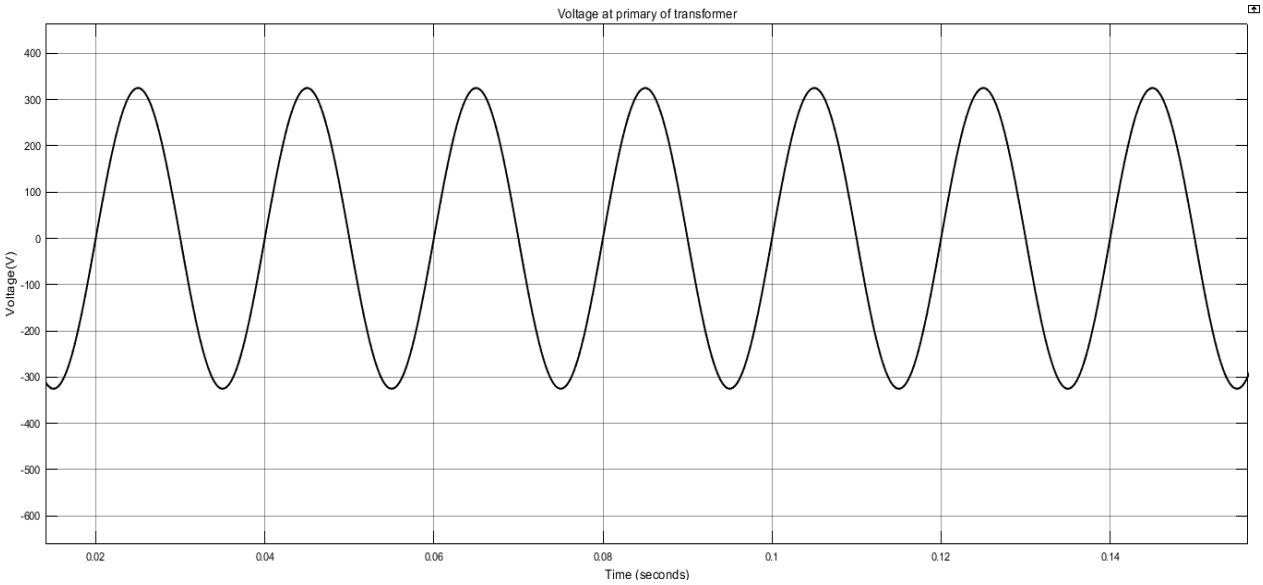

Fig 4.8. Voltage waveform at the primary of transformer

4.2.2. Output Voltage at the secondary of transformer

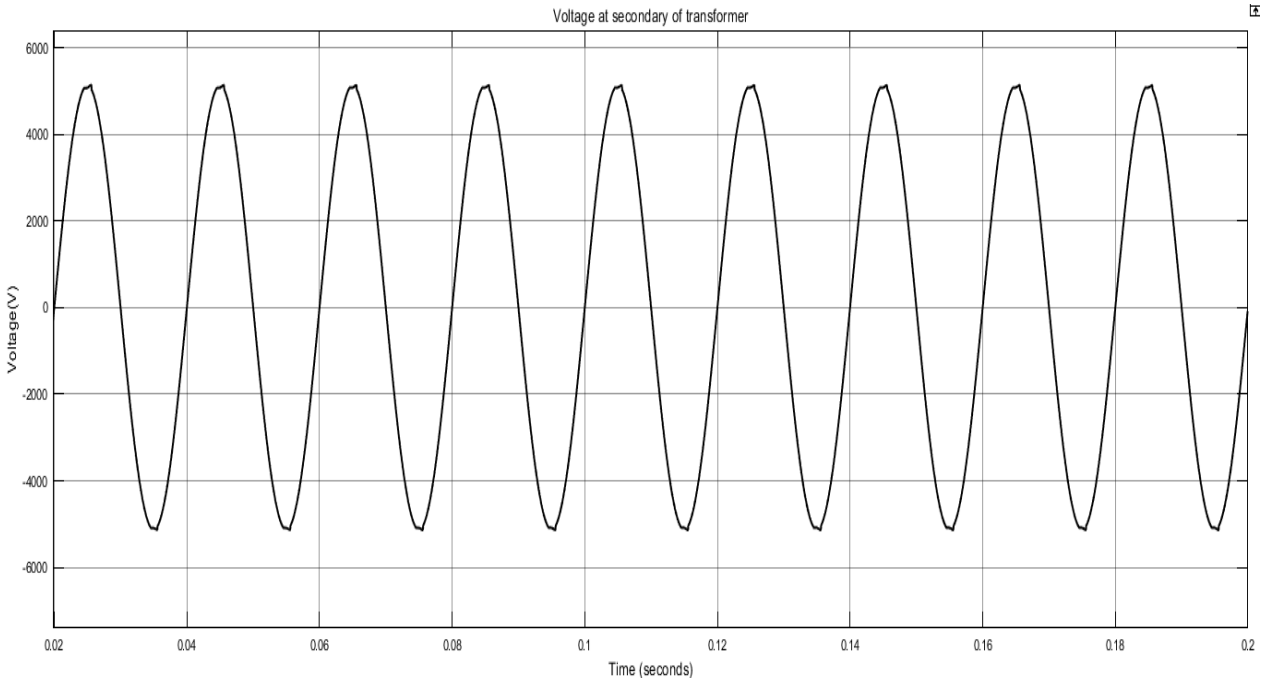

Fig 4.9. Voltage waveform at the secondary of transformer

4.2.3. Rectified Output voltage from diode bridge rectifier

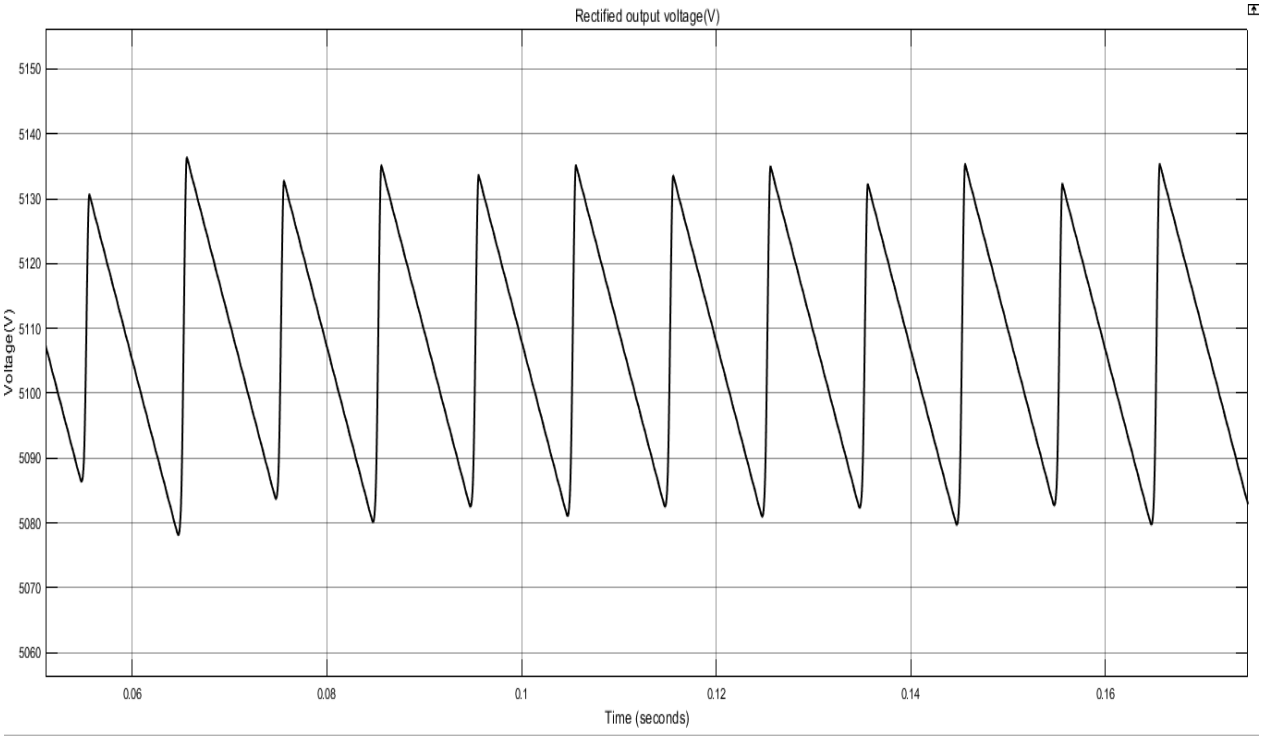

Fig 4.10. Output Voltage waveform from Rectifier with filter

4.3 Type E Guillemin PFN Network

PFN is a cascaded combination of inductors and capacitors which is used to store and release the energy to get the required pulse. Now there are various ways to connect them. Here, a PFN of type E is used with number of sections equal to n=10, given in Fig 4.11. In this PFN all section inductors and capacitors have same values. The values of inductors and capacitors obtained from theoretical calculations provided in chapter 7.

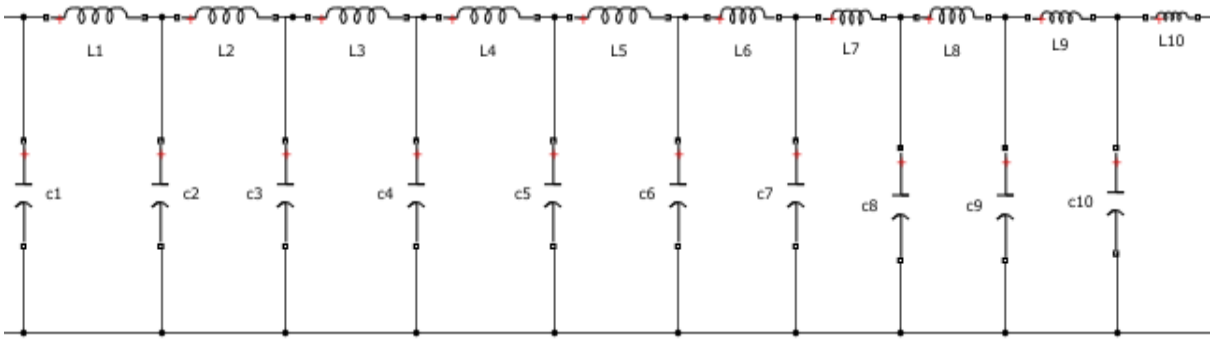

Fig 4.11. Ten section PFN

4.4 Charging circuit for PFN Network

The charging circuit consist of mainly the source, charging inductor and PFN. The charging inductor is used so that the PFN reaches the twice of the source voltage when MOSFET-1 is on. The charging is shown below in Fig.4.12. As soon as the PFN reaches to twice the source voltage, here in this case of 10kV, it discharges to the load by switching on the MOSFET-2 in the time period of 0.625 msec (i.e. 1/Ts= Fs= 1.6kHz).

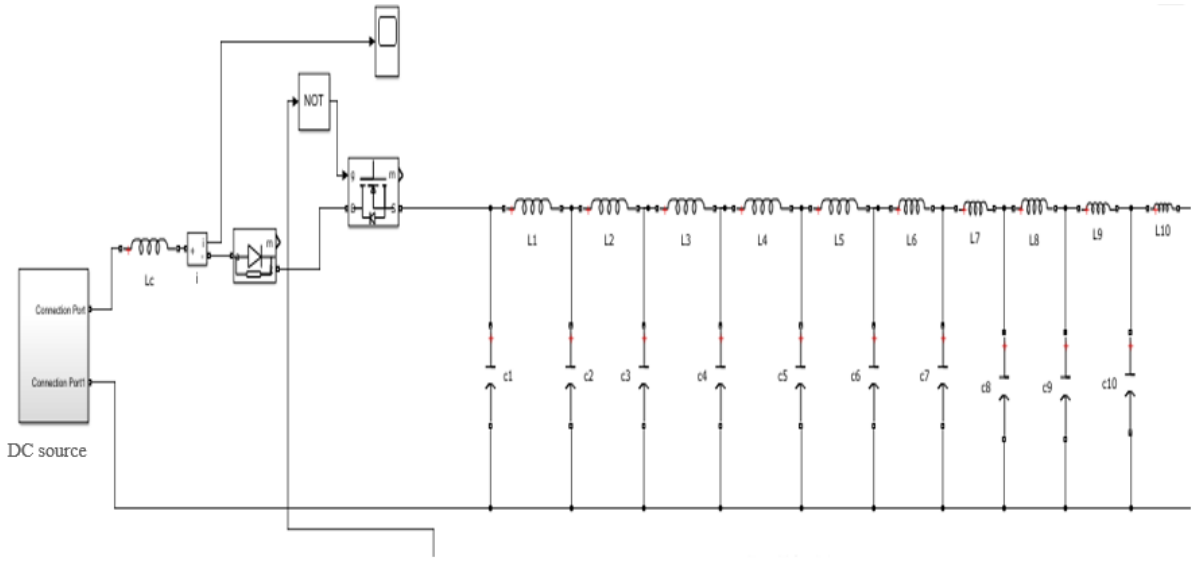

Fig 4.12. Charging circuit of PFN

4.4.1. Current waveform in the charging inductor

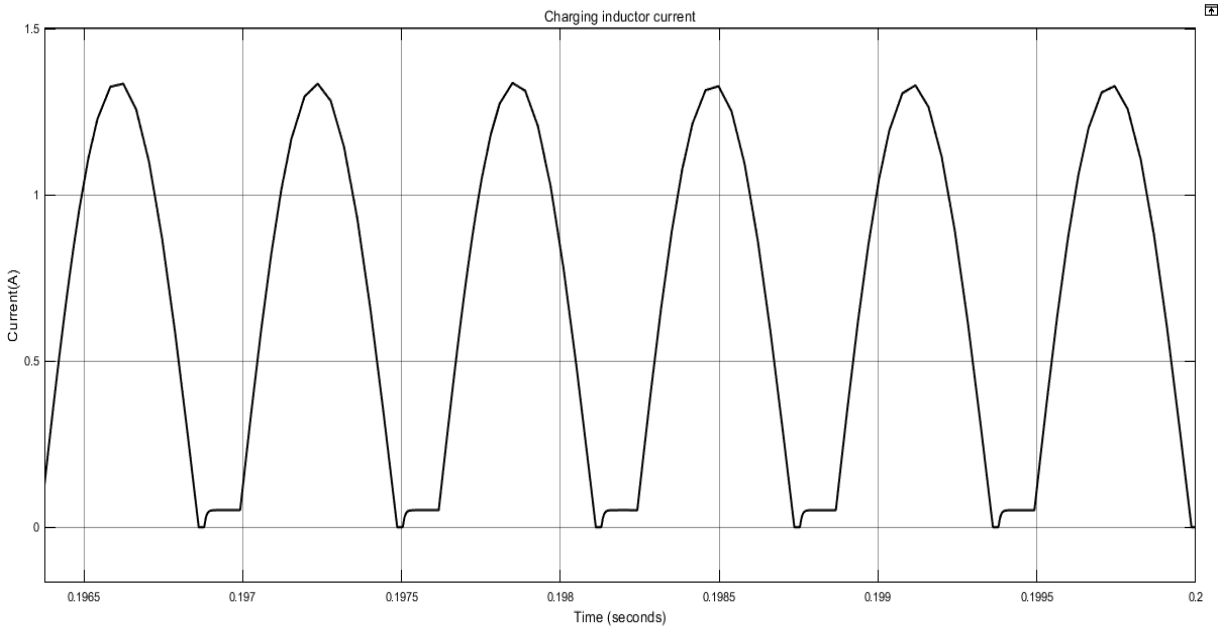

Fig 4.13. Charging inductor current waveform

4.5 Controlling technique for Switch

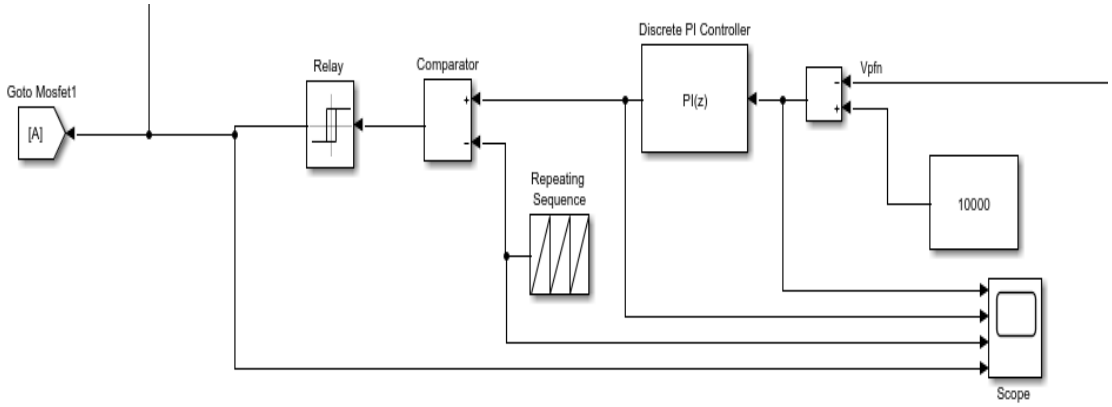

Fig 4.14. Voltage mode control by using PI controller for switching MOSFET

Here voltage mode control technique implemented by PI controller is used for generating ON and OFF pulses to MOSFET and its equivalent circuit is shown in Fig.4.14.The PI controller generates control signal which is compared with saw tooth signal as shown in Fig 4.15. The switching pulses generated from the comparator are given to MOSFET. The Kp and Ki values are set by trial and error tuning method. In the present design Kp= 0.00003, Ki= 0.00002.

4.5.1. Controlling circuit waveforms

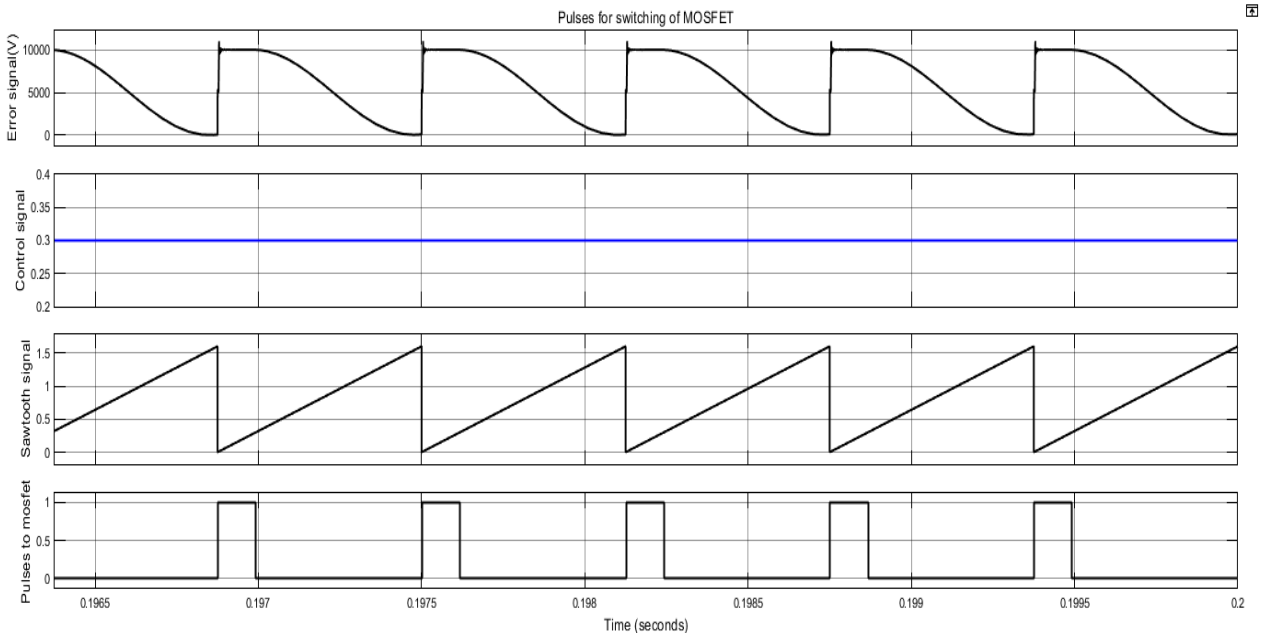

Fig 4.15. Waveforms obtained from the controlling circuit

4.5.2. Discharge of PFN capacitors

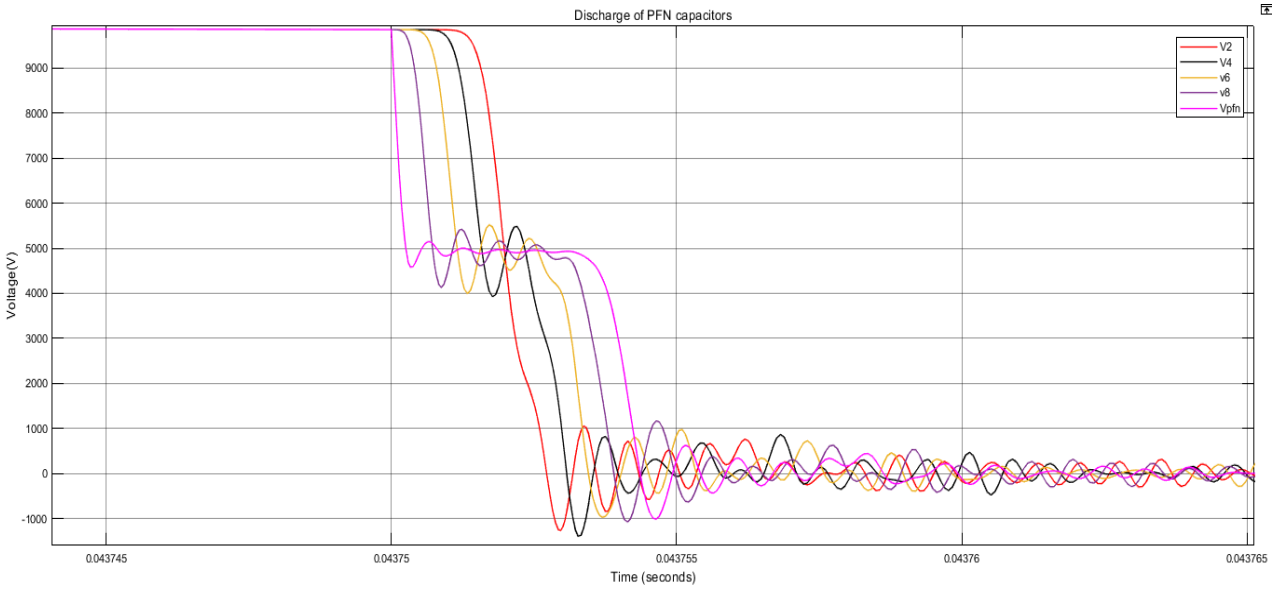

Fig 4.16. Voltage across PFN capacitors

As soon as the MOSFET at the load side is turned on PFN starts discharging as one can see in Fig.4.16. First the PFN capacitor near the load starts the discharging process. Then step by step other capacitors also starts the discharging process so that the voltage is maintained at the capacitor near the load is maintained constant for duration which is equal to the pulse width required at the output pulse.

4.6 Output Pulses from SIMULINK

The output pulses of current and voltage at the load side for the proposed system is shown below. The output pulses are rectangular type with required 4µs of pulse width and 1.6 kHz of pulse recurrence frequency.

4.6.1. Pulsed output current

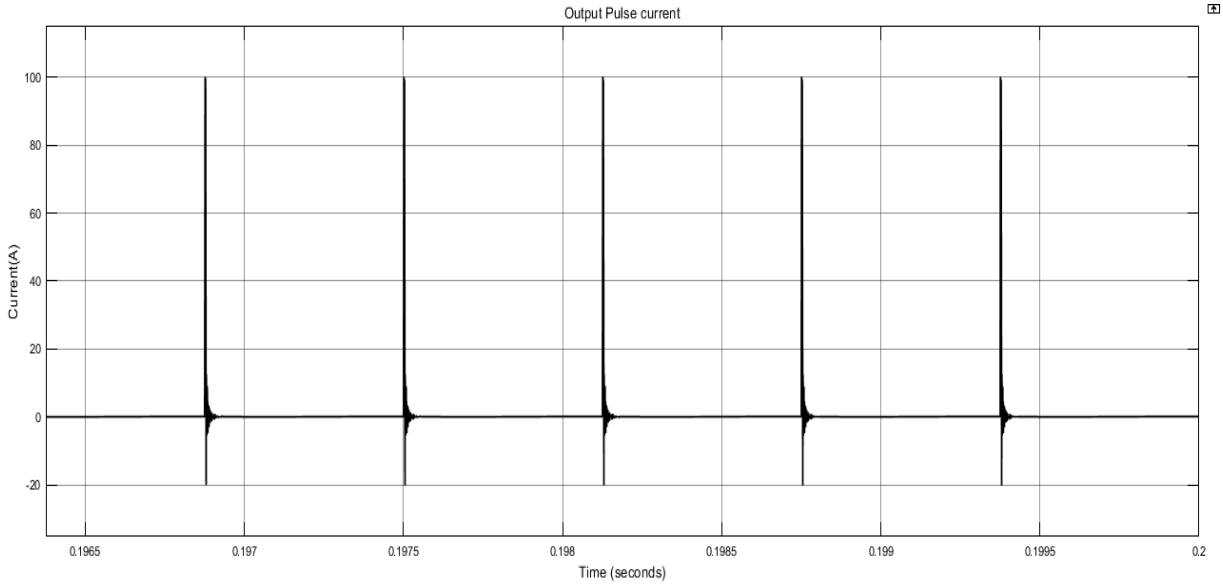

Fig 4.17. Output current waveform

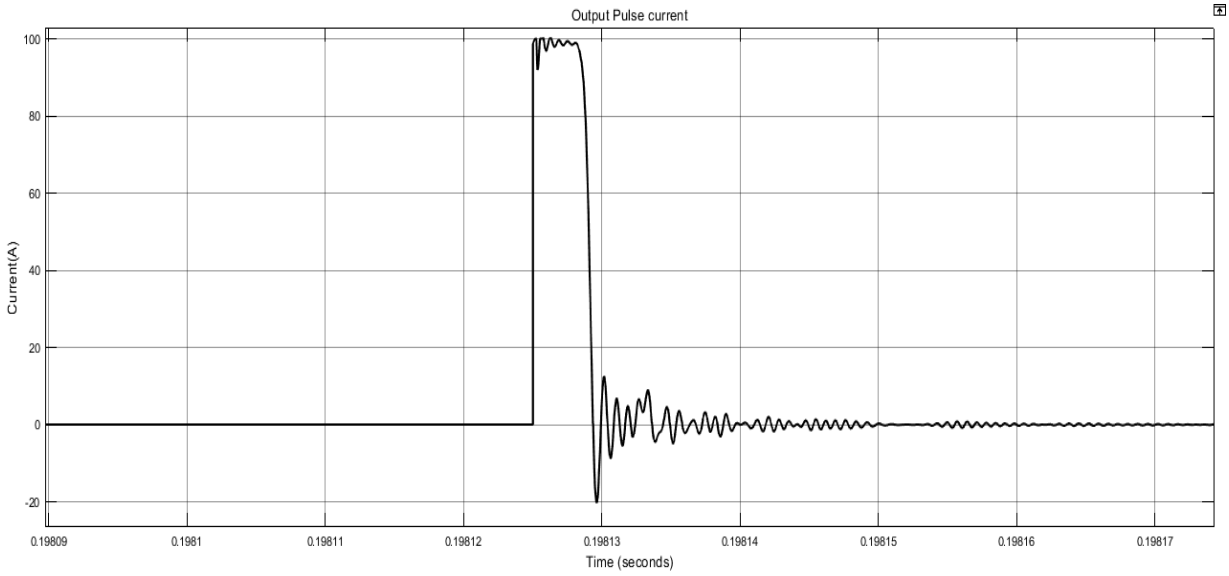

Fig 4.18. Output current waveform (one pulse)

4.6.2. PFN voltage and pulsed output voltage

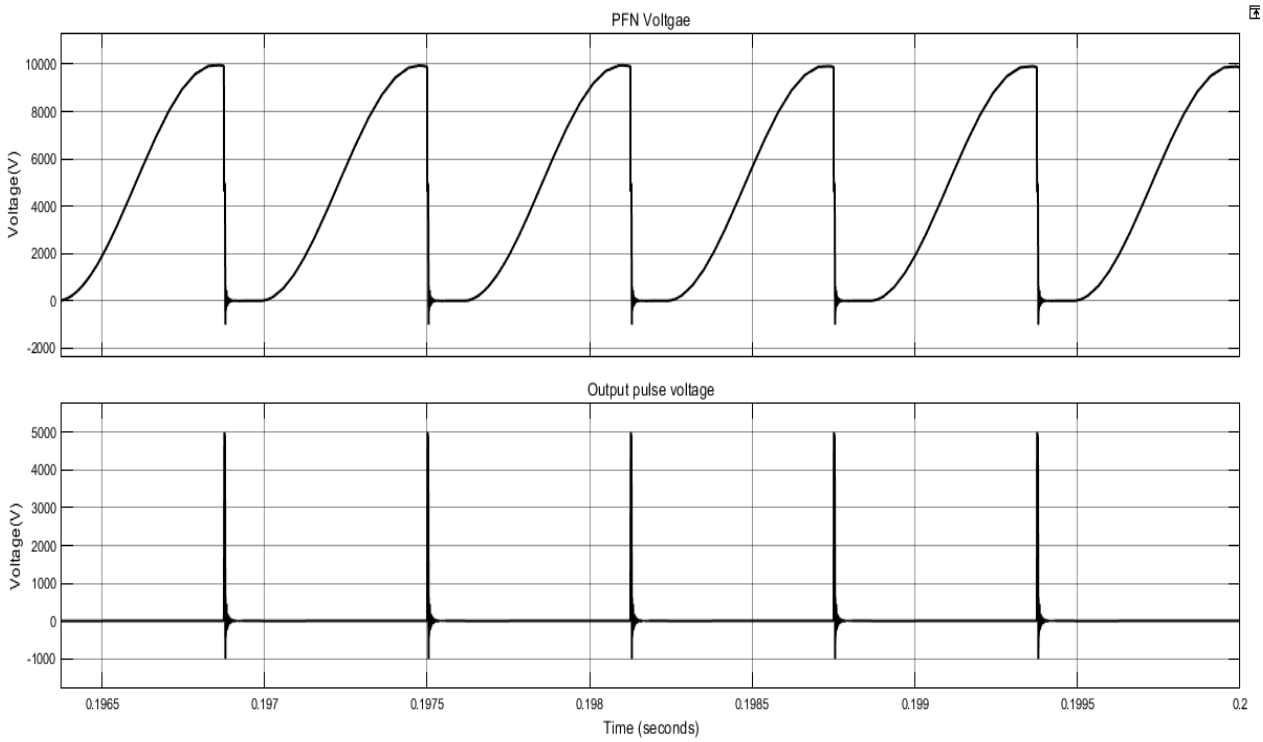

Fig 4.19. PFN voltage and output voltage waveform

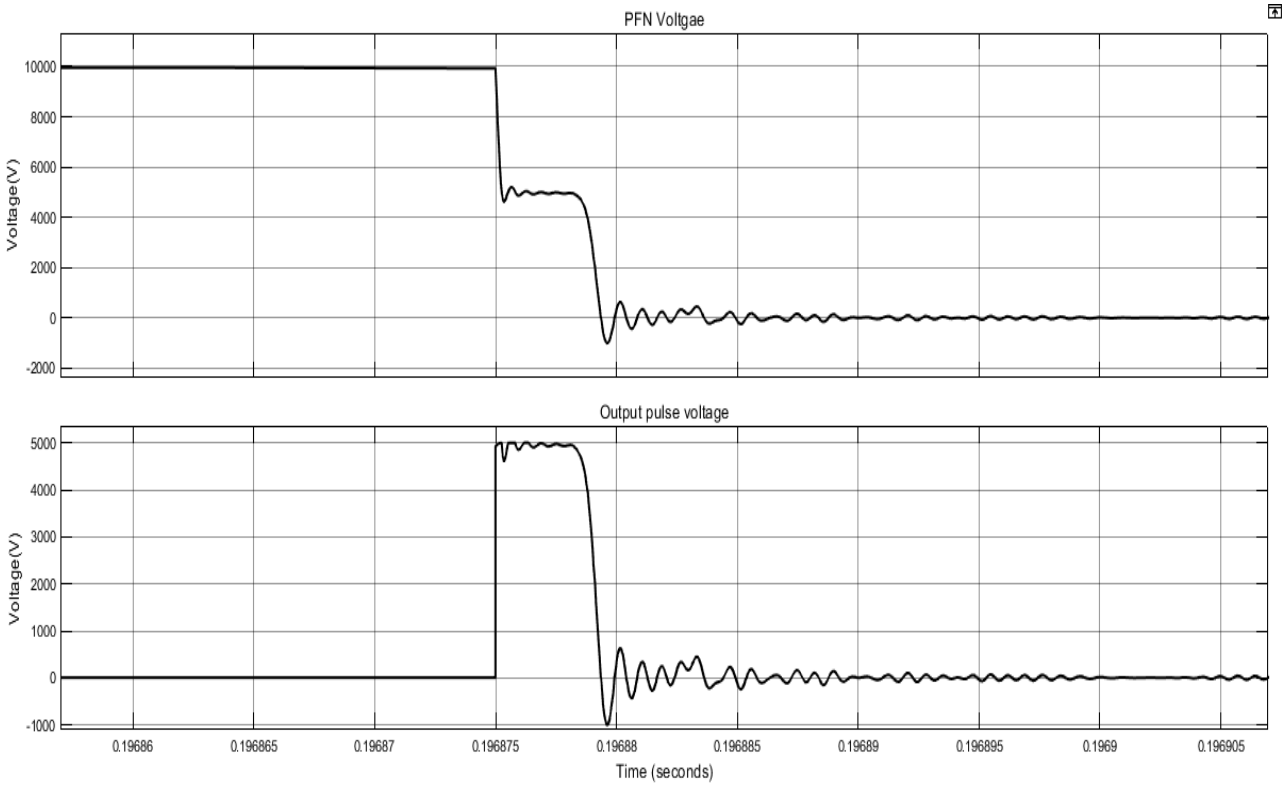

Fig 4.20. PFN voltage and output voltage waveform (one pulse)

4.7 FPGA Controller

FPGA stands for field programmable gate arrays. FPGA is basically an integrated circuit which is configurable i.e. programmable. Programmable components of FPGA are logic blocks and the interconnects i.e., interconnection between the logic blocks. The term field stands for programmable on the field i.e. the device function can be modified or configured or programmed in the lab or at the site where the device is installed. Advantages of FPGA are: They are inexpensive, easy realization of logic networks in hardware. So it is as simple as a software. Hardware of FPGA contains programmable logic devices (PLD), logic gates, RAM, and others such as DCM i.e. the clock manager and so on. FPGA contains a layout of a unit which is repeated in matrix form. The user can configure the function the each logic block, the input-output connects, the input-output ports and the interconnections between the logic blocks and input-output.

FPGA controller here of importance because they are used to provide gate pulses for switching the MOSFET. The gate pulse of required width which is found from simulation is developed using this FPGA controller. Here a low cost and compact high-speed digital controller of Atlys-Spartan 6 LX45 FPGA processor is used for generating the gate pulses for switching the MOSFET at a high frequency. Here the recurrence frequency used is of 1.6 kHz.

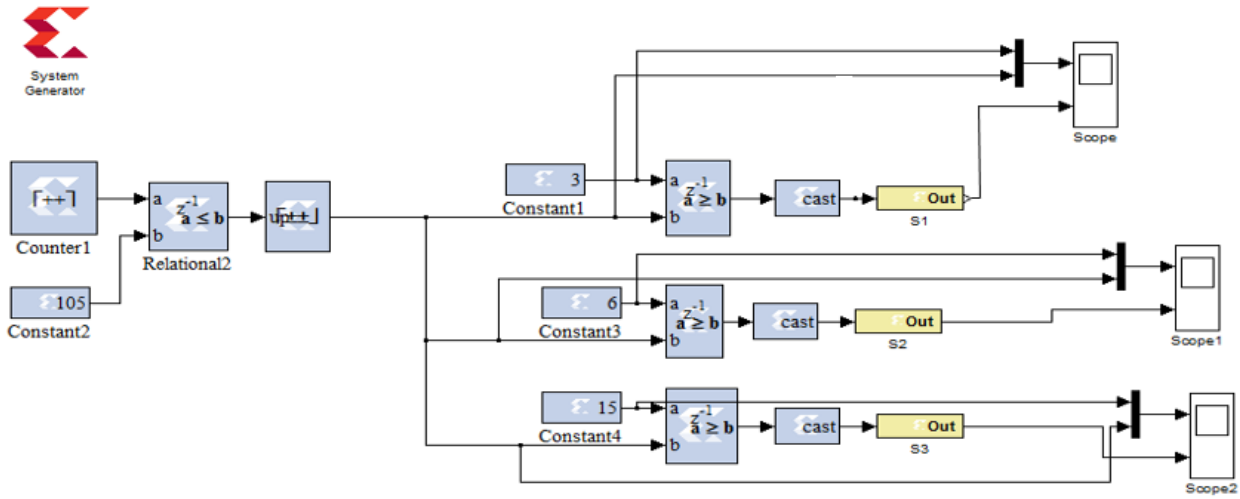

Fig 4.21. Simulink model to generate required pulses using FPGA

To develop the pulses of required width, the control scheme is developed in MATLAB simulation environment using Xilinx blocks which shown in Fig.4.21. The counter block generates either saw-tooth or triangular waveforms by either using up or up–down operational mode. The expression for selecting count value is shown in Eq.35 below:

$$\text{Count value} = \frac{f_{clcok}}{f_{desired} \times explicitperiod} \qquad \text{……..…(35)}$$

But the count value is limited by the number of bits with the relation 2^{nbits}> count value. For example, if the count value is 210, then the minimum number of bits selected should be 8. The explicit period normally is very small. The count value for 1.6 kHz frequency of saw tooth waveform generation with explicit value of approximately 10^{-6} is around 210. The clock frequency is made 1 to using system generator to match MATLAB simulation period. Saw tooth waveform obtained from the up counter block is of discrete type. Now a constant value of half of the count value is compared to the saw tooth waveform so as to get a 50% duty cycle of rectangular wave. Now it is applied to the up-down counter for which the signal increases linearly for high value and decreases linearly for low value. So from this up-down counter block a triangular signal is obtained. Now again this is compared with a constant value selected based on requiring the percentage of duty cycle to get the required gate pulse. The gateway out is used to assign proper I/O as per the pin assignment given in Atlys Spartan 6 user's manual. The developed model is converted into VHDL code using system generator and further programmed into the FPGA board via SPI programmable interface using ISE design suite.

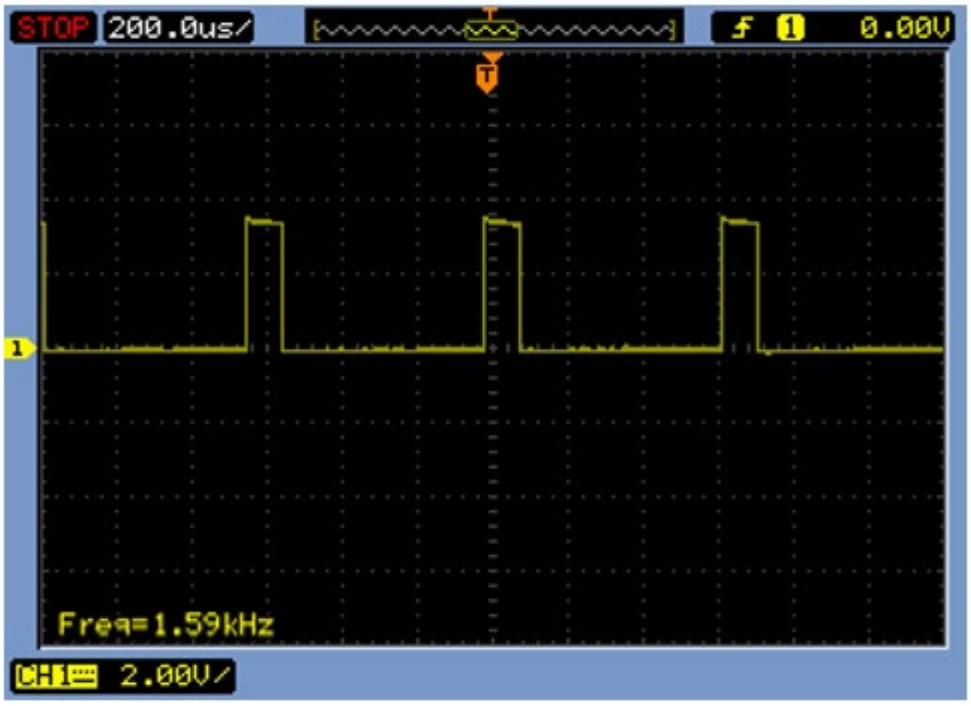

Fig 4.22. Gate pulses to the MOSFET

In this chapter Simulation model of overall subsystem generated. And simulated results analysis carried out along with FPGA based control and switching mechanism.

Chapter5

Design & Development of High Voltage High Pulse Power Supply

5.1 Design of Pulse Power Generation system

5.1.1 Design of Pulse Forming Network

The pulse power supply is designed for the below specifications:

Table 5.1. Specifications of pulse generation system

Parameter	Value	Unit
Load voltage	15	k Volt
Load Current	10	Amp
Pulse width	6	μ sec
Pulse repetition frequency	10-400	Hz

Assumed that the resistive load of 1.5 kΩ (approx.) and pulse power generating voltage of 15 kV.

Then, Pulse Current $=\frac{1.5x10^3}{1.5x10^3}$ = 10 amp. (Peak)

Let us take ratio of pulse transformer impedance = 1:11

Primary side impedance = $\frac{15x10^2}{N^2} = \frac{15x100}{11x11}$ = 12.5Ω

Primary side of pulse transformer impedance = 12.5Ω

The tri axial cable (RG-8) which is available of 50 Ω each impedance of cable.

Thus for maximum power transfer the transmission line impedance must be 12.5Ω, to match this we have to use 4 cable in parallel.

So that, Transmission line impedance = $\frac{50}{4}$ = 12.5Ω

The requisite pulse width for load is assumed is six microsecond for simplicity

Thus, PFN is designed for six μ second pulse width.

Total capacitance of PFN is = $\frac{t_p}{2Z_0}$

Where, t_p = pulse width

Z_0 = characteristic impedance of PFN and transmission line achieved for dynamic load,

because $C_n = \frac{t_p}{2Z_0}$

$C_n = \frac{6x10^{-6}}{2x12.5} = 0.24$ μF

To compensate for the loss in the pulse transformer the value of pulse transforming network capacitance is slightly increase.

The nearest available capacitor is 0.047 μ F.

To achieve the capacitor value in C_n to 0.24, we have use six capacitor for pulse forming.

Thus, Total capacitance C_n = 0.047 x 6 = 0.282 μ F.

The final output voltage across dynamic load is 15 kV and pulse transformer is having turn ratio of 1:11

So, primary voltage is $\frac{E_2}{E_1} = \frac{N_2}{N_1}$

$E_2 = \frac{N_2}{N_1}$ x E_1

$E_1 = 1363\ K\upsilon \approx 1.3\ K\upsilon$

The nearest available capacitor voltage is 1.5 kV.

Capacitor required have specification is as followed

Operating capacitor voltage = 1.5x2 = 3 kV

Capacitor value = 0.047 μ F

No. of capacitor = 6

We knew

Z_0 = characteristic impedance = $\sqrt{\frac{L_n}{C_n}}$

$L_n = Z_0^2$ x $C_n = 12.5^2$ x 0.28 x 10^{-6}, $L_n = 43.75\mu H$

The impedance of air wound can be represented as L = $\frac{0.2\times A^2\times N^2}{(3A\div 9B)}$

Where

L = Inductance in μ H

A = Mean diameter of the coil in inch

B = Length of the coil in inches

N = number of turns

We can make a coil made from copper tube of diameter 6 mm whose dimension will be:

Mean diameter A = 2.75 inches

Number of turns N = 82

So the length of coil B will = 24.5 inches

This gives the require inductance of 43.73 μ H

To provide 15 KV pulse, we have to charge the capacitor up to 2 kV approximate

A capacitor value of 0.047 μ F, Inductance of PFN is 43.75 μ H.

5.1.2 Charging choke

Higher the inductor of the charging choke better the isolation from switching device from the EHT side, but it will slower the rate of charging of Pulse forming network.

Thus,

The compromise is made between charging time and isolation. Smaller charging time also increase the peak charging current in charging diode.

The maximum Pulse Repetition Frequency at which we are going to operate the pulse power generation is 200 pulses per second.

So, the quiescent duration between the two pulses for main switching device = $\frac{1}{200}$ S = 5ms

Thus, we can take charging time as 1.5 msec. This charging time is actually half the period of resonance between charging choke and pulse forming network capacitor.

Hence, the charging time T is represented as T=$\pi\sqrt{LC}$.

Where

L = inductance of charging choke

C = capacitance of pulse forming network

Hence, L = $\frac{T^2}{\pi^2 \times C} = \frac{\left(1.5\times10^{-3}\right)^2}{\pi^2\times0.282\times10^{-6}}$ = 0.808 H.

We can take L=1H & Lower side operating voltage = 1.5 kV,

Higher side operating voltage = 3 kV.

5.1.3 Charging diode

Six number of charging diode is required whose blocking capacity is = 500V.

Type = Fast recovery diode

Connected in series to charge the pulse forming network and block to charge the pulse forming network capacitor into the charging choke i.e. only positive part of the resonance cycle is used to charge the pulse forming network.

5.1.4 Dequing

Pulse to pulse regulation provides constant input so as to get constant output from the RF. DEQ solid state switch in series with resistance capacitor network is connected across the charging choke.

As soon as pulse forming network changes to set level, the part of voltage across the pulse forming network is compared to a low level D reference which in turn trigger DEQ switch and remain energy in the choke is dissipated in the resistor connected in the DEQ circuit.
The resistance is of the order of 2.5 kΩ.
So, the decay time constant of the dequing circuit is represented as

$T_q = \frac{L_{chargingchoke}}{R_{deq}} = \frac{1}{2.4\times10^2}$ = 0.416 msec.

Pulse charging average current is represented as, $I_{av} = \frac{Q}{T} = \frac{CV}{T}$

$= \frac{0.28\times10^{-6}\times3\times10^{-3}}{1.5\times10-3}$ = 0.56 amp ≈ 0.6 amp

Hence,

Peak current I through charging choke will be represented as $I = \frac{\pi}{2} \times I_{av}$

$= \frac{\pi}{2} \times 0.8 = 1.25$ amp.

DC current flowing through the choke will be represented as

$I_{dc} = I_{av} \times duty ratio = 0.8 \text{ x } \frac{T_{on}}{T_{on+T_{off}}} = 0.8 \text{ x } \frac{1.5\times10^{-3}}{5\times10^{-2}} = 0.24$ amp.

Hence the specification of charging chokes as follows:

Choke inductance at DC current of 0.25 is = 1H

Winding current capacity = 0.25 amp.

Main switch specification:

The main pulse transformer turn ratio 1:11, Pulse transformer secondary current is 10 amps.

Primary current = 11 x 10 = 110 amp.

So, suitable switch is IGBT which can handle Peak forward current 100amp to switch on IGBT a Gate Drive Circuit is required with isolation. In, deal condition for matching the load can never be achieved.

So the pulse transformer design for matching the load is made in such a way that there is always some negative mismatch resulting the pulse forming network getting negatively charged.

To limit the negative charge on the PFN to about less than 600V. A shunt diode circuit is used for 600V blocked a series resistance to limit the current in the diode is chosen in such a way that the shunt current is 10% approximately of load current.

So, $The value of resistnace is = \frac{V}{I}$

10% of load current = 10% x 110 = 11 amp.

$R_{shuntdiode} = \frac{600}{11} = 54.5\ \Omega \approx 60\ \Omega$

Hence, the shunt diode resistance of around 100Ω with diode reverse voltage = 600V,

Instead of fixed resistance, we used thyristor.

5.1.5 EHT Power Supply and Rectifier Circuit

The filter capacitor value such that the energy stored in the capacitor is almost 10 times greater than the energy stored by pulse forming network for a charging pulse.

The energy stored in pulse forming network as, E = $\frac{1}{2} \times C \times V^2$

$= \frac{1}{2} \times 0.28 \times 10^{-6} \times (3 \times 10^3)^2 = 1.26$ Joule

So, the energy in the filter capacitor is equal to 1.26 x 10 = 12.6 J.

The energy being stored at 1.5KV in which the drop in choke and rectifier are also considered.

Hence, the capacitance of filter is represented as $C_f = \frac{2\times E}{V^2} = \frac{2\times 12.6}{(1.5\times 10-3)^2}$ = 11.2 μF.

So, we use capacitor of 12 μ F for the filter. The equivalent capacitor

Transformer:

The R.M.S. voltage on secondary V_{rms} = 0.74x DC_{avg} = 0.74 x 750 = 555 volt.

Secondary line current is I_{sec} = 0.816x I_{dc} = 0.816 x 0.24 = 0.195 amp.

On safe side, we take it a 0.20 amps.

Protection circuit:

A) Inverse Current Protection (shunt diode fault):

A Toroidal transformer is compared with the reference and that comparator gives the fault signal, if the inverse voltage goes above the set value, fault signal through the relay operate EHT contractor.

B) Over Current Protection:

A return charging current is sensed through a small resistor of 1 Ω. The voltage across this resistor is compared with a reference and the comparator gives the fault signal output to switch off the EHT.

Specification of Load:

Load Current = 10 amp (Peak)

Resistive load = 1.5KΩ

Operative voltage = 15KV

Peak power dissipation on the load = $P_{l(peak)}$ = I^2 x R_l

$P_{l(peak)}$ = 10^2 x 1.5 x 10^3

$P_{l(peak)}$ = 150KW

Duty of pulse on load = $\frac{T_{on}}{T}$

Let

Max. Operating frequency = 400Hz

Pulse width of pulse = 6μsec.

Duty = $\frac{6\times 10^{-6}}{\frac{1}{400}} = 2.4 \times 10^{-3}$

Avg. Power Dissipation = $150 \times 10^{-3} \times Duty$

$P_{l(avg)} = 360W.$

5.1.6 Hardware Development

The system has been developed for closed loop control containing the following blocks:

- Power Circuit
- Charging and Pulse Generation
- Snubber Circuit
- Pulse Amplification and Isolation Circuit
- Current Sensing Circuit
- Voltage Sensing Circuit
- Power Supplies
- Power Circuit

Fig 5.1 shows the power circuit of high voltage high pulse power supply. The 230V, 50 Hz ac input is fed through 1:2 isolation transformers. Secondary of pulse transformer is connected to fuse link and circuit breaker. High recovery diode is used for rectification to generate DC voltage supply the pulse generator. These power devices are placed on heat sinks made of aluminum sheet to dissipate the excessive heat.

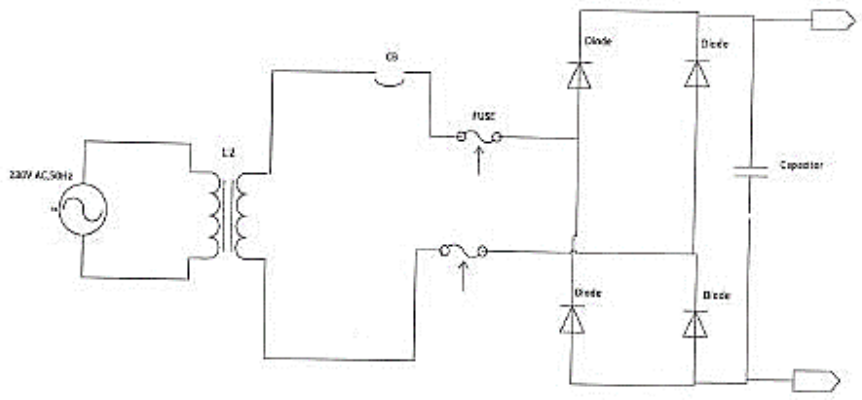

Fig 5.1. Basic power circuit of pulse power supply

Specifications

- Single phase diode bridge dc 602-9108 (1000V, 10A): 1 nos shown in Fig 5.2.

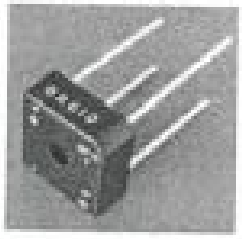

Fig 5.2. Single phase diode bridge

- Heat sinks (2.5” x 2.5” top surface, 5mm sheet thickness): 04 Nos

5.1.7 Charging and Pulse Generation

Initially charging choke the PFN through forward diode to twice the fed voltage. This charging voltage is sensed by fast compensation network and trigger signal is generator by SPARTAN 3 FPGA kit of requite pulse duration and repetition frequency. The actual charging current, is sensed using current sensor circuit and these currents are given as inputs to the pulse generation circuit which is shown in Fig 5.3.

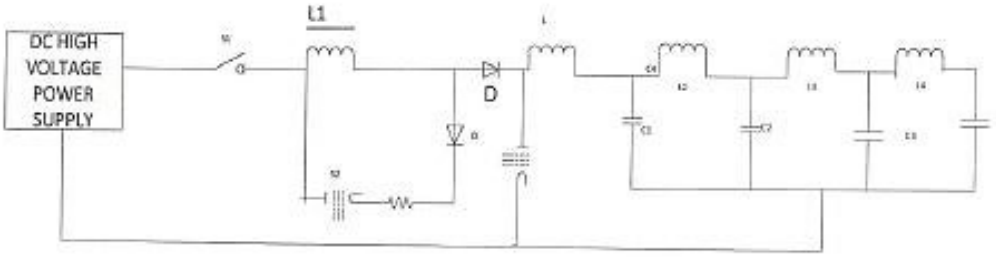

Fig 5.3. Charging and Pulse Generation

5.1.8 Pulse Amplification and Isolation Circuit

- The pulse amplification circuit for MOSFET is shown in Fig 5.4. The opto-coupler MCT-2E provides necessary isolation between the low voltage isolation output amplifier transistor 2N2222. When the input gating is +5V level, the transistor saturates, the LED conducts and the light emitted by it falls on the base receives no base drive and remains in the cut-off state and a +15V pulse (amplified) appears as its collector terminal.
- MOSFET-IRFP 460 (500V, 20A): 40 nos

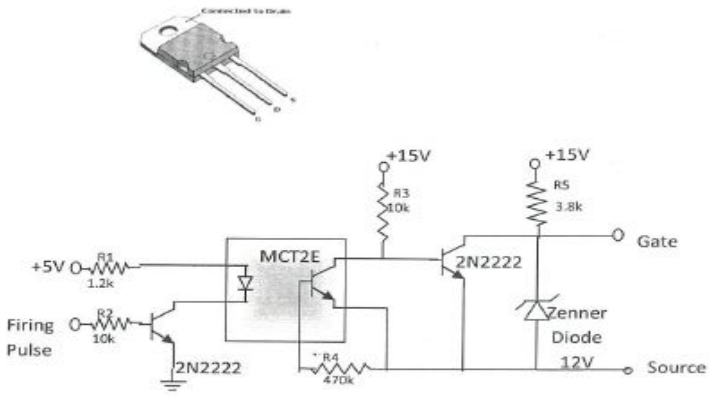

Fig 5.4. Pulse Amplification and Isolation circuit

When the input gating pulse reaches ground level, the input switching transistor goes to cut-off state and LED remains off, thus emitting no light and therefore the photo-transistor remains off. The output transistor receives base drive and saturates, hence the output falls to ground level. Therefore, the circuit provides proper amplification and isolation.

Further, since slightest spike above 20 can damage the MOSFET, a 12V Zener diode is connected across the output isolation circuit, this clamps the triggering voltage 12V.

Further to the +15V power supply was fabricated on the same PCB using 7815 chip.

Components

- Opto-coupler MCT-2E: 04 nos.
- Output amplifier transistor (2N2222): 04 nos.
- Resistance: -10 Ω: 08 nos, 1.2 Ω: 04 nos, 470 Ω: 04 nos, 3.8 Ω: 04 nos.
- Zener diode (+12V): 04 nos.
- Copper clad sheet (4” x 2”) for making 4 PCBs.

5.1.9 Snubber Circuit

Since the power handle by the prototype bridge converter is less (up to 10A) an RC Snubber circuit has been used for protection of the main switching device. Switching high current in short time gives rise to voltage transients that could exceed the rating of the MOSFET. Snubbers are therefore needed to protect the switch from transients. Snubber circuit for MOSFET is shown in Fig 5.5. The diode prevents the discharging of the capacitor via the switching device, which could damage the device due to large discharge current. An additional protective metal oxide varistor (MOV) is used across each device to protect against over voltages across the devices.

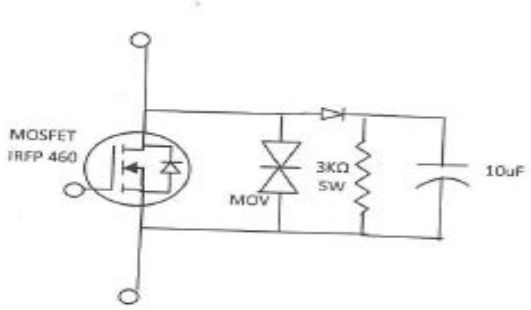

Fig 5.5. Snubber circuit for MOSFET protection

Components

- Snubber circuits: 04 nos
- Dimensions of each PCB: 2.5” x 2.5”
- Capacitance : 10 µF/450V
- MOV (metal oxide varistor): 510V
- Diodes IN5408 : 04 nos

Current Sensing Circuit

The actual charging current is sensed using the current sensing circuit of 1Ω assembly shown in Fig 5.6 and is given as input to the pulse generation.

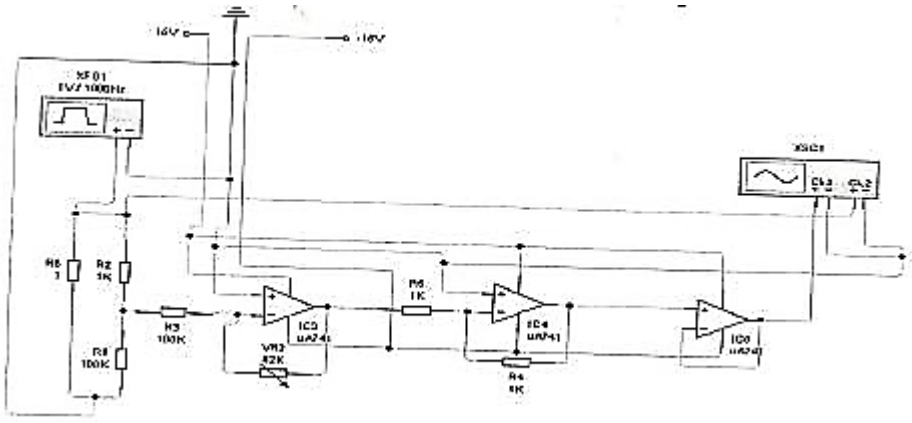

Fig 5.6. Current Sensing Circuit Voltage Sensor:

The source voltage is sensed using voltage sensing circuit which is soldered on PCB. The output of the voltage sensor circuit is given to the ADC channel of SPARTAN 3kit. Fig 5.7. shows the voltage sensing circuit, the input to the voltage sensor i.e., the input source voltage is first applied to a potential divider arrangement. This reduces the voltage by a factor of 100. This reduced voltage is applied to the input terminals of AD202 which is an isolator/ amplifier. The output of AD 202 is fed to a buffer of IC 741 and then to gain block again of IC741. The gain block has an adjustment POT. This POT is adjusted to give an overall gain of 0.05 to the output voltage.

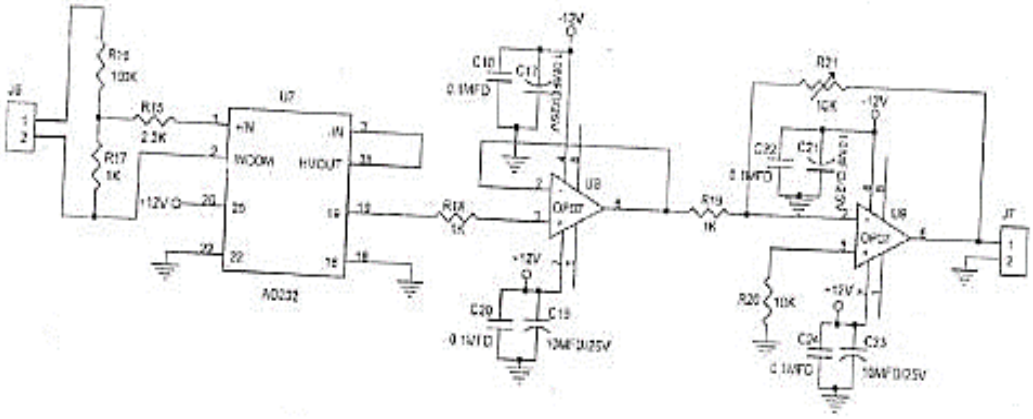

Fig 5.7. Voltage Sensing Circuit

Components

- AD202: 01no
- IC741: 02no
- Resistors (0.25W): 100 Ω: 01 no., 1 Ω : 03no., 2.2 Ω: 1 no., 10 Ωf: 1no.
- Trim POTs: 01 nos
- Capacitors (25V):- 10 μF:2nos., 0.1 μ F :02 nos
- Connectors:- 2 pin: 08nos

Power Supplies

DC regulated power supplies (+15V, +12V,-12V,+5V) are required for providing biasing to various circuits like pulse amplification and isolation, voltage sensor circuits and analog inputs providing reference frequency and voltage using ICs 7815,7812,7912 and 7805 for +15V,+12V,-12V and +5V respectively.

Primary side of 230V/12V single phase transformer is fed through a single phase 230V, 50Hz supply, secondary side is connected to a diode bridge, 1000 μ F, 25V capacitor is connected at the input supply of the regulator, 1000 μ F, 25V capacitor is connected at the output of the IC voltage regulator of each supply for obtaining the constant ripple free DC voltage.

Components

- + 12V supply : 10 nos
- - 12V supply : 1 no
- + 5V supply : 1 nos
- IC 7812 : 10 nos
- IC 7912 : 1 nos
- IC 7805 :1 no
- Capacitors 1000 μ F/ 50V : 12 nos., 100 μ F, 25V : 12 nos
- Diodes : 48 nos
- Single phase transformer 230V/12V :12 nos

5.2 Need of driver circuit for MOSFET

The structure of a MOSFET is as that the gate produces a nonlinear capacitor. The device is turned on when gate capacitor is charging and permits current to flow between drain and source terminals, when the capacitor is discharging it makes the device off and a high voltage can be obstructed between the drain and source terminals. The voltage (minimum) with which the gate capacitor is charged and the device just about conduct is the threshold voltage (V_{TH}). For working a MOSFET as a switch, a voltage adequately larger than V_{TH} ought to be connected between the gate and source terminals.

Consider a digital logic circuit with a microcontroller that can yield a PWM signal of 0 V to 5 V to one of its I/O pins. This PWM would not be sufficient to completely turn on a power device utilized in power circuits, as its overdrive voltage by and large surpasses the standard CMOS/TTL logic voltage. Accordingly, an interface is required between the logic/control circuitry and the powerful device. This can be actualized by driving a logic level n-channel MOSFET, which, thus, can drive a power MOSFET .In majority of the electrical application, there is a need of a switch which should operate at an appropriate at a particular recurrence period to provide desired results. Since for all intents and purposes perfect switches are not there, so as a rule we go for use MOSFET as a switching device. MOSFET has its preferences just as drawbacks. For all intents and purposes it isn't that simple to turn off/on a MOSFET. It requires a driver circuit to play out the on/off task at a specific frequency. At the point when the power-supply IC and MOS transistor are chosen, it is particularly essential to choose a fitting driver circuit to associate the IC to the transistor.

5.3 Requirements of a good driver circuit:

- When the MOSFET is turned on, the drive circuit ought to have the option to give a sufficiently substantial charging current to quickly build the voltage between the gate and source terminals of the MOSFET to the required esteem, guaranteeing that not just the MOSFET can be immediately turned on yet additionally there is no high-recurrence oscillation on the rising edge.
- At the time when the switch is turned on, the driver circuit can guarantee that the voltage between the gate and source terminals of the MOSFET stays stable and dependably turned on.
- During switching off, the driver circuit can provide as low impedance as conceivable to rapidly release the capacitor's voltage between the gate and source terminals of the MOSFET, guaranteeing that the switch can be immediately switched off.
- The circuit structure ought to be basic, effective and completely reliable.
- Electrical isolation is provided accordingly.

Here, an opto-coupler is used as an isolation element. An opto-coupler is an element that isolates control circuit from the power circuit so that high frequency signal does not flow to the control circuit which can damage the control circuit. The opto-couplers are used in various applications from communications to monitoring systems to power circuits. Here an opto-coupler A3120 is used.

MOSFET driver circuit:

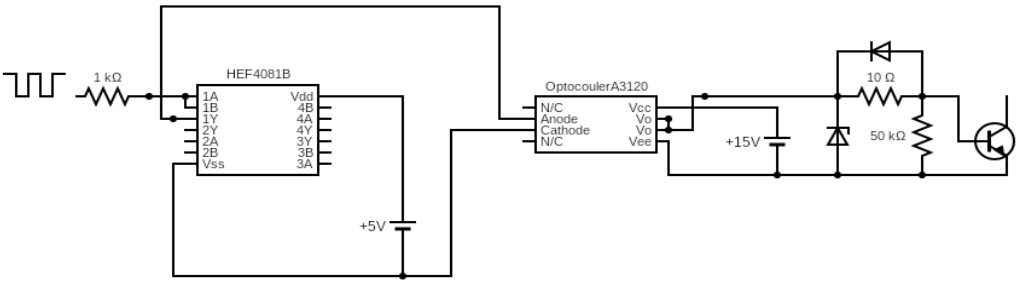

Fig 5.8. Gate Driver Circuit for MOSFET

Here, the AND gate is used as a buffer to protect the opto-coupler, so that if any ripples are there at the input, it will be removed by the AND gate. Now when the pulse is high i.e. both

the inputs to the AND gate is high the output is high. Now the +5V is given to the anode of the opto-coupler and cathode is connected to the ground. So the photodiode which is internally connected to the anode and cathode of the opto-coupler emits photons and turns on the phototransistor of the opto-coupler and high output voltage is obtained at the output pin. Since slightest of spike can damage the MOSFET, a Zener diode of 15V is connected across the MOSFET. This clamps the triggering voltage to 15V. So the MOSFET is turned on when input pulse is high. Now when the input pulse is low, low output from the AND gate is applied to the opto-coupler photodiode which cannot emit photons and hence low output voltage is obtained at the output pin of the opto-coupler and hence cannot drive the MOSFET for switching on in other words when input pulse is low MOSFET is off. The schottky diode connected across the resistor is used to make the turn off process fast. The schottky diode is preferred for high frequency applications because of their short reverse recovery time and during forward bias condition due to their low voltage drop. The circuit is given in Fig 5.8.

5.4 DC power supply for driver circuit

The power supply for MOSFET is required to drive the MOSFET so that it is turned ON or OFF at a particular frequency. The power supply basically consist of four stages. They can be shown as a block diagram as in Fig 5.9. below:

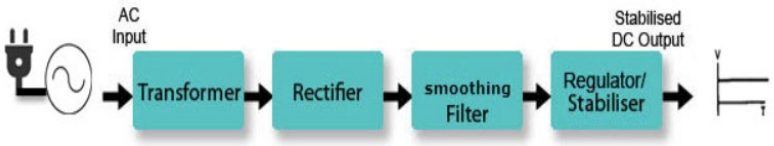

Fig 5.9. Power supply block diagram

The complete steps to generate the regulated power supply one by one is discussed below:

First there is need of stepping down high AC voltage to a low AC voltage. Transformer is used for stepping down the voltage to a desired level. A transformer is an electromagnetic energy conversion device and also constant frequency device because it transfers energy from one circuit to another without change in frequency. Basically a transformer is a coupled circuit. Flux that is produced by the source voltage in the primary links with the secondary to induce a voltage in secondary terminals. Now since we have step down the voltage so the turns in the secondary is less than the primary.

Now after stepping down the voltage to a desired level, the AC voltage that we get from the supply has to be converted into DC. For that a rectifier need to be used. A rectifier converts

an AC voltage to a DC one. Rectifiers of various combinations are there. Most preferred one here is the diode full bridge rectifier which is discussed below:

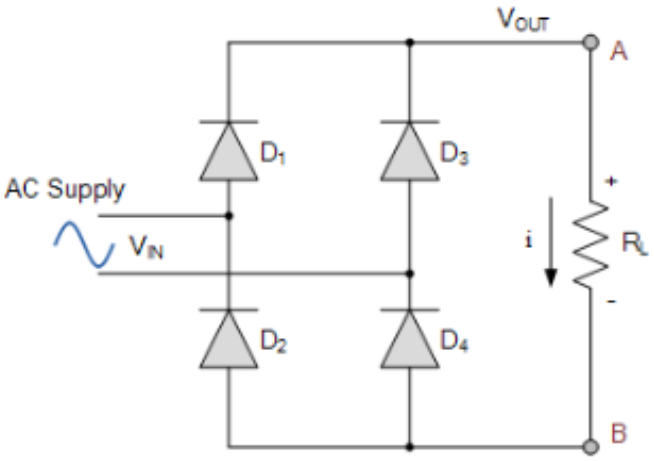

Fig 5.10.Single phase full bridge diode rectifier

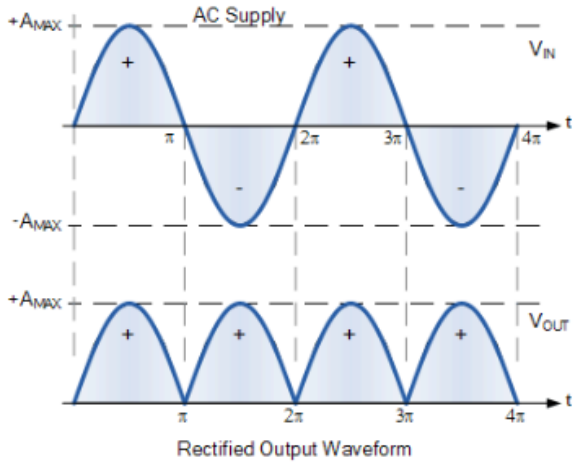

Fig 5.11.Rectified output waveform

Single phase full bridge diode rectifier consists of four diodes which are being powered from an AC supply as shown in Fig 5.10. During the positive half cycle of the supply voltage the diodes D1 and D2 gets forward biased and conduct. The power is supplied from the supply through diodes D1, D2 and load. During negative half cycle of supply voltage the diode D3 and D4 gets forward biased and conducts. These type of circuits mainly used in industrial applications. When V_{IN} is positive then D1 and D2 conducts then $V_{OUT}=V_{IN}$ and $I=I_{IN}$. When V_{IN} goes negative, diodes D3 and D4 conducts then $V_{OUT}=V_{IN}$ and $I = -I_{IN}$.

Now the ripples that is there in the output of the rectifier has to be removed using capacitor filter. The pulsating DC from the rectifier is applied to the filter capacitor. This smoothing capacitor will remove the unwanted ripples in the pulsating DC. The rectifier without

filter will create pulses at the output as appeared in Fig 5.11. These vacillations can be decreased if a portion of the energy can be put away in capacitor or in inductor while rectifier is producing the ripples and is permitted to release from capacitor or inductor in the middle of pulses. A circuit that limits or disposes of the ripple rectified output is known as filter. Filter frameworks by and large are made out of a capacitor, an inductor, or both. Capacitor filters are utilized for lower control applications. Then again, inductor filters are utilized in high-control applications. The single stage diode rectifier with capacitive filter appears as in Fig 5.12.

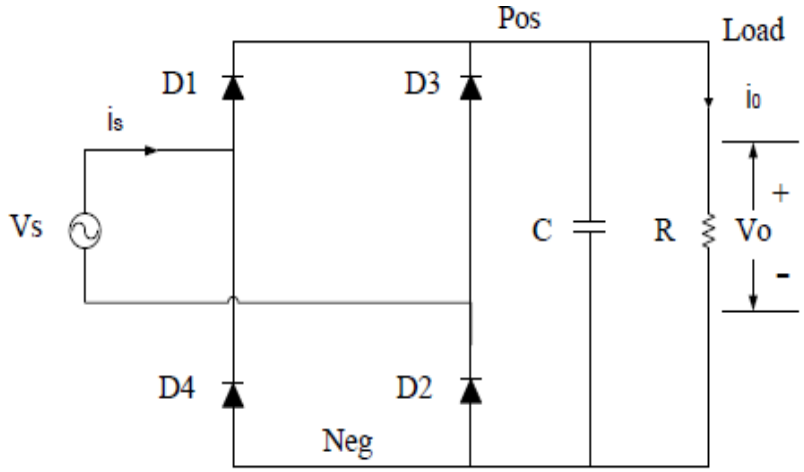

Fig 5.12. 1-Ø Full Bridge diode Rectifier with 'C' filter

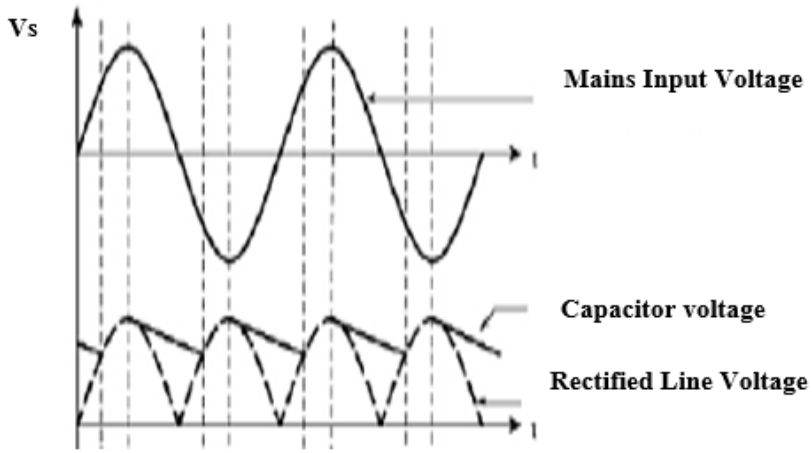

Fig 5.13.Rectifier waveforms with 'C'filter

The capacitor which is used to smoothen the rectified output voltage converts the full wave rectified output into a more smooth DC having very much less ripple factor. When supply voltage is greater than capacitor voltage then capacitor charges to maximum supply. When supply voltage is lower than capacitor voltage then capacitor starts discharging. The advantage of using C filter is that AC component flows through C and DC component alone will flows through load R. The rectified output voltage waveform utilizing capacitive filter is shown in Fig. 5.13.

Now the DC voltage has to be regulated to a desired level using a regulator. A voltage regulator usually regulate the voltage to a lower value and the main thing is to make the voltage available constantly over time. In the world of electronic parts, the voltage controller is a standout amongst the most generally utilized. Any electrical or electronic device that keeps up the voltage of a power source inside adequate cut-off points is called a voltage regulator. The voltage regulator is expected to keep voltages inside the endorsed range that can be endured by the electrical hardware utilizing that voltage.

These voltage regulators are generally utilized in engine vehicles of various types to coordinate the output voltage of the generator to the electrical load and to the charging necessities of the battery. Voltage controllers likewise are utilized in electronic gear in which high variations in voltage can be harmful. Electronic voltage controllers use solid state semiconductor devices to smooth out variations in the flow of current. By and large, they work as variable resistances; that is, resistance diminishes when the electrical load is high and increments when the load is less. The complete pin out for voltage regulator can be shown in Fig 5.14. below:

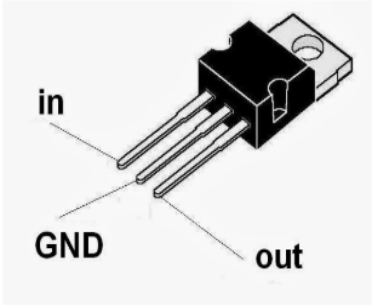

Fig 5.14. Voltage regulator

The first pin is the input pin, second pin is the ground/common and third pin is the output. The output from the filter capacitor is connected to the is connected to the input of the voltage regulator to regulate the voltage at the required level and the output from the regulator which is constant DC voltage is further connected to the output capacitor which removes any other ripples if it is there in the circuit.

The complete circuit diagram for a regulated power supply is shown in Fig 5.15. below:

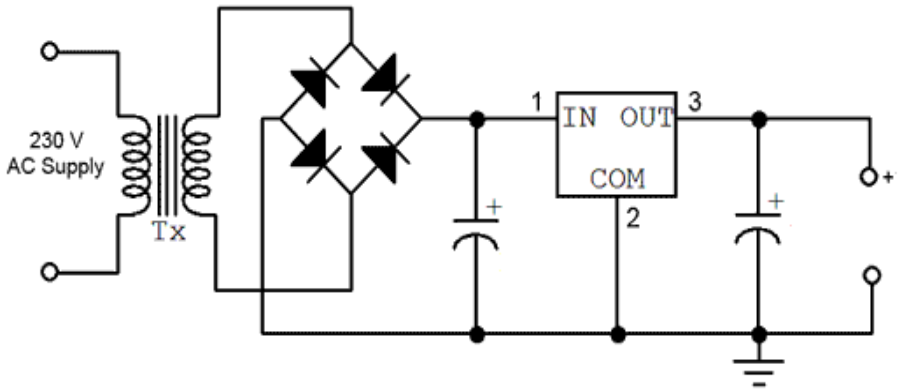

Transformer | Rectifier | Filter cap. | Voltage reg. |O/P cap. | DC O/P

Fig 5.15. Regulated Power supply for switching of MOSFET

5.5 Control Strategy

The output voltage of a Pulse Generator is kept steady with the assistance of a closed loop control technique. The estimation of the output voltage i.e. actual voltage is compared to a reference voltage i.e. nominal voltage. The difference among the actual and nominal voltage controls actually the duty cycle of the Switch.

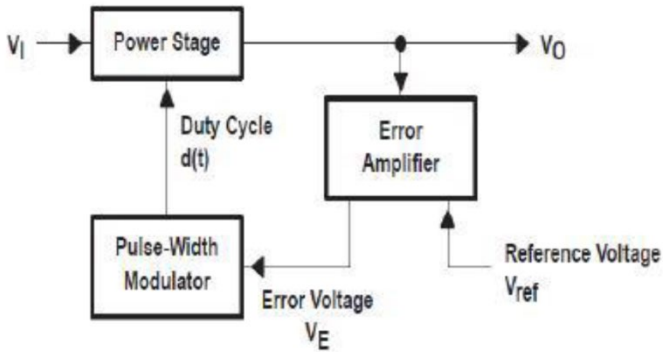

Fig 5.16. Controlling Technique of Power Stage

Control circuit manages output by either varying the ON time of switch or fixing the switching frequency or by fluctuating switching frequency and fixing ON or OFF time of switch. The primary controlling is done in pulse width modulation (PWM) Technique and second method is utilized in switch mode power supplies (SMPS) as shown in Fig 5.16. Control circuit which is used in SMPS has a few important functions. Control circuit keeps up output voltage consistent regardless of whether there is any adjustment input voltage or load, amid steady state activity. Control circuit secures all parts, amid transient task by restricting external pressure on them. Duty cycle i.e. the ratio of on time switch to the total time and input voltage are the two

inputs applied to the power stage. By varying the duty cycle of the switch by generating the necessary control signal after error signal is applied as input to the controller, necessary PWM signals can be generated.

5.6 Controlling technique types

The most popular closed loop control methods used for generating PWM signals for switch are namely the voltage mode control, current mode control and hysteretic control. All of the above mentioned control methods can be used for different applications.

5.6.1 Voltage Mode Control

Voltage-mode control (VMC) is broadly utilized on the grounds that it is anything but difficult to design and implement, and has great immunity to disturbances at the references input. Voltage mode control just contains single feedback loop from the output voltage as appeared in Fig 5.17. A single loop voltage mode control is utilized to compare the output voltage and reference voltage and it is amplified by Compensator. The output from the compensator is then compared with a fixed frequency saw tooth waveform by utilizing Pulse Width Modulator (PWM). The output from PWM is utilized to control Switch task.

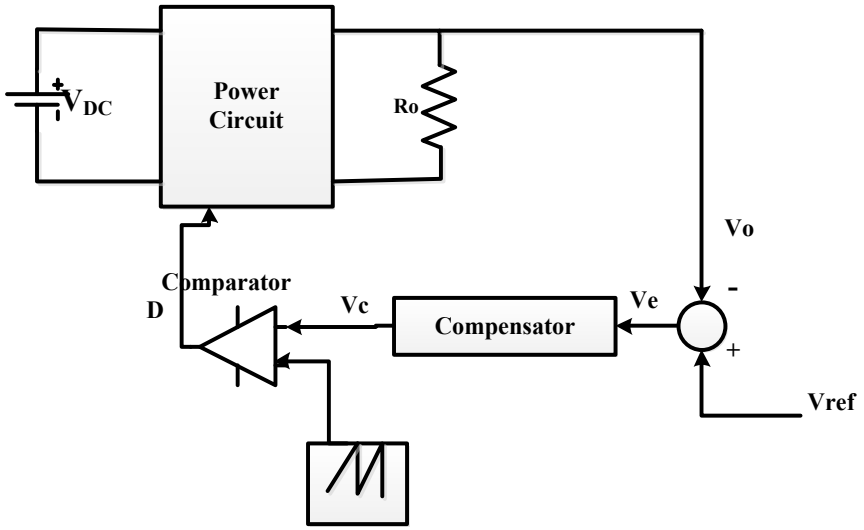

Fig 5.17. Voltage Mode Controller

5.6.2 Current Mode Control

Current Control strategy can control both output voltage and output current of the circuit. Contrasting to voltage-mode control, current-mode control gives an extra internal control circle

control. The converter output voltage is detected and it is compared with the reference voltage and produces an error signal. The control voltage is created by the compensator which is compared with the consistent amplitude saw tooth waveform. The detected signal from the internal loop is not continuous but saw tooth and will in this way be utilized as the PWM producing saw tooth. The comparator produces a PWM signal that is nourished to drivers of controllable switches. The current and the voltage feedback signal (V_C) are fed into a comparator and will characterize the state that is connected to the reset pin R. At each cycle (characterized by the clock), the pin S of the latch is set to high while its reset pin is at first low, PWM is in this way likewise at high (pin Q i.e. the output). In the event that amid this cycle $V_C$decreases than the present current feedback value the reset pin will go high and PWM will go to low.

This outcomes in a sufficient adjustment of the PWM sign to ensure an unfaltering output voltage. The duty (D) i.e. the time the switch is on in the circuit of the PWM signal relies upon the estimation of the control voltage. Additionally the recurrence of the PWM signal produced is same as the recurrence of the saw tooth waveform. An inward control loop which feeds back the inductor current signal, and this current signal, changed over into its voltage type, is compared with the control voltage. The current controller circuit is shown below in Fig 5.18.

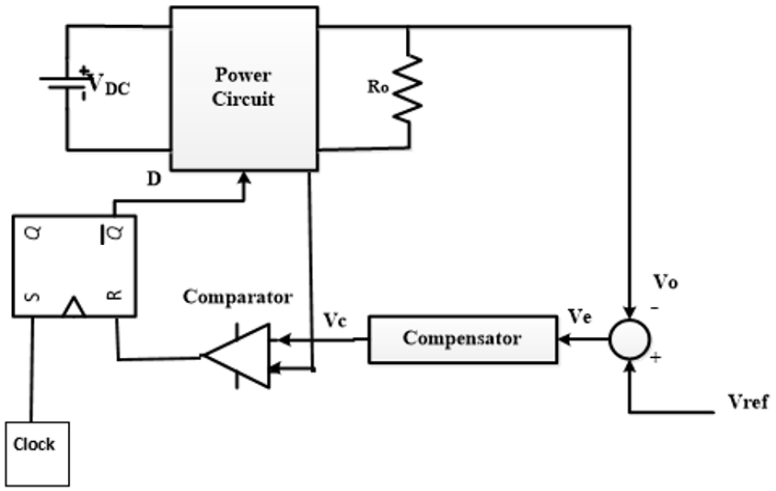

Fig 5.18. Current mode Controller

5.6.3 Hysteresis Mode Control

In contrast to previously seen PWM-based control, hysteresis based control introduces a two-state threshold voltage called hysteresis (VDC1 and VDC1 - Vhyst) given in Fig 5.19. As in previous methods, every time the sensed signal crosses a threshold voltage the state of the switch is changed.

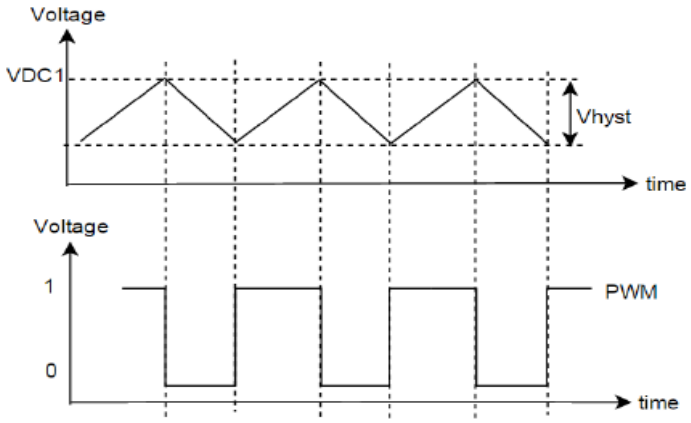

Fig 5.19. Hysteresis PWM generation

Again, as in PWM based control, depending on the sensed signal, it can be hysteretic current mode control or hysteretic voltage mode control. Each of these control schemes has its own pros and cons. Hysteresis Mode Control provides quick response and very much simple in design and usage. It reacts to unsettling influences and load change directly after just the transient happen, so that they give incredible transient execution. Additionally, they don't require the components for compensation in the closed loop network. This diminishes the component count value and also the solution size estimate in execution. The above preferences make hysteresis control a decent answer for power circuit. Despite the favourable circumstances, one noteworthy worry of utilizing hysteresis control technique is the steadiness issue lack of immunity against the load disturbances.

5.7 PI Controller

So as to manage the output voltage, voltage mode controller is utilized. The voltage mode control uses the PI controller as compensator. A PI is a very popular used in feedback loop mechanism and widely utilized in the industry sector. A PI controller tries to reduce the error between the reference value and the calculated value by producing the control signal which is to be further processed to reduce the error.

In order to reduce the error the proportional term plays a very important role as it produces the change in output in proportional to the present error value. The corresponding proportional response can be adjusted by multiplying the error value with a constant term Kp called as proportionality constant. In fact there are many applications which uses only the proportionality constant it performs quite well also. If more is the error after comparing the reference and calculated value, more is the proportional output and if the error diminishes the

proportional output also diminishes. In order to obtain a very good steady state response the integral term is used.

The integral term is proportional to both magnitude and duration of the error. The value of integral term Ki defines the contribution of the integral term in the control action for reducing the error. In most of the applications the derivative action can be eliminated as it requires a very high gain for signals with high frequency. So by eliminating derivative action proportion and integral actions are tuned. In most of the industrial applications combinations of proportional and integral term are used to obtain a very good steady state response.

5.8 Methods of Tuning PI Controller

Now it is very important to determine the optimum values of proportional term and integral term so as to produce a proper control action from the PI controller in order to obtain a very good performance from the system is called tuning. This is a very important part for all closed loop systems. Now there are various forms of tuning methods that are there to obtain required performance from the system. Among them trial and error tuning method and Ziegler-Nichols' tuning method are the two most popular tuning methods. Among them trail an error method is the simplest one.

5.8.1 Tuning of PI controller using Trial and Error method

It is the most straightforward method for tuning the PI controller. If we get the clear idea of proportional and integral term, this method becomes relatively easy.

- First Set integral term to zero and afterward increment the proportional term until the output of the control loop oscillates at a consistent rate. Proportional term should be increased in such a way that the response becomes faster without making the system unstable.
- As soon as the response is fast enough, start increasing the integral term in order to reduce the oscillations. Increase in the integral term K_i should be increased till the error is reduced to almost zero and steady state response is improved.

5.9 Control and Impedance Matching Philosophy

- FPGA based controllers are always compact, reliable, simpler and of emerging technology. FPGA based controller works in a shielded environment for EMI and EMC protection. FPGA controls the charging requirement of the pulse forming network as well as the main switch operation. Further it controls impedance matching and logical flow of power.
- To implement control and impedance matching, pulse to pulse voltage is monitored through voltage compensation network and the same is used as feedback for comparison with ideal pulse shape defined. When the pulse shape deteriorates due to positive and negative impedance mismatch beyond 10% (acceptable limit defined by the user), a trip command is issued by the controller to stop output voltage generation.

5.9.1 Impedance matching algorithm implementation

- Pulse Forming Network has multiple sections of LC tank based on pulse width requirement. A novel technique is introduced to create an option for impedance matching at the source end. In this technique, several round of inductance coil are used to meet the impedance matching requirement. The source voltage is sensed with the help of voltage sensor circuit. The flow chart for implementation is shown in Fig 5.20.

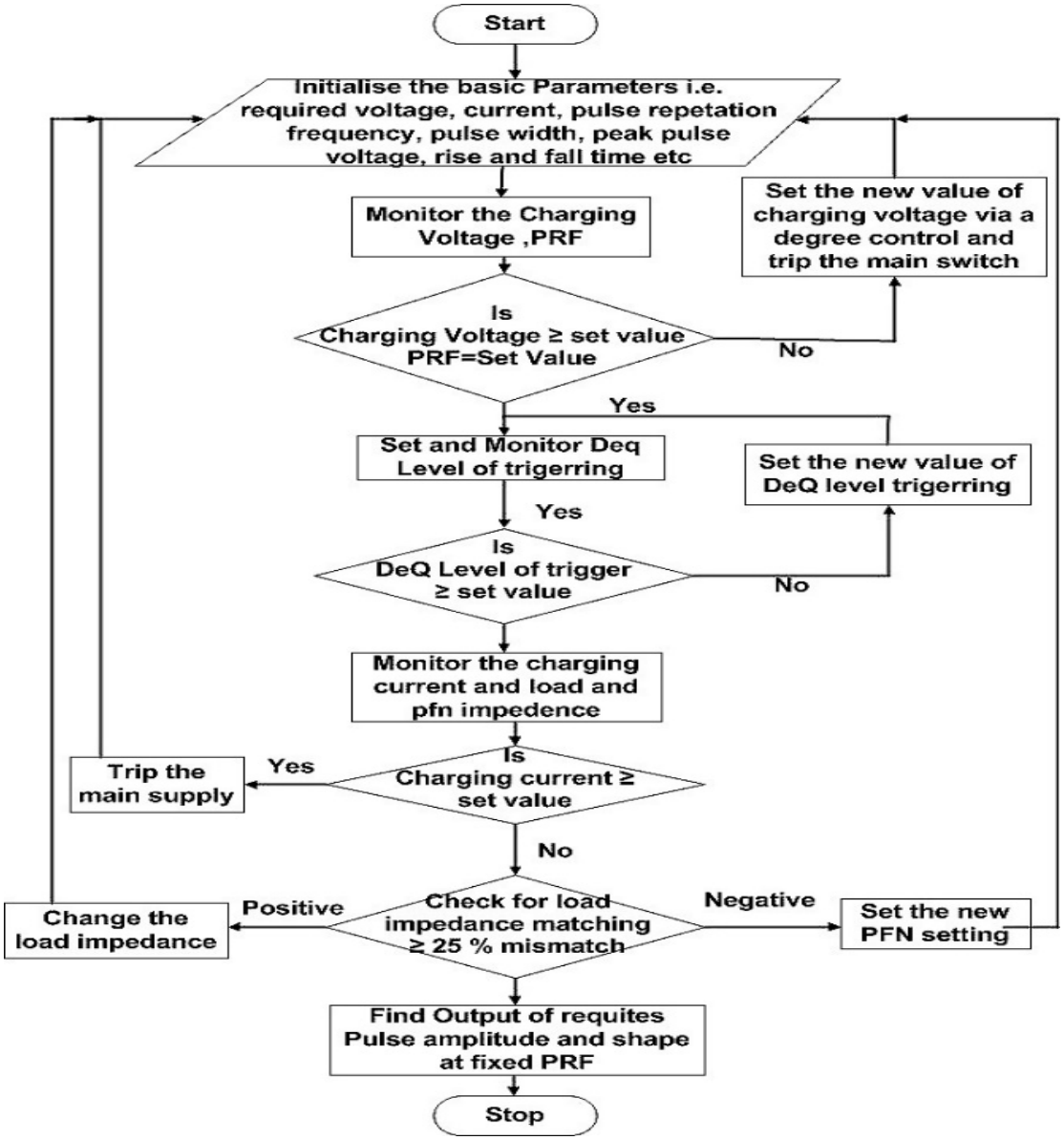

Fig 5.20. Flow chart for power flow and control

- The generated reference signal is compared with the set values. Finally the switching signals are given to the devices through pulse amplification and isolation circuits.
- The detailed algorithm for Dynamic Impedance matching evolved and implemented as prototype hardware.

5.10 Output Pulses from hardware implementation

The output pulses are obtained after PFN discharges its energy to the load. As the PFN capacitors reaches to approximately twice the applied voltage i.e. of 60V switching pulses from the FPGA controller is applied to the MOSFET so that output pulses is obtained at the resistive load at a pulse recurrence frequency of 1.6 kHz.

To verify the Experimental Results obtained from simulation, a scaled down hardware implementation of the proposed line type pulser is assembled using a six section PFN and a charging inductor. The complete hardware implementation is shown in Fig.5.21 below.

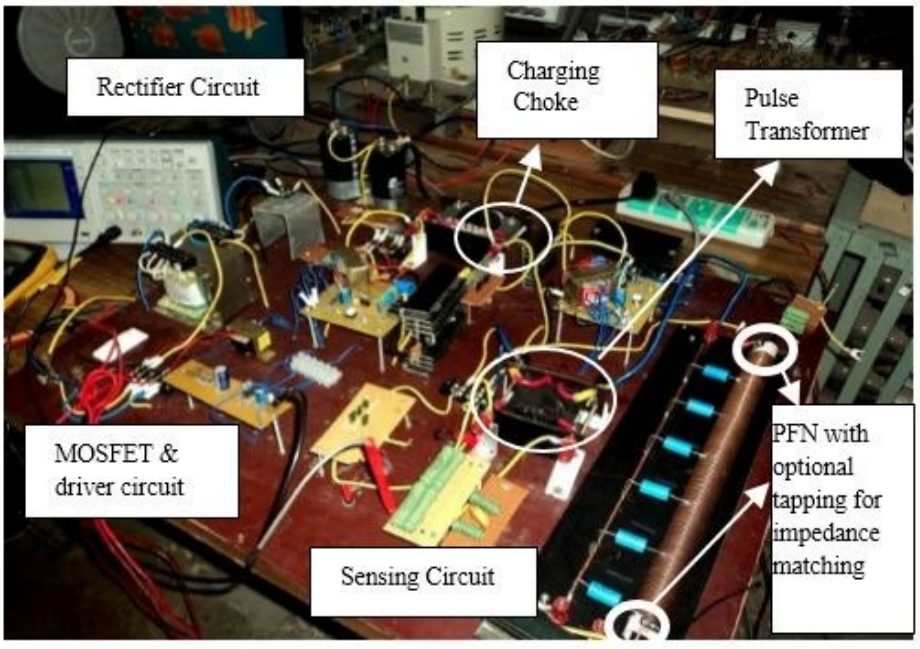

Fig 5.21. Hardware implementation of the proposed system Source: DRDO,MOD,INDIA

The capacitor and inductor values are chosen based on the theoretical calculations presented in chapter 7. Each section consist of capacitor of 4nF and inductor of 10μH. Hence the characteristic impedance of the PFN is of 12.5 Ω. Since the load impedance is of 12.5ohm, maximum amount of energy will be discharged to the load. Here air core inductors are used. Air core inductors refers to the inductors where ferromagnetic material is not used as a core. Though the inductance obtained from air core inductors are less but it is very useful in high frequency circuits since the losses called core losses will be less compared to a ferromagnetic core which increases with the increase in frequency.

It is imperative that the all of the energy is discharged to the load of 50 Ω and again recharged to the equal required level of voltage during the interpulse interval so that equal magnitude of voltage is obtained for each pulse.

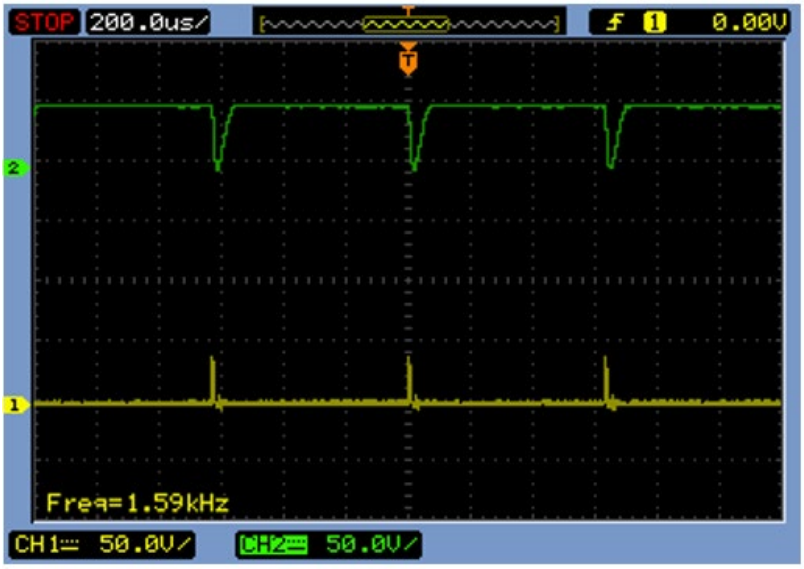

Fig 5.22. PFN and load voltage

Now looking at the single output pulse, it is seen that a pulse which is very close to rectangular shape is obtained according to our requirement. The pulse is having a rise time which is less than even 100ns as given in Fig 5.23. So we can say that the response is very fast or pulse rise time is very small. The fall time obtained from the system is around 720ns which is more than the rise time. Initially a minimal overshoot is obtained due to the release of energy from the PFN which can be neglected.

The voltage obtained in the output pulse is around half of the PFN voltage which is 30V since equal voltage drops 30V will be there in the PFN since the load resistance and the characteristic impedance of the PFN are equal. Now as one can see according to our design a pulse waveform of approximately 4μs is obtained from the proposed system. The output rectangular pulse is shown in Fig 5.23. Since we know the pulse width is calculated from the formula $2n\sqrt{L_{sec}C_{sec}}$, where 'n' is the number of PFN sections, L_{sec} and C_{sec} are inductance and capacitance values of each section.

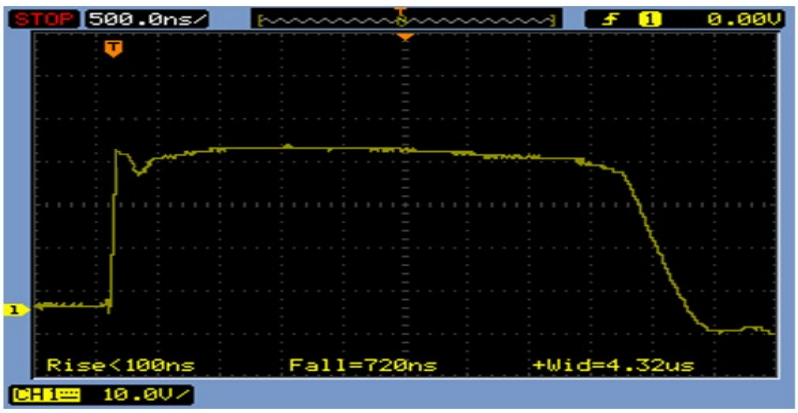

Fig 5.23. Output voltage pulse

This chapter presents Design of High Voltage Pulse Power Supply, Design of Pulse Power Generation system, Design of Pulse Forming Network, Charging choke, charging diode, Dequing, EHT Power Supply and Rectifier Circuit, Hardware Development, Control strategy for Switch, types of controlling procedures, PI controller significance, tuning strategy for PI controller, control and impedance matching philosophy.

Chapter 6

Prototype Hardware Development and Analysis

6.1 Case Study –I of Pulse Deformation

Developed High Voltage High Pulse Power Supply tested with pulse transformer connected through four RG8 (tri-axial) cables to match the transmission line impedance of 12.5 Ω. The system is fed from 3ϕ Phase AC Voltage Source with a voltage of 415V, 50Hz frequency as shown in Fig 6.1. below.

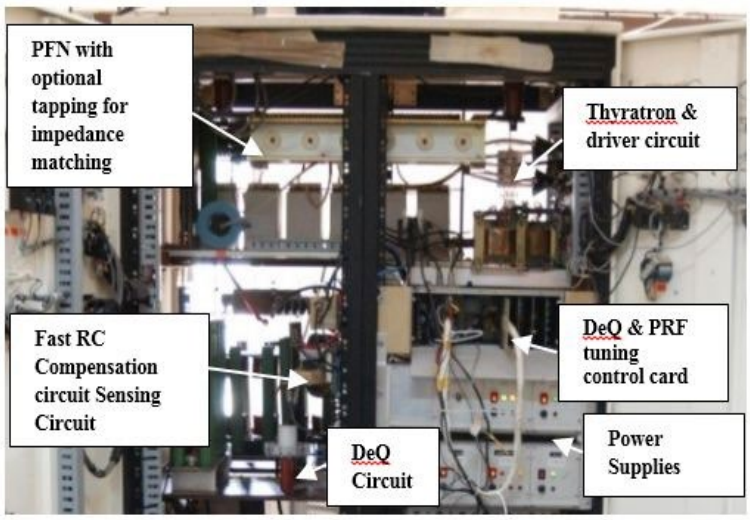

Fig 6.1. Hardware of high voltage high pulse power supply (HVHPPS); Source: DRDO, MOD, INDIA

Collection, evaluation and analysis of performance data of multiple standing wave bi-model electron linear accelerator systems.

The systems under consideration 7Mev, 9Mev magnetron systems and 15Mev klystron systems. The Rg8 tri axle cables in multiple provides impedance matching between PFN and Pulse Transformer. Klystron is best RF source with frequency range higher than 3.0 GHz. Klystron has high gain of around 50 d B. Klystron is a voltage driven device and if applied voltage is stable, phase property is excellent. It is a matured device with its simplicity, availability and long life. It is a best device for average and peak power capability.

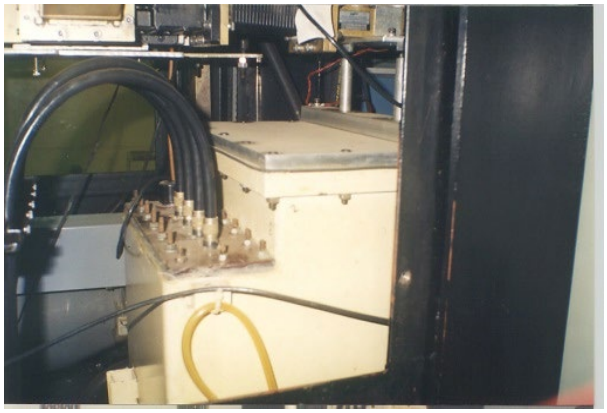

Fig 6.2. Klystron tank assembly Source: DRDO,MOD,INDIA

Fig. 6.2. shows Klystron tank assembly. Klystron consists of key components such as electron gun, RF cavity, drift tube, RF window, beam collector, focusing magnet, and cooling system. Electron is velocity modulated in the input cavity and forms bunch i.e. density modulation. Bunches are de-accelerated in the output cavity (beam energy to RF power) which is inverse process of accelerator (RF power to beam energy).

Table 6.1. Parameters of Klystron

Operation Frequency	2.998 GHz
Cathode Voltage	132 kV
Beam Current	92 A
Max. RF Peak Power	6 MW
RF Pulse Duration	1.5ms
Repetition Rate	Upto 170 Hz
RF Average Power	6 kW
Efficiency	65%
Gain	48.2dB
Solenoid Power	6kW
Length	2.5m
Lifetime (goal)	~40000h

Klystron characteristics is as follows,
Child's Law- In space charge limit current, emission current is,

$$I = P_r V^{3/2} \qquad (1)$$

Where P_r is Perveance, I is current and V is applied voltage
Then Power is,

$$P = I.V = P_r V^{5/2} \qquad (2)$$

Power's variation,

$$\frac{\delta P}{P} = \frac{2.5 P_r V^{3/2} \delta V}{P_r V^{5/2}} = \frac{5}{2}\frac{\delta V}{V} \qquad (3)$$

Klystron's Impedance,

$$Z = \frac{V}{I} = \frac{V}{P_r V^{3/2}} = \frac{1}{P_r \sqrt{V}} \qquad (4)$$

Therefore, Klystron's impedance varies with applied voltage. The systems under consideration are 15 MeV klystron based LINAC systems. The impedance matching between PFN, Pulse Transformer and load gives Klystron Current Waveform obtained at the time of installation are at the full rated value with perfect matching condition as shown in Fig 6.3.

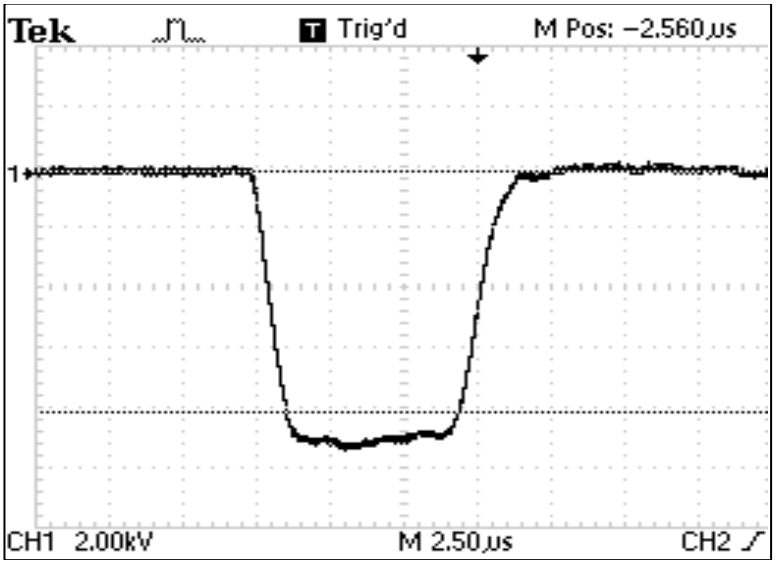

Fig 6.3. Klystron current at the time of installation

After two to three year of continuous use of these systems, there was deterioration in the output power of Klystron used and after increasing the filament voltage more than 10% of permissible values the Klystron current were not increased significantly. Thus, the time of filament heating increased and found that the time delay given is 11 min which is not sufficient to get maximum Klystron current.

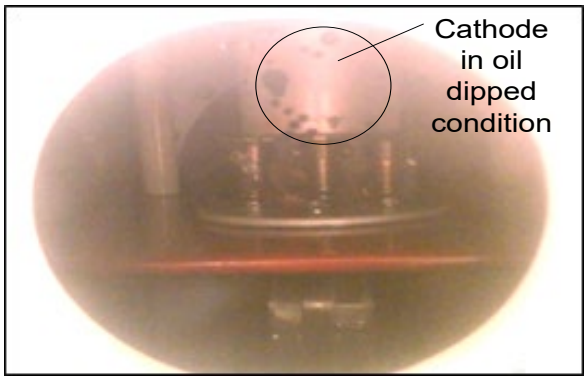

Fig 6.4. Cathode Oxidation due to Aging, Source: DRDO,MOD,INDIA

It was taking 30 min of time to reach the maximum value based on one month of noticeable behaviour with similar pattern. It was confirmed that the cathode is not getting sufficient electron to the output power. After operating the assembly which was oil dipped found that carbonation has happened on to the contact due to that the Klystron was not giving proper output power. As Fig 6.5. shows a drastic deteriorate of Amplitude and Shape in Klystron current with 15 min heating time delay.

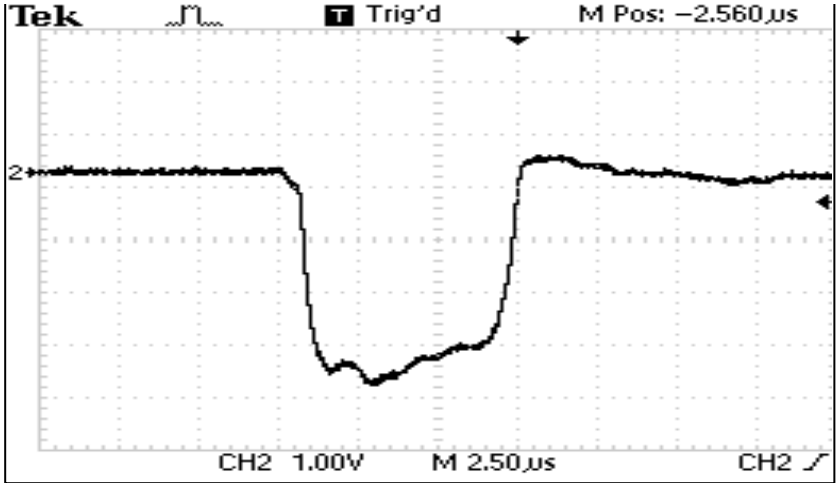

Fig 6.5. Klystron current with 15 min heating time delay

Table 6.2. Output performance with time and klystron current value

Klystron gun/filament voltage (AC)	Klystron heater time	Klystron current (A)	Days of experiment
6.3 volts	15	80	1-10
6.3 volts	20	82	10-20
6.3 volts	25	83	20-30
6.3 volts	30	83	30-40
6.3 volts	45	84	40-50
6.3 volts	60	84	50-60

Table 6.3. Variation in Klystron Filament Voltage with current and time

Klystron filament voltage	Klystron heat time	Klystron current	Days of experiment
6.3 ±1%	15	80	1-2
6.3±2.5%	15	80	2-4
6.3±3%	15	80	4-6
6.3±4%	15	80	6-8
6.3±4.5%	15	80	8-10
6.3±6%	15	80	10-12
6.3±7%	15	80	12-14
6.3±8%	15	80	15-16

The above table shown that variation in output Klystron current is slightly changing from 80A to 84A with increasing the Klystron filament heating current from 15 min to 80 min.

6.2 Case Study –II

An experimental hardware developed for varying the length of the tri-axial cable between pulse forming network and klystron load. Also a High Voltage High Pulse Power Supply is developed and tested with a 1.5 kΩ resistor connected over four tri-axial cables each having 50Ω line impedance. The overall equivalent impedance of transmission line will be 12.5Ω. Fig 6.6. shows functional block of experimental hardware.

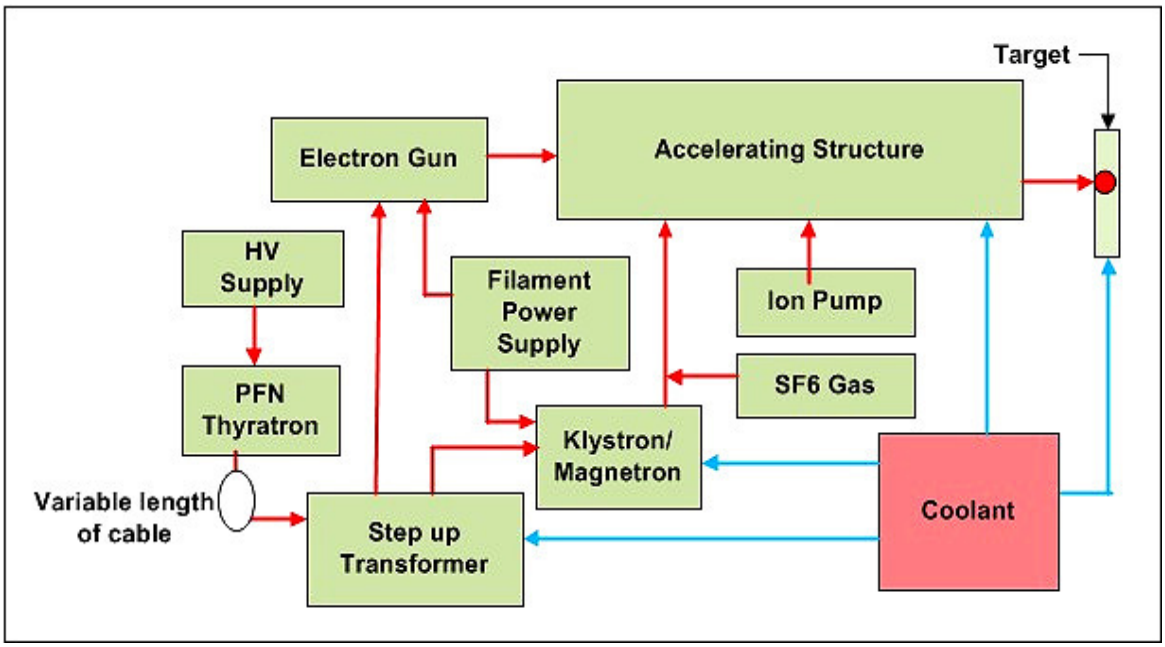

Fig 6.6. Block diagram of experimental hardware

The overall hardware specification of the above system is as below,

Table 6.4. Hardware Specifications

Parameter	Value
Pulse Output Voltage	12 kV
Output Current	1000 A
Pulse width (Variable)	6 µsec
Repetition rate (Variable)	10-200Hz
Load impedance(R_L)	12.5 Ω
Turns Ratio of Pulse Transformer	1:10
Duty Cycle	0.001

The inside view of high voltage high pulse power supply is shown in Fig 6.7. The system is energized by three phase 415V AC each time for a particular cable length; vital waveforms i.e. charging voltage, discharging voltage are captured by Yokogawa DL1520 and Tektronix TD1002. In this way the cable length is varied for ten different values and its effect on High Voltage High Pulse Power Supply is captured.

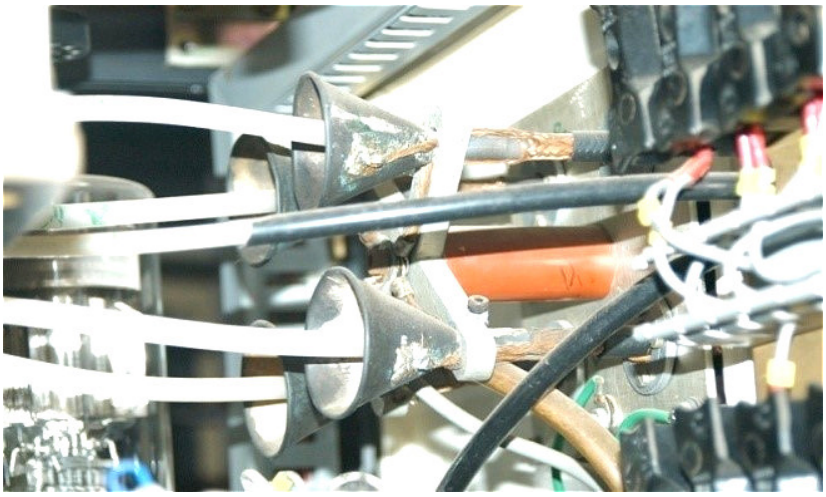

Fig 6.7. Photograph of cone structure of discharge of high voltage high pulse power supply (HVHPPS), Source: DRDO,MOD,INDIA

The degree of simulation will improve as the number of elements increases for the given network type. The PFN output pulse will be approximately equal to rectangular pulse network pulse is a good approximation of the rectangular pulse only during the pulse interval. The network pulse may show undershoot, overshoot and varying oscillations, at the beginning and end of the pulse. The pulse shapes were obtained for six uniform section pulse forming network

supplied to matched resistance load, when $R_\ell = Z_N$ .The calculated and experimental pulse shapes are very close and the major difference is in the initial overshoot, so the calculated value is approximately twice the observed value. The experiment is done on 12KV of HVDC at 7.0 Amps of charging current, to get a pulse of 12.0 KV rectangular shapes for 6 micro seconds for the above mentioned Pulse Forming Network configuration. The actual hardware of 12 kV pulse output PFN based modulator as shown in Fig 6.8. is used for the experiment.

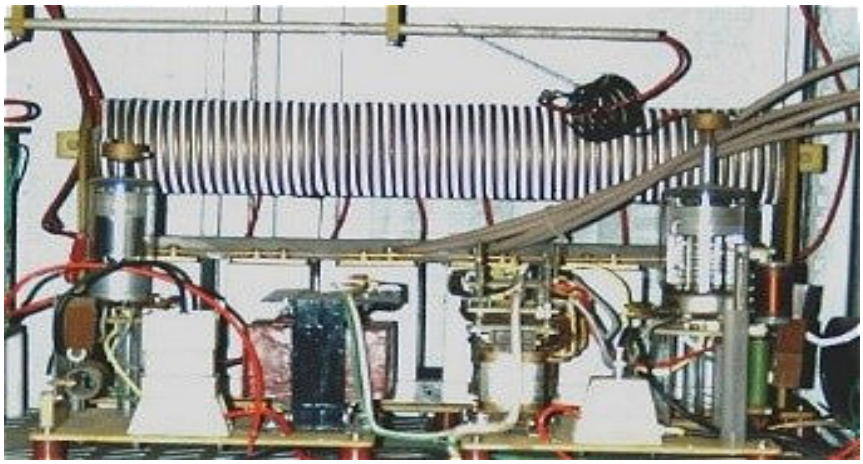

Fig 6.8. Experimental Modulator Hardware; Source: DRDO,MOD,INDIA

In this experiment, all the time cable length of the system changes and cable connection for high voltage supply is ensured. In this case, klystron of 6 MW peak power and 6kW average power has been taken into account and the results were obtained experimentally.

6.3 Length of cable: high voltage pulse with 10 meters

When the length is less, the top of the pulse is found to be flat in shape. The initial overshoot and undershoot is at a minimum level and as per calculated value. As the length of the tri-axial cable is less, the load impedance is lower and, the mismatch is also minimum as in Fig 6.9.

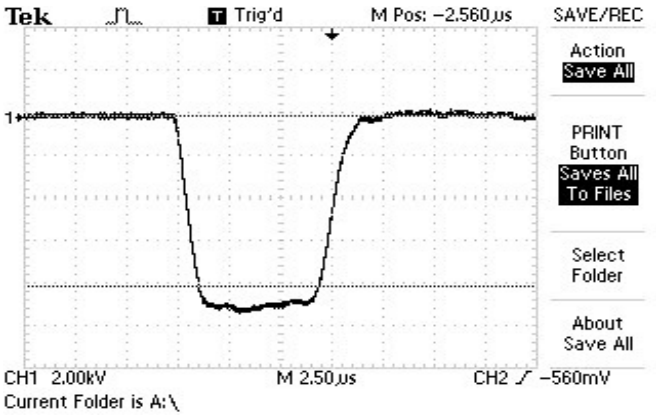

Fig 6.9. Voltage waveform in 10 m long cable

6.4 Length of cable: high voltage pulse with 30 meters

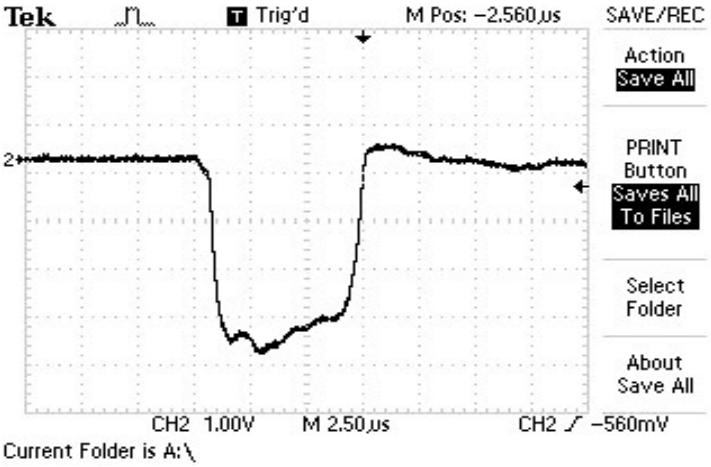

Fig 6.10. Voltage waveform in 30 m long cable

When the length is increased moderately, given in Fig 6.10. the top of the pulse is disturbed by ripples. The initial overshoot and undershoot increase moderately. The load impedance changes as per $\sqrt{\frac{L_N}{C_N}}$ with an experimental change of $\sqrt{\frac{L_N+\Delta L}{C_N+\Delta C}}$ and accordingly, the pulse width ($2\sqrt{L_N C_N}$) change is negligible, whereas the amplitude of the pulse shows marginal reduction due to waveform distortion compared to earlier flat top wave shape.

As per the derivation, the pulse current $\frac{V_N}{2\sqrt{\frac{L_N}{C_N}}}$ changes due to the impact of impedance change.

6.5 Length of cable: High voltage pulse with 50 meters

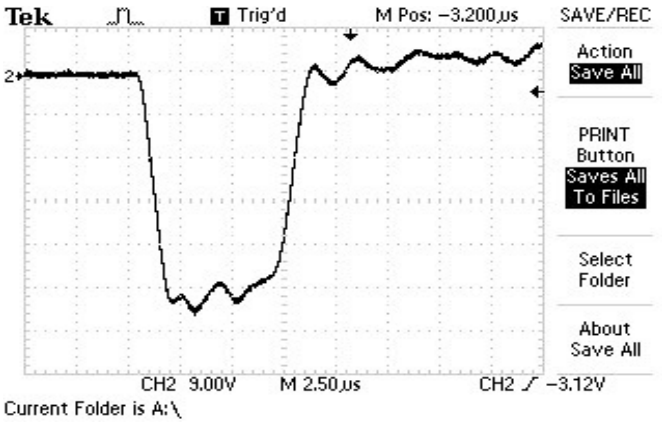

Fig 6.11. Voltage waveform for 50 m Cable

When the length is increased further, see Fig 6.11. The top of the pulse is disturbed by ripples and negative mismatch. If we compare the Pulse shape parameter with earlier wave forms at 30m cable length, as the length we find that increased, pulse width also increased i/e the pulse current amplitude had significant reduction.

6.6 Length of cable: high voltage pulse with 70 meters

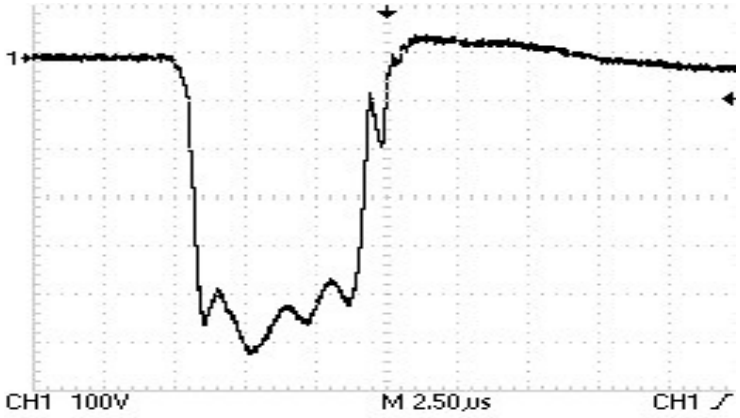

Fig 6.12. Voltage waveform for 70 m Cable

The phenomena still follows the same pattern like the rectangular portion of the wave and the quantity of the overshoot and undershoot. After microscopic analysis of wave shape, it is found that average pulse current amplitude has significant reduction compared to 50m of cable length pulse current, while pulse width reports marginal changes as given in Fig 6.12.

6.7 Length of cable: high voltage pulse with 90 meters

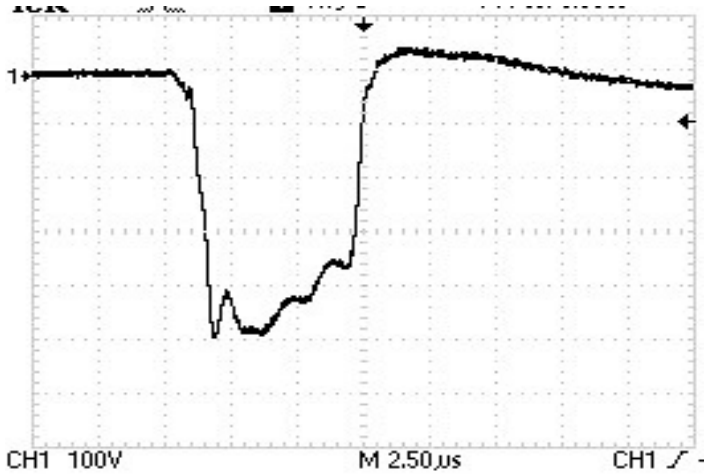

Fig 6.13. Voltage waveform for 90 m Cable

The above pulse shape shown in Fig 6.13. was badly distorted at the same when the pulse flat top was disturbed. The pulse width also got changed and average pulse current had drastic

reduction due to incorporation of ΔL and ΔC. This type of pulse shape utilization will not be effective for microwave power generation.

Table 6.5. Comparative Analysis of Wave Shape and Mismatch

Length of cable (m)	Initial over shoot (%)	Under shoot (%)	Type of mismatch
10	Minimum	Minimum	Matched
30	01	0.5	Negative
50	03-04	01-02	Negative
70	06-07	03-04	Negative
90	10	6	Negative

As shown in Fig 6.8. hardware of High Voltage High Pulse Power Supply developed for implementation of impedance matching offline which delivers 12kV, 0 - 200Hz frequency, approximate 1000 A current with 6 micro sec pulse duration for primary of pulse transformer when the load is klystron microwave amplifier.

This chapter comprises of Theoretical calculations of present design, experimental study of pulse deformation due to aging effect discussed and analyses the reasons .in case study 2 the effect of cable length on pulsed deformation carried out and concluded the effect of cable length on pulse deformation. The cable end termination and effect of minor change also analyzed.

Chapter 7

Impedance matching and Pulse Shaping of High Voltage High Pulse Power Supply

All High Voltage High Pulse Power Supply were designed to deliver the output pulse for a specific or targeted load and in this case Klystron is the load. A novel technique for - pulse shaping is introduced to meet the dynamic impedance mismatch due to subsystem parameter changes because of continuous operation, component fatigue, subsystem operational temperature effect and environmental conditions as discussed in earlier chapter. It has been observed that due to change in dynamic parameter of the subsystem causes output pulse deformation like overshoot, low rise time, wide amplitude variation etc. The novel technique of pulse shaping of High voltage high pulse power supply for Klystron type of load. The developed pulse shaping mechanism implemented on Klystron based High Voltage High Pulse Power Supply for microwave generator. The output result of pulse shaping validated and analyzed on actual industrial hardware results.

High energy linear accelerated system used for particle acceleration to generate high energy photons for medical and industrial application. Fig. 7.1. below shows the functional block of Klystron based High energy linear accelerated system.

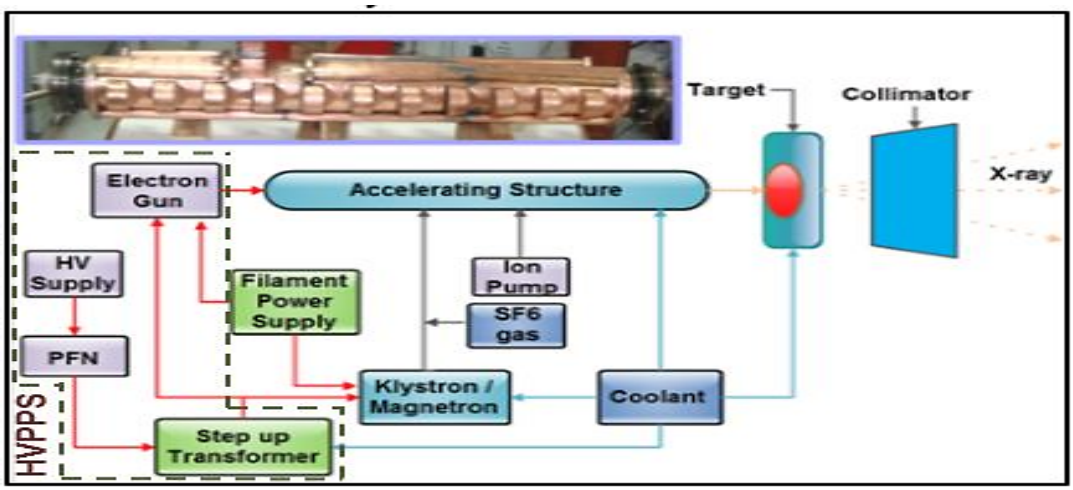

Fig 7.1. Klystron based High Energy Linear Accelerated System

The overall specifications of Klystron based LINAC system are following,

Table 7.1. Specifications of Klystron Based High Energy Linear Accelerated System

Parameter	Value
Energy	15Mev
Pulse Output Voltage	132 kV
Output Current	100 A
Peak output Power	6MW
Average output power	6kW
Pulse width (Variable)	6 µsec
Repetition rate (Variable)	10-200Hz
Load impedance(RL)	1500Ω
Turns Ratio	1:10
Duty Cycle	0.001

The energy delivered by LINAC is 15MeV photons and RF filed excitation provided by Klystron. Klystron requires 130 kV pulse voltage on the cathode to deliver 6 MW peak power. To meet the above output voltage and current a pulse transformer of 1:11 is used. There is a pulse generation system comprises of pulse forming network, charging inductor, high voltage switches and sensing network. The same is used for radar application to energise the transmitters.

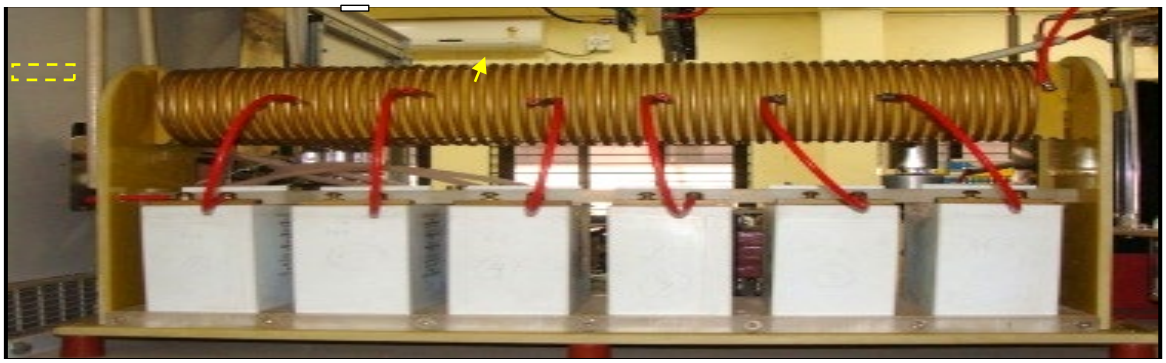

Fig 7.2. Novel Pulse-Forming Network (PFN); Source: DRDO,MOD,INDIA

The pulse shaping technique with variable impedance module, control by forward or reverse micro displacement through linear stage actuator of having micro motion. The data of linear actuator as given in Table 7.2.

Table 7. 2. Data of linear actuator

Parameter	Value
Load Capacity	3.0kg Direct Top Load
Linear Travel	25 and 50mm
Weight	165 to 264 gms
Repeatability	1μm/ 25.4 mm
Slider Backlash	1 μm
Speed	1.6mm/sec
Gearhead Backlash	<2 μm
Encoder Conversion	0.49609 μm count

The reference voltages are served through fast compensation / pulse sensor, which can change the charging voltage with the help of fast RC voltage sensor circuit. The sensed source voltage is given as analog input to ADC of FPGA kit. This is converted into digital form and then the reference is generated. The generated reference signal is compared with set value of requirement. Finally the switching signals are given to the devices through pulse amplification and isolation circuits.

Based on the feedback of wave shape, the micro actuator moves (forward and backward) to meet the required dynamic impedance, load impedance at the same side. The impedance of PFN Sub-section maintains the rectangular flat top for each pulse as per logic implementation shown in flow chart in Fig 7.3.

In order to check the LINAC System performance, an experimental set-up was assembled. It consists, basically, of a High voltage power supply that feeds the PFN through the charging inductor, fast blocking diode and hydrogen thyratron used to switch the PFN and a pulse transformer (1:11) with a secondary circuit winding bifilar, using comparator RC Network.

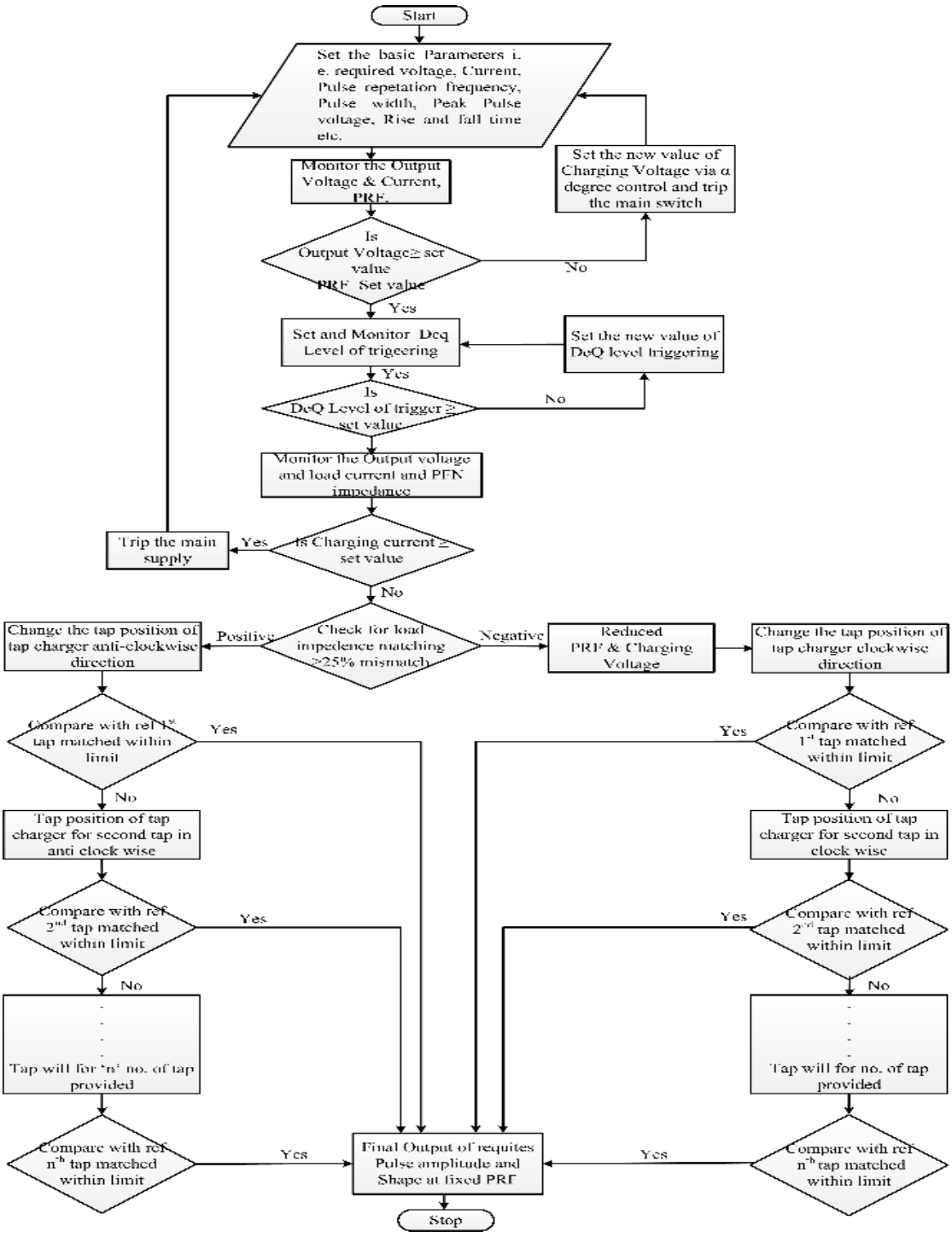

Fig 7.3. Flow Chart for Implementation of Pulse Shaping technique

Fig. 7.4. shows the hardware of the High Voltage High Pulse Power Supply developed for implementation of impedance matching which delivers 12 kV, 10 – 400 Hz (selectable) frequency, approximately 8 A current (Primary of Pulse transformer) with 6 μ sec pulse duration and transmission line impedance of 12.5 Ω, where the load is klystron microwave amplifier.

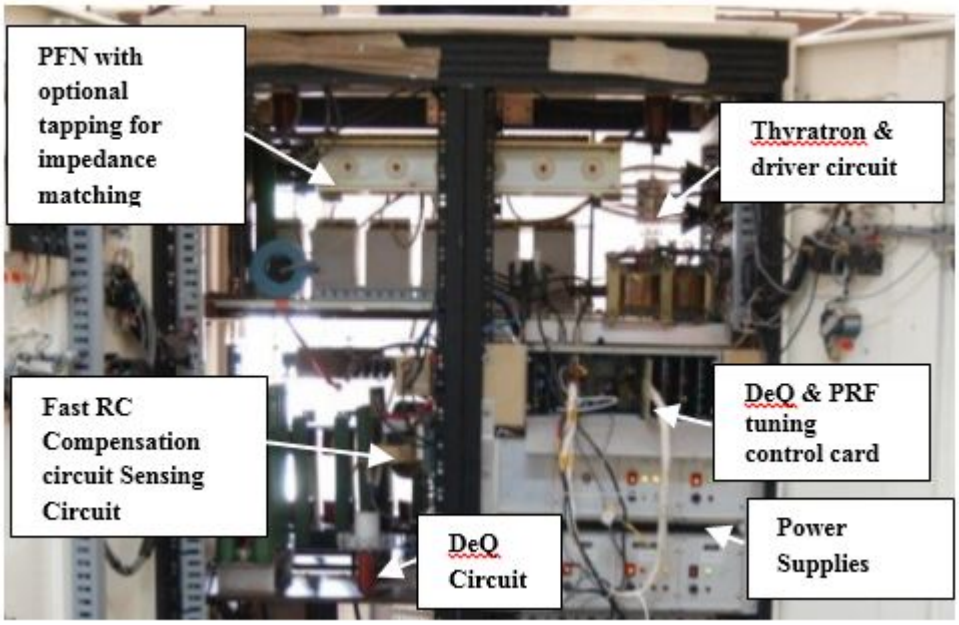

Fig 7.4. Actual hardware of high voltage high pulse power supply (HVHPPS); Source: DRDO,MOD,INDIA

As shown in Fig.7.5. a negative impedance matched klystron current waveform was observed during the experiment with manual taped change option created for impedance matching.

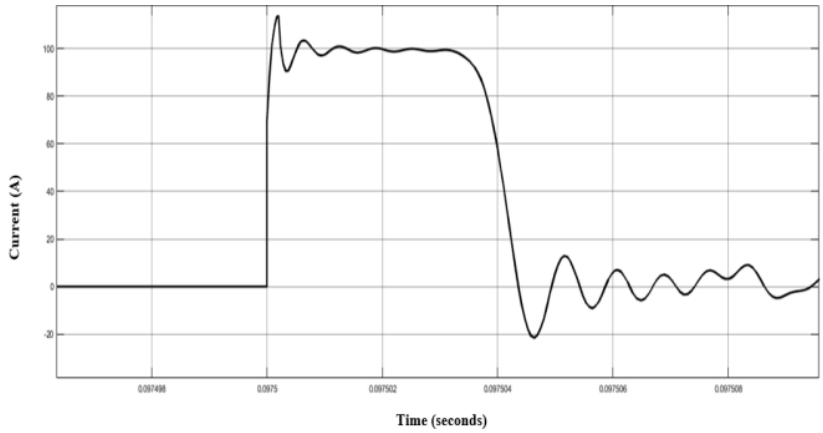

Fig 7.5. Reference Klystron current waveform observed in perfectly matched condition

The rise time, pulse width, fall time and overshoot of 8µsec, 6µsec, 1.2µsec and over shoot of 2A obtained respectively.

A) Negative Mismatch Tuning

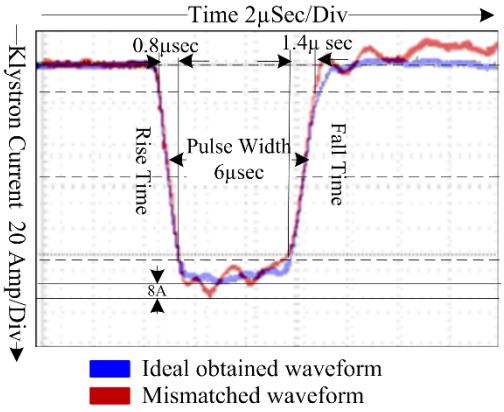

Fig 7.6. Klystron current waveform with -ve mismatch

As per Fig. 7.6. over shoot of 8A was observed and 1.4µsec of fall time was obtained which was due to positive mismatch (Z_l>Z_o) of PFN. Initial tapping of PFN increased i.e. line inductance was enhanced to compensate positive mismatch by adding the number of turns (Ln) to obtain the reference waveform for klystron.

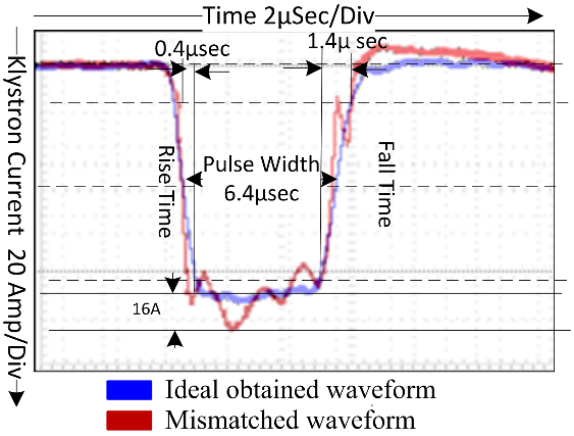

Fig 7.7. Klystron current waveform with +ve mismatch

As per Fig. 7.7. Klystron output current showed negative mismatch (Z_l<Z_o) of upto 18 % of the reference value. This negative mismatch was detected and measured to give a suitable command for output voltage amplitude and frequency correction.

To compensate the overshoot, pulse width, fall time and rise time, PFN tapping at the trailing edge was done in such a way that some of the air wound coils (Ln) were eliminated from the PFN.

B) Positive Mismatch Tuning

Fig. 7.8. shows that when impedance mismatch is high the controller will work in time domain and issue corrective command based on deterioration of the output voltage pulse parameters.

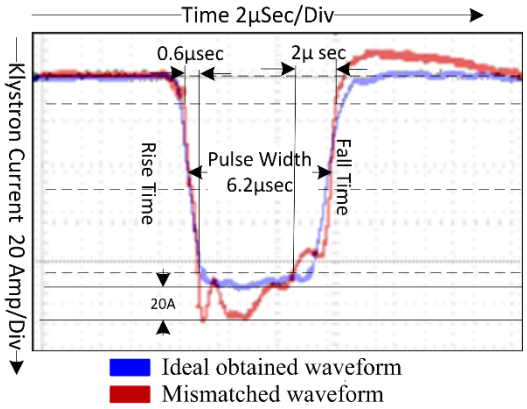

Fig 7.8. Klystron current waveform with high mismatch

After observation and comparative analysis with reference waveform, tripping command is issued by FPGA controller. Based on the mismatch condition the developed hardware option for impedance matching correction is utilized offline and impedance matching of PFN at the source end and finally ideal pulse as shown in Fig.7.9. is achieved, which is a perfectly impedance matched condition.

The modified Pulse forming network of High voltage high pulse power supply will have pulse shaping component, which can be controlled through actuators. The klystron pulse deformation discussed and seen into the system and found the reason. The various impedance mismatch condition and case problem identified, discussed for their appropriate solution. The control flow chart implemented in the actual HVHPPS hardware (Klystron based LINAC System) obtained the requisite pulse shape (flat top, rise and fall time control) and achieved the impedance matching condition. In future scope of work FPGA may be in the HVHPPS to impart various technique of control philosophy i.e. Artificial Neutral Network, fuzzy logic, and genetic algorithm. For dynamic loads rapidly changing their impedance, which is the usual behaviour of loads in most. This controller will take the HVHPPS into the new domain of dynamic control and pulse to pulse shaping.

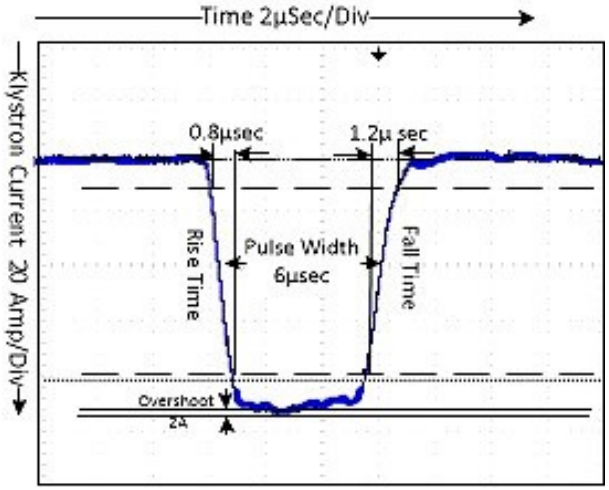

Fig 7.9. Klystron current waveform observed in perfectly matched condition

As shown in Fig 7.9. perfectly impedance matched klystron current waveform observed during the experiment with manual taped change option created for impedance matching.
This chapter comprises of Impedance matching and Pulse Shaping of High Voltage High Pulse Power Supply for Klystron.

In this chapter the dynamic impedance matching algorithms implemented and result were obtained. The various impedance mismatch condition created and dynamic impedance matching obtained on actual hardware.

Chapter 8

Conclusion and Future Scope

8.1 Conclusion

In this work, High Voltage High Pulsed Power with continuous pulses to excite a load with required width, frequency and magnitude. Simulation and experimental results have been performed to get the desired results. The main results obtained is discussed as below:

- The modelling of the Pulse Forming Network (PFN) for HVPPS are done which is used for storing and discharging of the energy to get required pulses. The L and C can be connected in various combinations to form PFN and it is observed that PFN of type E gives optimum performance.
- It is observed that, when Inductor is used as a charging element, the PFN voltage reaches to twice of the source voltage so that there is minimum requirement in the input voltage.
- As for the discharging circuit, PFN discharges energy to the load through a switch. It is observed that semiconductor switches are of more advantageous and here MOSFET is used as a switch.
- In the simulation, a voltage mode control is used where the error signal (difference between the reference and actual signal) is passed through a controller to generate the necessary control signal which is then compared with a saw tooth pulse to generate the gate pulses for MOSFET so that it is always switched on only when the PFN voltage reaches the required voltage. In the Hardware circuit, FPGA controller is used for giving appropriate gate pulses based on simulation results.
- After switching on the MOSFET at a particular frequency, pulses of required magnitude, width and pulse recurrence frequency is obtained.
- A proof of concept hardware was developed for Compact High Voltage High Pulse Power System which delivered 15KV, 10 amp pulse with sharp fall and rise time in micro seconds. Sharp fall and rise times are achieved using MOSFET and ferrite core pulse transformer. Using Virtex FPGA controller, the output pulse can vary pulse repetition frequency from 10 Hz to 400 Hz and voltage from 1 KV to 15 KV can be attained.
- Impedance matching mechanism and algorithm were tested in scale down model. The same was implemented in actual hardware as klystron load (klystron amplifier of 6MW,

6 micro sec, and 0.001 duty cycle) and impedance matching was tested and offline impedance matching tuning mechanism was achieved.

- Pulse shaping are achieved through linear actuators servo control technologies for online PFN tuning in power supply in wide band as universal HVHPPS.

8.2 Future scope

In this work a fixed load is used whose impedance is matched with characteristic impedance of the PFN to transfer maximum energy to load, if a pulse transformer is installed at the load side, loads of variable impedance can be used because by varying the transformer parameters load and PFN impedance can be matched. Also there will be less voltage requirement at the source side and at the PFN capacitors so that capacitors of minimum size can be used in the PFN.

Faster and higher power solid-state devices are constantly being introduced that offer significant advantages for pulse power applications. These devices are being incorporated into significant number of modulator designs and used in various projects for specific applications. As the performance of these devices continues to improve they will replace more of the conventional switch technologies. A sub-nanosecond solid state pulse generator is under investigation, which is expected to produce an electrical field that is fast enough to penetrate the inner part of the cancer cells.

The most important work is in the of putting Artificial Intelligence into the system for fault prediction and dynamic impedance matching to make system more agile and wide band performance.

REFERENCES

1. Rai, K.K., Giridhar, A. V., Jahagirdhar, D., Rai, A., & Paul, A. (2022). Investigation on the Effect of Cable Length on Pulse Shape of High Voltage High Pulse Power Supply. In Defence Science Journal,72(2),243-249,May 2022.
   DOI: https://doi.org/10.14429/dsj.72.17548

2. Krishna Kumar Rai, Dr. A.V Giridhar, Dr. D R Jahagirdhar, Ashish Rai, Akash Kumar Paul. Mathematical Modeling and Analysis of High Voltage High Pulse Power Supply Performance on Various Loads. In Proceedings of the 1st International Conference on Power Electronics and Energy, IEEE, India 2021.

3. K. K. Rai, A. V. Giridhar, D.R. Jahagirdar, and A. Rai, "Design and Development of High Voltage High Pulse Power Supply using FPGA for Dynamic Impedance Matching", IEEE Transactions on Plasma Science Journal, On page(s): 1-6, Print ISSN: 0093-3813, Online ISSN: 1939-9375, July 2023 DOI: 10.1109/TPS.2023.3278976

4. Akash Kumar Paul, A.V Giridhar, Krishna Kumar Rai, A. Kirubaharan. Generation of Pulsed Power for Radar Application. In Proceedings of the 1st International Conference on Power Electronics and Energy, IEEE, India, 2021.
   DOI:10.1109/ICPEE50452.2021.9358689

5. H. Akiyama, S. Sakai, T. Sakugawa and T. Namihira. Invited Paper - Environmental Applications of Repetitive Pulsed Power. IEEE TDEI, 2007, 14(4), 825-833.
   doi: 10.1109/TDEI.2007.4286513.

6. H. Li, Z. Yan, C. Zhang, Y. Wang, M. Gao and G. Zou. Experimental Study of Inductive Pulsed Power Supply Based on Multiple HTSPPT Modules. IEEE TPS, 2016, 44(6), 950-956.
   doi: 10.1109/TPS.2016.2558663.

7. N. Carleto and C. C. Motta. Design, construction and characterization of a line-type pulse modulator for driving high power magnetron. In SBMO/IEEE MTT-S International Conference on Microwave and Optoelectronics, 2005, pp. 330-333.
   doi: 10.1109/IMOC.2005.1580011.

8. Y. Wang et al. Design of Series Resonant High-voltage Constant Current Power Supply. In IEEE 4th Advanced Information Management,Communicates, Electronic and Automation Control Conference (IMCEC), 2021, pp. 471-475.
   doi:10.1109/IMCEC51613.2021.9482281

9. Q. Wang, Y. Gao, C. Liang and J. Zhao. Design of series resonant high voltage capacitor charging power supply. In 16th IET International Conference on AC and DC Power Transmission (ACDC 2020), 2020, pp. 1294-1297.
   doi: 10.1049/icp.2020.0309.

10. A. Ponomarev, S. Korzhenevskiy, A. Komarskiy, O. Krasniy and A. Chepusov. Power Supply for Powerful Generators with High Pulse Repetition Rate. In 7th International Congress on Energy Fluxes and Radiation Effects (EFRE), 2020, pp. 315-316.
    doi: 10.1109/EFRE47760.2020.9242016

11. J. h. Kim, C. g. Park, M. H. Ryoo, S. Shenderey, J. s. Kim and G. h. Rim. IGBT Stacks Based Pulse Power Generator for PIII&D. In IEEE Pulsed Power Conference, 2005, pp. 1065-1068.
    doi: 10.1109/PPC.2005.300503

12. S. Jin, J. Chen, Z. Li, C. Zhang, Y. Zhao and Z. Fang. Novel RDD Pulse Shaping Method for High-power High-voltage Pulse Current Power Supply in DBD Application. IEEE TIE, 2022, 1-1.
doi: 10.1109/TIE.2022.3140515

13. L. Zhou et al. High Overload Power Supply System and Its Energy Synchronization Control Method for Short-Term High-Energy Pulse Load, IEEE TSG, 2022, 13(2), 849-860.
doi: 10.1109/TSG.2021.3122442

14. Falong Lu, Xinyi Nie, Yu Wang, Weirong Chen, and Zhongming Yan. Influence of the Mutual Inductance between Two HTSPPT Modules on Three Discharge Modes of Superconducting Pulsed Power Supply. IEEE TPS, 2018, 46(8), 2993-2998.
DOI:10.1109/TPS.2018.2852706.

15. Zhenmei Li, Haitao Li, Xiaotong Zhang, Cunshan Zhang, Shucun Liu, and Tong Lu. Modeling and Simulation of Railgun System Driven by Multiple HTSPPT Modules. IEEE TPS, 2018, 46(1), 167-174.
DOI:10.1109/TPS.2017.2777699.

16. Sizhuang Liang, Youtong Fang, and Xiaoyan Huang. Simulation of an Electromagnetic Launcher with a Superconducting Inductive Pulsed Power Supply. IEEE TAS, 2016, 26(4).
DOI:10.1109/TASC.2016.2521427.

17. A.V. Akimov, P.V. Logachev, V.D. Bochkov, D.V. Bochkov, V.M. Dyagilev and V.G. Ushich, “Application of F TPI1-10k/50 Thyratron for building a modulator, intended for supply of inductive-resistive load in double pulse mode” IEEE International Pulsed Power Conference, Vol.2, pp-1339-13, 2007.

18. C. -G. Cho, H. -J. Ryoo, "Design of Compact Solid - State Modulator for High–Power Electromagnetic Pulse Generation," In IEEE Journal of Emerging and Selected Topics in Power Electronics, vol. 9, no. 5, pp. 6059-6068, Oct. 2021,
doi: 10.1109/JESTPE.2021.3079330.

19. Dongdong Wang, Jian Qiu and Kefu Liu, “All-Solid State Repetitive Pulsed-Power Generator using IGBT and Magnetic Compression Switches”, IEEE Transactions on Plasma Science, Vol.38, No.10, pp-2633-2638, October2010.

20. Yifan Wu, Kefu Liu, Jian Qiu ,Xiao Xu Liu and Houxiu Xiao, “Repetitive and High Voltage Marx Generator Using Solid-state Devices”, IEEE Transactions on Dielectrics and Electrical Insulation, Vol. 14, No. 4, pp-937-940, August 2007.

21. Falong Lu, Yu Wang, Xiufang Wang, Xiaoyong Liao, Zhengyou He, and Zhongming Yan. Study on the Collaborative Discharge of a Double Superconducting Pulsed Power Supply Based on HTSPPT Modules. IEEE TAS, 2017, 99(1-1).
DOI:10.1109/TASC.2017.2776269.

22. Haitao Li, Yadong Zhang, Cunshan Zhang, Mingliang Gao, Yunzhu An, and Tao Zhang. A Repetitive Inductive Pulsed Power Supply Circuit Topology Based on HTSPPT.IEEE TPS, 2018, 46(1), 134-139.
DOI: 10.1109/TPS.2017.2776564

23. Haitao Li, Cunshan Zhang, Zhenmei Li, Yuanchao Hu, Mingliang Gao, and Xinxin Zheng. An Inductive Pulsed-Power Supply Circuit Consisting of Multiple HTSPPT Modules With Capacitor Reuse Methodology. IEEE TPS, 2017, 45(7), 1139-1145.
DOI: 10.1109/TPS.2017.2697915.
DOI:10.1109/ICPEE50452.2021.9358787

24. G. N. Glosoe and J. V. Lebacqz, “Pulse Generators” New York: Mc- Graw-Hill, 1948.

25. H.Li, H.J.Ryoo, J.S.Rim, Y.B.Kim, and J.Deng, “Development of Rectangle-Pulse Marx Generator Based on PFN’’, IEEE Trans. Plasma Sci., Vol.37,pp.190-194,2009.
26. M. Akemoto, S. Gold, A. Krasnykh and R. Koontz “Design of a PFN for the NLC Klystron Pulse Modulator”, Presented at 1st Asian Particle Accelerator Conference (APAC 98), C98-03-23.3, p.175-177.
27. N. Carleto, C. R. B. Miranda and C. C. Motta “Design of an Pulse-Forming Network for driving High Power Magnetron”
28. https://www.researchgate.net/publication/265009076_Design_of_an_Pulse-Forming_Network_for_Driving_High_Power_Magnetron.
29. Francis Lassalle , Alain Morell, Arnaud Loyen, Thierry Chanconie, Bernard Roques, Martial Toury, and René Vezinet “Development and Test of a 400-kV PFN Marx With Compactness and Rise Time Optimization”, IEEE Transactions on Plasma Science, Volume:46,Issue:10 , OCTOBER 2018.
30. A. Musolino, M. Raugi, and B. Tellini, “Pulse forming network optimal design for the power supply of EML launcher,” IEEE Trans. Magn., vol. 33, no. 1, pp. 480–483, Jan. 1997.
31. Carleto, N., and C. C. Motta. "Design, construction and characterization of a line-type pulse modulator for driving high power magnetron." In SBMO/IEEE MTT-S International Conference on Microwave and Optoelectronics, 2005. pp. 330-333. IEEE, 2005.
32. H.A.H. Boot, J.T.Randall, “The cavity magnetron”, Journal of the Institution of Electrical Engineers- PART IIIA: Radiolocation, Volume:93, Issue:5,1946.
33. Dipit Khare A Srivastava, J Dutta, D P Chakravarthy, D N Barve, H.A Mngalvedekar A S Paithankar Dixit, “Development of New Solid State Pulse Modulator, IEEE Transactions on Dielectrics and Electrical Insulation Volume: 16, Issue: 4, August 2009.
34. S Krishnaveni and V Rajini, “Implementation of an Economical and Compact Single MOSFET High Voltage Pulse Generator” Indian Journal of Science and Technology, Vol 8, issue 2017.
35. Barrera-Cardenas, Rene, Takanori Isobe, and Marta Molinas,"Optimal design of air-core inductor for medium/high power dc-dc converters." In 2016 IEEE 17th Workshop on Control and Modeling for Power Electronics (COMPEL), pp. 1-8. IEEE, 2016.
36. Balogh, Laszlo. "Fundamentals of MOSFET and IGBT gate driver circuits." Texas Instruments–Application report, SLUA618-March (2017).
37. Truntič, Mitja, and Miro Milanovič. "Voltage and current-mode control for a buck-converter based on measured integral values of voltage and current implemented in FPGA." IEEE Transactions on Power Electronics 29, no. 12 (2014): 6686-6699.

LIST OF PUBLICATIONS

SCI / SCIE Journals

1. K. K. Rai, A. V. Giridhar, D.R. Jahagirdar, and A. Rai, "Design and Development of High Voltage High Pulse Power Supply using FPGA for Dynamic Impedance Matching", IEEE Transactions on Plasma Science Journal, On page(s): 1-6, Print ISSN: 0093-3813, Online ISSN: 1939-9375, July 2023 DOI: 10.1109/TPS.2023.3278976

2. K.K. Rai, A. V. Giridhar, D.R. Jahagirdar, A. Rai, and A. Paul, "Investigation on the Effect of Cable Length on Pulse Shape of High Voltage High Pulse Power Supply", Defense Science Journal, vol. 72, no. 2, pp. 243-249, May 2022
   DOI: https://doi.org/10.14429/dsj.72.17548

3. K. K. Rai, A. V. Giridhar, D.R. Jahagirdar, and A. Rai, "Novel Technique of Pulse Shaping of High Voltage High Pulse Power Supply for Klystron", IEEE Transactions on Plasma Science Journal. **(Under Review)**

International Conferences

4. Krishna Kumar Rai, Dr. A.V Giridhar, Dr. D R Jahagirdar, Ashish Rai, Akash Kumar Paul. Mathematical Modeling and Analysis of High Voltage High Pulse Power Supply Performance on Various Loads. In Proceedings of the 1st International Conference on Power Electronics and Energy, IEEE, India 2021.
   DOI:10.1109/ICPEE50452.2021.9358787

5. K. K. Rai, A. V. Giridhar, D.R. Jahagirdar, and A. Rai, "Analytical Approach for Fault Diagnosis of High Voltage High Pulse Power Supply for High Power Klystron" International Conference on Plasma Science and Pulse Power Electronics, "IEEE" PPC/SOFE 2021.

6. Akash Kumar Paul, A.V Giridhar, Krishna Kumar Rai, A. Kirubakaran. Generation of Pulsed Power for Radar Application. Proceedings of the 1st International Conference on Power Electronics and Energy, IEEE, India, 2021. DOI:10.1109/ICPEE50452.2021.9358689